AD-603 233

LIGHTNING PROTECTION MEASURES FOR AIRCRAFT FUEL SYSTEMS: PHASE II

Christian C. Bolta, et al

Atlantic Research Corporation
Alexandria, Virginia

May 1964

DISTRIBUTED BY:

NTIS

National Technical Information Service
U. S. DEPARTMENT OF COMMERCE
5285 Port Royal Road, Springfield Va. 22151

This document has been approved for public release and sale.

603233

AD No.____
DDC FILE COPY

FAA ADS-18

TECHNICAL REPORT
ADS-18

LIGHTNING PROTECTION MEASURES FOR AIRCRAFT FUEL SYSTEMS

Phase II

Submitted By

Christian C. Bolta, Raymond Friedman,
Gary M. Griner, Michael Markels, Jr.
Matthew W. Tobriner, Guenther von Elbe

Atlantic Research Corporation
Alexandria, Virginia
Contract No. FA 64WA-4955

DDC
RECEIVED
AUG 6 1964
DDC-IRA C

for

FEDERAL AVIATION AGENCY

WASHINGTON, D.C. MAY 1964

Reproduced by
NATIONAL TECHNICAL
INFORMATION SERVICE
Springfield, Va. 22151

repo[illegible]
tribution. It does not [illegible]
[illegible]ect FAA policy in all respects and it
[illegible] not, in itself, constitute a standard,
[illegible]ification or regulation.

N O T I C E

THIS DOCUMENT HAS BEEN REPRODUCED FROM THE BEST COPY FURNISHED US BY THE SPONSORING AGENCY. ALTHOUGH IT IS RECOGNIZED THAT CERTAIN PORTIONS ARE ILLEGIBLE, IT IS BEING RELEASED IN THE INTEREST OF MAKING AVAILABLE AS MUCH INFORMATION AS POSSIBLE.

11,031

TO: Thorion Industries, Inc JOB NO. #26

DEPARTMENT OF COMMERCE CONTRACT NO. #2-35641

DATE SUBMITTED 7-13-72 ORIGINAL WITH JOB:

TITLE AD-603233 YES ✓

NO. OF PAPER PLATES [redacted] 201 (1up) NO _____

NO. OF COPIES REQUIRED 20 Dup. 4,020

COVER PRINTS ONE SIDE ONLY (PGS. 3 AND 4 OF COVER BLANK)

TEXT PAGES PRINT HEAD TO HEAD

PAPER STOCK - COVER - FRONT - PRINTS ON YELLOW LEDGER

BACK - PLAIN YELLOW LEDGER

TEXT - WHITE OFFSET - C.W. SUB 100

INK: BLACK

TRIM SIZE: 8½ X 11 INCHES

BINDING: GATHER AND STITCH WITH TWO (2) WIRE STAPLES ON LEFT SIDE

DELIVER TO: OFFICE OF PUBLICATIONS
MICROREPROGRAPHIC DIVISION
ROOM 1219 - DOCK NO. 3
5285 PORT ROYAL ROAD
SPRINGFIELD, VIRGINIA 22151

THIS JOB IS DUE TO DELIVER ON 7-19-72

SIGNATURE OF AUTHORIZED OFFICIAL E. MacFarland 7/13.

PRINTING OFFICER DATE

OP/MRG #1
TEST FORM
8-70

Worksheet attached -

Worksheet - Thorion Ind. Job No. 26

AD - 603233 - 1 up 20 cps.

		Blanks
1 pg.	(N.T.I.S. Cover.) O.S.O.	1
2 pgs.	(Doc. Cover + Notice) H. to H.	—
2 pgs.	(F.A.A. rpt. (pp. 1+2.) H. to H.	—
* 9 pgs.	(Pgs. i thru xi) H. to H.	3
157 pgs.	(Pgs. 1 thru 157) H. to H.	1
1 pg.	(Appendix A.) O.S.O.	1
12 pgs.	(Pgs. A-1 thru A-12) H. to H.	—
1 pg.	(Appendix B.) O.S.O.	1
3 pgs.	(Pg. B-1 thru B-3) H. to H.	1
1 pg.	(Appendix C.) O.S.O.	1
12 pgs.	(Pg. C-1 thru C-13) H. to H.	2
201 pgs.	total c.c. Back Cover	2
+13 blanks.	Total Blanks -	13
214 total text pages.		

* Pages ii and iv are blank.

FEDERAL AVIATION AGENCY
Washington, D. C., 20553

July 20, 1964

Reports on Lightning Protection Measures
For Aircraft Fuel Systems

The enclosed reports are the results of a two-phase, short-range program of study, test, and experimentation conducted under Federal Aviation Agency contracts. The two reports are identified as follows:

1. ADS-17 "Lightning Protection Measures for Aircraft Fuel Systems Phase I", dated May 1964.
2. ADS-18 "Lightning Protection Measures for Aircraft Fuel Systems Phase II", dated May 1964. AD603233

The work was initiated as a result of the accident which occurred to a jet transport near Elkton, Maryland, on December 8, 1963. The accident occurred during a severe storm in which heavy lightning discharges were observed. Examination of the wreckage indicated that a lightning strike may have ignited fuel vapors. The official CAB investigation of this accident is in progress.

Although the accident investigation is not yet complete, sufficient evidence existed early in the investigation to warrant immediate short-range studies and tests to:

a. Secure a better understanding of the possible mechanisms by which lightning strikes could be hazardous to fuel systems,
b. Develop means to protect aircraft against such hazardous conditions,
c. Determine design criteria for the protective means, and
d. Examine the protective means for characteristics which might have an otherwise adverse effect on safety.

Pursuit of these broad aims is reflected in the more specific objectives spelled out in each of the enclosed reports.

In order to carry out an accelerated short-range effort, it was necessary to restrict deliberately the scope of the investigations. The work was confined to limits which resulted from the assumption that lightning, in some manner, had provided an ignition source either at the fuel tank vent or at some point within the fuel tank. A determination of the validity of this assumption is not within the scope of these efforts.

An airworthy outer wing panel, a wing tip and several production fuel vent systems were used in the testing. This approach was dictated by the need to test production aircraft materials, fits, bonding, electrical continuity, and assembly techniques. Components tested were selected as being typical of FAA approved jet-powered transport designs in which careful consideration had been given to possible hazards from lightning based upon knowledge available at the time of certification.

These programs have shown areas which can be improved in many aircraft; some of which could be accomplished in the near future and others which would require more development and testing. In addition, the programs have provided direction for future testing to assure that maximum flight safety is attained.

The FAA and the project contractors are indebted to the Boeing Company and Pan American World Airways whose cooperation, assistance, and equipment helped assure that the work would provide practical results in the minimum time.

George P. Bates, Jr.
Acting Director
Aircraft Development Service

Enclosures

LIGHTNING PROTECTION MEASURES FOR AIRCRAFT FUEL SYSTEMS

PHASE II

Submitted by

Christian C Bolta, Raymond Friedman,
Gary M. Griner, Michael Markels, Jr.
Matthew W. Tobriner, Guenther von Elbe

Atlantic Research Corporation
Alexandria, Virginia

Contract No. FA 64WA-4955

for

Federal Aviation Agency
Air Development Service
Washington, D. C.

May 1964

ACKNOWLEDGEMENTS

In keeping with the high level of effort and short duration of this program, Atlantic Research Corporation established the following corporate team to carry out the program. Dr. Raymond Friedman, corporate Vice President, was in over-all charge of the project and provided insight into problems of combustion and flame dynamics. The program work was carried out under the technical direction of Dr. Michael Markels, Jr., Director of the Nuclear Engineering Division. Dr. Guenther von Elbe served as senior technical consultant and provided much of the theory of flame propagation discussed in this report. Mr. Christian Bolta, Project Engineer, was responsible for the coordination and timely execution of all phases of the program.

Mr. Matthew Tobriner, with the technical aid of Mr. Kenneth Clark, Mr. William McCarthy, and Mr. Kenneth McKee, performed the experimental work. Mr. Stanley Lazerus, Head of Engineering Development Laboratory, fabricated the equipment and supported the test program. Mr. Robert Kindel was resident engineer at the Lightning and Transients Research Institute and performed most of the Atlantic Research tests at that facility. Mr. Gary Griner performed the detailed analysis of the icing phenomena.

The authors wish to acknowledge the guidance provided by Mr. Harvey Hansberry, Federal Aviation Agency Program Manager, Mr. Robert Auburn, Chairman, and members of the Technical Committee on Lightning, especially Dr. Gilbert Kinser of the Weather Bureau who provided a technical review of the manuscript. Fine cooperation and support were provided by Professor Morris Newman, Mr. John Robb, and Mr. James Stahmann of Lightning and Transients Research Institute. Mr. Donald Nordstrom, of the Boeing Company, was extremely helpful in obtaining technical information concerning the Boeing 707 vent system, and Mr. Joseph Gillis of Fenwal, Inc., provided engineering assistance during portions of the test program.

PRECEDING
PAGE BLANK

TABLE OF CONTENTS

PRECEDING PAGE BLANK

TABLE OF CONTENTS (Continued)

TABLE OF CONTENTS (Continued)

LIST OF ILLUSTRATIONS

LIST OF ILLUSTRATIONS (Continued)

LIST OF ILLUSTRATIONS (Continued)

LIST OF TABLES

1.0 SUMMARY

A four-month, short-range program was conducted to develop technology leading to methods of overcoming the aircraft lightning strike hazards which could have been responsible for the crash of the Pan American 707 Aircraft N709PA near Elkton, Maryland, on December 8, 1963, and to investigate the potential hazards introduced by these methods. The program included experimental and analytical investigations of (a) flame propagation characteristics through the 707 vent system as a result of ignition by simulated lightning discharges and specially developed laboratory ignition equipment, (b) the effectiveness of flame arresters of various designs located at different sections of the vent system with simulated lightning and laboratory ignition equipment, (c) explosion suppression techniques utilizing an explosively disseminated chemical agent to prevent explosion in aircraft tanks upon sensing a flame propagating through the vent tube, (d) the previously reported ultra-high blast pressure effects and large volume plasma generation as a result of simulated lightning discharge in the area of the vent outlet. In addition, analytical evaluations were performed concerning, (e) the addition of air to the combustible vapor mixture to obtain high-velocity effluent from the vent outlet to prevent flashback, (f) the use of mechanical valves to isolate vent passages, and (g) the use of bladders as fuel containers. A purely theoretical analysis was performed to evaluate the potential hazards due to icing of selected flame arrester designs.

Flame propagation and arrester experiments were performed with the use of the high-voltage and high-current facilities of Lightning and Transients Research Institute and repeated in the combustion laboratory using a drive tube to simulate the lightning effects. Propagation of flame through actual 707 vent systems containing flammable fuel-air mixtures was demonstrated and characteristic flame speeds and pressure pulses were measured and duplicated in the laboratory apparatus. The apparatus provided a range of conditions from low flame speeds of 5 ft/sec to speeds of several hundred ft/sec. Flame arresters were designed to quench flames propagating at high

speeds through the vent duct and were tested at two locations in the system. Pressure drop and flame holding characteristics of the best arrester were experimentally determined.

Several general conclusions were developed in the program. Flame propagation tests using simulated lightning discharges directly to the vent outlet showed that flame speeds higher than the usual turbulent speeds are achieved due to the large mass flows caused by an organ pipe action of the vent system. Flame arresters near the vent outlet were compromised while those further inboard were effective. Explosion suppression systems were effective against flames propagating at speeds typical of those generated by the simulated lightning strike. No evidence was found of plasma penetration into the vent duct and maximum pressures in the system due to simulated lightning discharge did not exceed one atmosphere gauge as measured by fast response blast gauges. The analysis concerning flashback prevention by increased vent exit velocities showed that a rather large outflow may be required in order to assure a continuous net outward flow against flames propagating at high speeds into the vent system. Icing calculations showed that the best flame arrester would not be sealed by icing during the worst descent rates and environmental conditions and that several descents could be performed under normal conditions before serious icing developed.

Specifically, it is concluded that a suitable modification of the best flame arrester tested could be installed in the 707-type vent system and that such an arrester would protect the fuel tanks from flames propagating through the vent system. Further work is needed to optimize the arrester design with respect to cell size, position, area, thickness, geometry, pressure drop, pressure relief and icing characteristics. This would permit full evaluation of the approach and the integration of the arresters into the aircraft after which a flight test program could commence. Further work is warranted in the use of explosion suppression systems, increased vent velocity and inerting techniques as effective protection schemes.

2.0 INTRODUCTION

2.1 PROGRAM OBJECTIVES

As a result of the crash of Pan American 707 Aircraft N709PA near Elkton, Maryland, on December 8, 1963, the FAA has sponsored studies of aircraft-lightning strike hazards. As of the date of this report, the accident investigation is not complete; however, sufficient evidence was found early in the investigation to warrant an intensive four-month study of the problem of decreasing the probability of aircraft fuel ignition by lightning. Assuming that the final analysis of the Elkton accident bears out the preliminary assessment, this represents the first known instance in which a commercial aircraft was destroyed by the ignition of jet fuel by lightning.

Many valuable research programs of the past, directed toward the protection of aircraft from lightning hazards, have been carried out by Government agencies and by industry. The results of these programs provide the background for this program. However, the solutions of this program are not general in nature but are directed toward the development of specific modifications and hardware of specific aircraft and components. Accordingly, the basic objectives of this short-range program are to develop technology leading to methods of overcoming the hazards which could have been responsible for the crash of the Pan American 707 Aircraft N709PA near Elkton, Maryland, and to investigate any new potential hazards introduced by these methods.

The short-range program covered by this report is divided into two concurrent phases; one phase conducted by Lightning and Transients Research Institute and the other by Atlantic Research Corporation. Lightning and Transients Research Institute's program comprised methods of preventing internal arcing in the fuel tanks from direct strikes to skin surfaces, filler caps, access doors, and fuel probes, and determination of types and locations of lightning diverters to prevent sources of ignition at the vent. The results of this phase of the program are reported in FAA Report No. ADS-17.

Atlantic Research Corporation's program is directed toward studying methods of preventing propagation of flames through the vent system to the fuel tanks. Specifically, the objectives of Atlantic Research Corporation's program are:

1. To determine the conditions under which ignition of fuel vapors outside the vent produces flame propagation through the vent, vent duct, and surge tank, capable of triggering an explosion within the reserve tank.

2. To evaluate the protection offered by:
   a. Flame arresters
   b. Explosion suppression systems
   c. Providing increased vent exit velocities by adding air
   d. Isolation valves in the vent lines
   e. Flexible mechanical interface between the fuel surface and the air in the vent space.

3. To determine the speed and effective length of the plasma resulting from a lightning strike, if such a plasma exists.

4. To determine flame speed and pressure surges resulting from flame propagation through the vent system initiated by simulated lightning strikes and by electrical sparks.

5. To determine design criteria for the best methods, techniques, or devices for stopping flame propagation through the vent system.

6. To investigate whether the means of stopping flame propagation add other problems or hazards to aircraft operations.

The successful conclusion of the short-range program will provide input to a follow-on long-range program. This long-range program will have as its objectives the refining of the rough results of the short-range program, expanding those results to yield a broader band technology applicable to all jet transports having similar problems, conducting advanced studies on lightning and fuel hazards beyond the scope of the present program, and finally, developing advanced protection concepts. This long-range program, in turn, will lead to engineering test programs with flight testing of actual hardware.

2.2 PROGRAM PLAN

The short-range program was completed in fourteen weeks. Because of the limited time allotted for study, the program was divided into three concurrent tasks:

1. Analysis - to provide design criteria for equipment and components and to provide theoretical evaluation of the phenomena under study.

2. Experimental - to design and fabricate test equipment needed to perform flame propagation tests through a 707 vent system and to test flame arresters and explosion suppression systems.

3. Hazards Review - to perform theoretical and/or experimental evaluations of the added hazard to aircraft operation due to the installation of the prevention systems studied.

The details and results of these tasks are described fully in the following sections.

2.3 GENERAL BACKGROUND INFORMATION

2.3.1 Natural and Simulated Lightning

There are several good texts on the mechanisms, characteristics, and effects of natural lightning.[1, 2, 3, 4] The important properties are shown in Table 1. The values listed were obtained in discussions with personnel of Lightning and Transients Research Institute and the United States Weather Bureau. It should be noted that the maximum properties are those which have been measured or calculated from the effects of actual strokes, while those listed as possible upper limits are the maximum properties which are believed to be possible. Those listed as severe strokes have been used as United States Air Force design criteria for protective devices.

Lightning and Transients Research Institute (LTRI) has converted a 180-foot cable laying ship, Thunderbolt, into a laboratory in which experiments requiring simulated lightning strikes can be performed. The facilities were designed to duplicate the measured and observed effects of lightning discharges.

Table 1. Properties of Natural Lightning Discharges.

	Average	Severe	Maximum	Possible Upper Limit
Current, amperes	5×10^4	10^5	5×10^5	10^6
Initial Rate of Rise of Current, amperes/μsec	10^4	2×10^4	2×10^5	5×10^5
Charge Transfer, coulombs	50-200	200	600	1000
Voltage, volts	10^8	2×10^8	5×10^8	10^9

Lightning discharges produce various effects which depend on the materials and configuration of the object struck as well as the characteristics of the discharge. In these experiments the facilities were arranged to reproduce the particular characteristics of lightning thought to be significant in studying ignition and flame propagation into vent tubes and through flame arresters. This required currents and rates of rise of currents of maximum amplitude. The facility which produces the high-current discharges, located at the bow of the ship, is shown in Figure 1. This generator gives peak currents of up to 250,000 amperes at 25 kv. The rise time is of the order of 50 μsec, and the decay time is about 300 μsec. This generator provides large heating effects in the discharge path with associated pressure blasts. The generator at the stern of the ship, shown in Figure 2, develops high initial rates of rise (50,000 amperes/μsec) of current and high peak voltages (10^8 volts) which reproduce inductive sparking and streamering effects. The pertinent features of the two generators are listed in Table 2. A more complete discussion of the above points is found in Appendix A and in FAA Report No. ADS-17.

2.3.2 Fuels, Ignition, and Combustion

A wealth of information exists on the ignition, combustion, and detonation of fuels. The most pertinent include references 5, 6, 7, 8 and 9. The prerequisites for ignition are a flammable mixture and a concentrated energy source. It has been shown[6,7] that ignition can occur in homogeneous combustible mixtures, with energies of less than 1 millijoule so that flammable mixtures can be spark-ignited by commonly occurring electrostatic discharges. For instance, an average-sized man, with capacitance of about 300 $\mu\mu$f and charged to 10,000 volts by walking across a rug on a dry day, could conceivably initiate a discharge of energy ($1/2\ CV^2$) equal to 15 millijoules. It is obvious that lightning discharge can be a potent ignition source.

The presence of JP-4 or kerosene in jet aircraft provides a flammable mixture in the fuel tank and/or vent lines over a rather extensive range of altitudes and temperatures. This is shown in Figure 3 obtained from reference 10. In addition to the fuel vapor-air mixture, a flammable

NOT REPRODUCIBLE

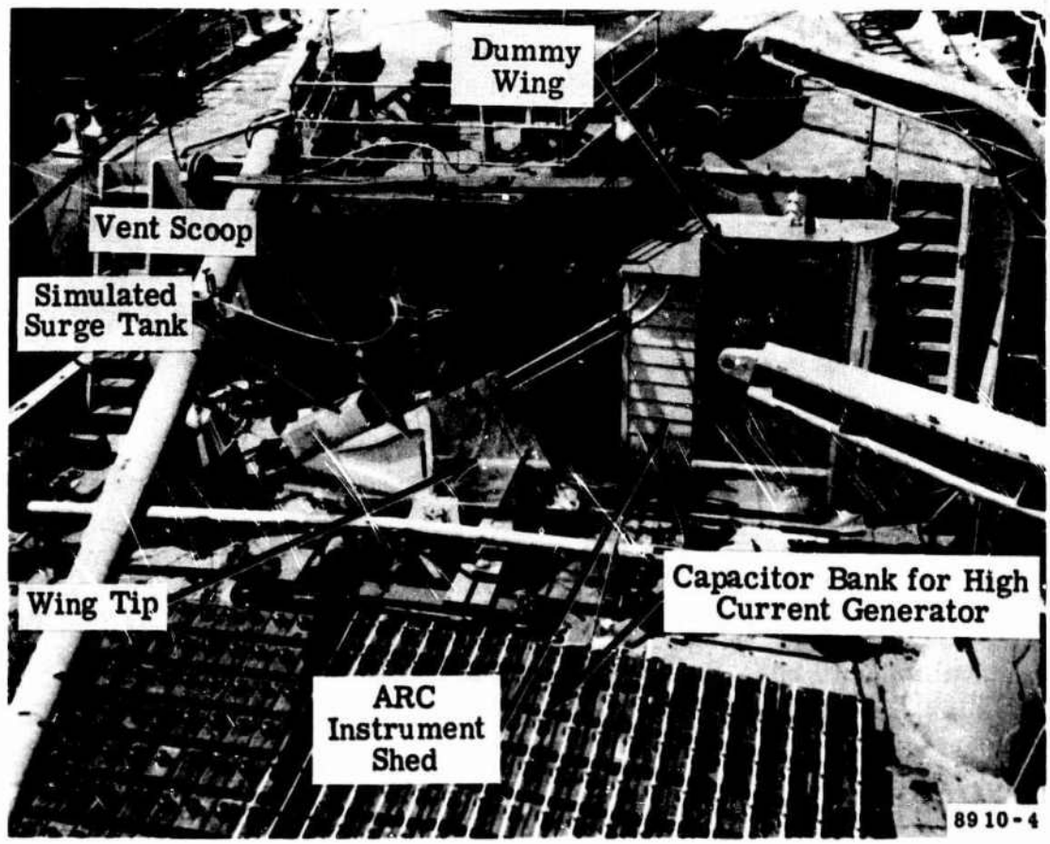

Figure 1. Lightning and Transients Research Institute High-Current Generator.

603233

NOT REPRODUCIBLE

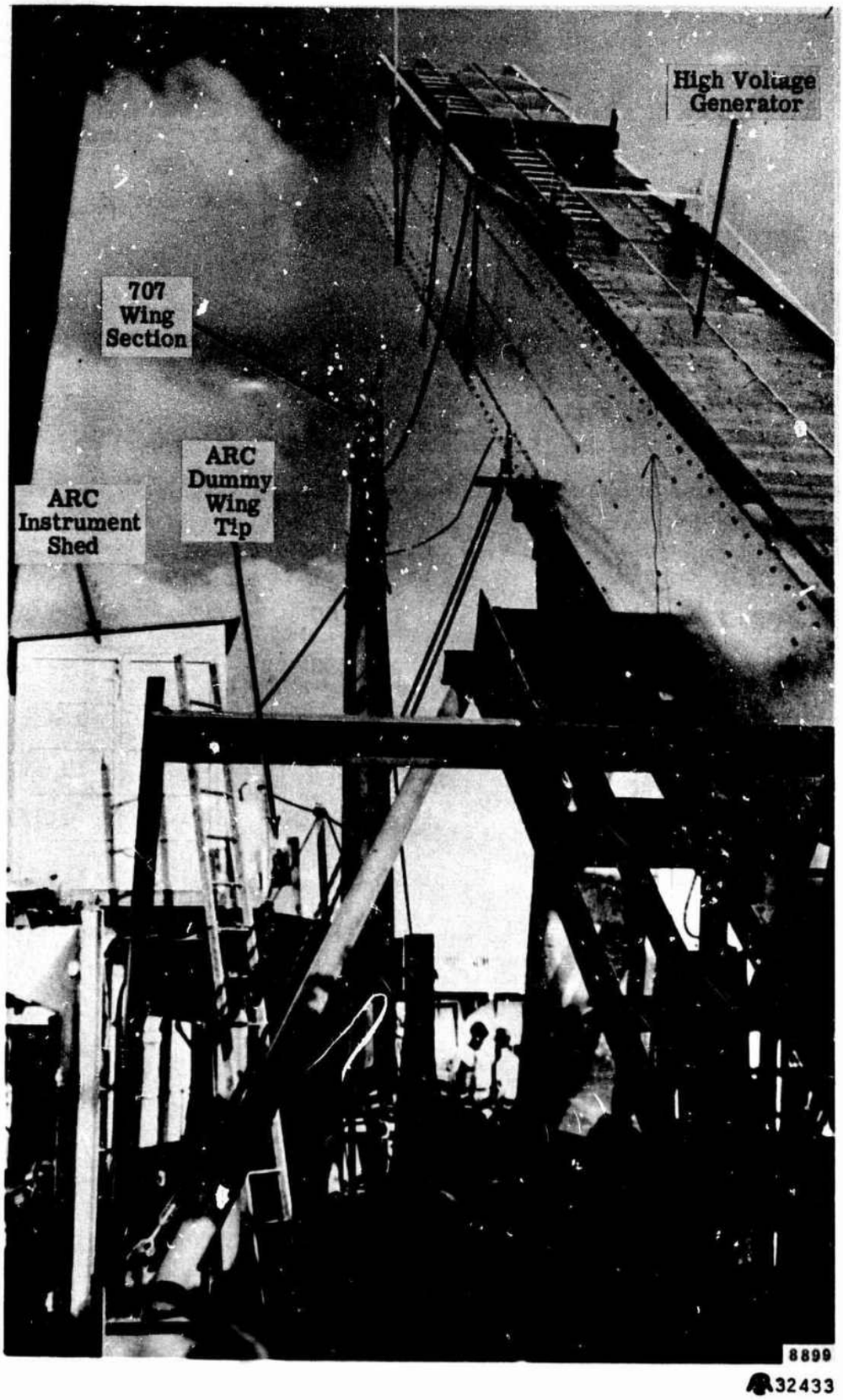

Figure 2. Lightning and Transients Research Institute High-Voltage Generator.

603233

Table 2. Properties of the Lightning and Transients Research Institute Facilities on the "Thunderbolt".

	High-Current Generator	High-Voltage Generator
Rated Current, amperes	250,000	100,000
Max. Current, amperes	500,000	---
Max. Experimental Current, amperes[a]	250,000	50,000
Initial Rate of Rise of Current, amperes/μsec	6,000	200,000
Capacitance, μf	36[illegible]	0.0077
Rated Energy Release, joules	114,000	385,000
Max. Energy Release, joules	456,000	---
Rated Charge Transfer, coulombs	9	0.077
Rated Voltage, volts	25,000	10,000,000
Max. Voltage, volts	50,000	---
Max. Experimental Voltage, volts[a]	25,000	325,000

[a] Maximum conditions obtained for Atlantic Research Corporation tests.

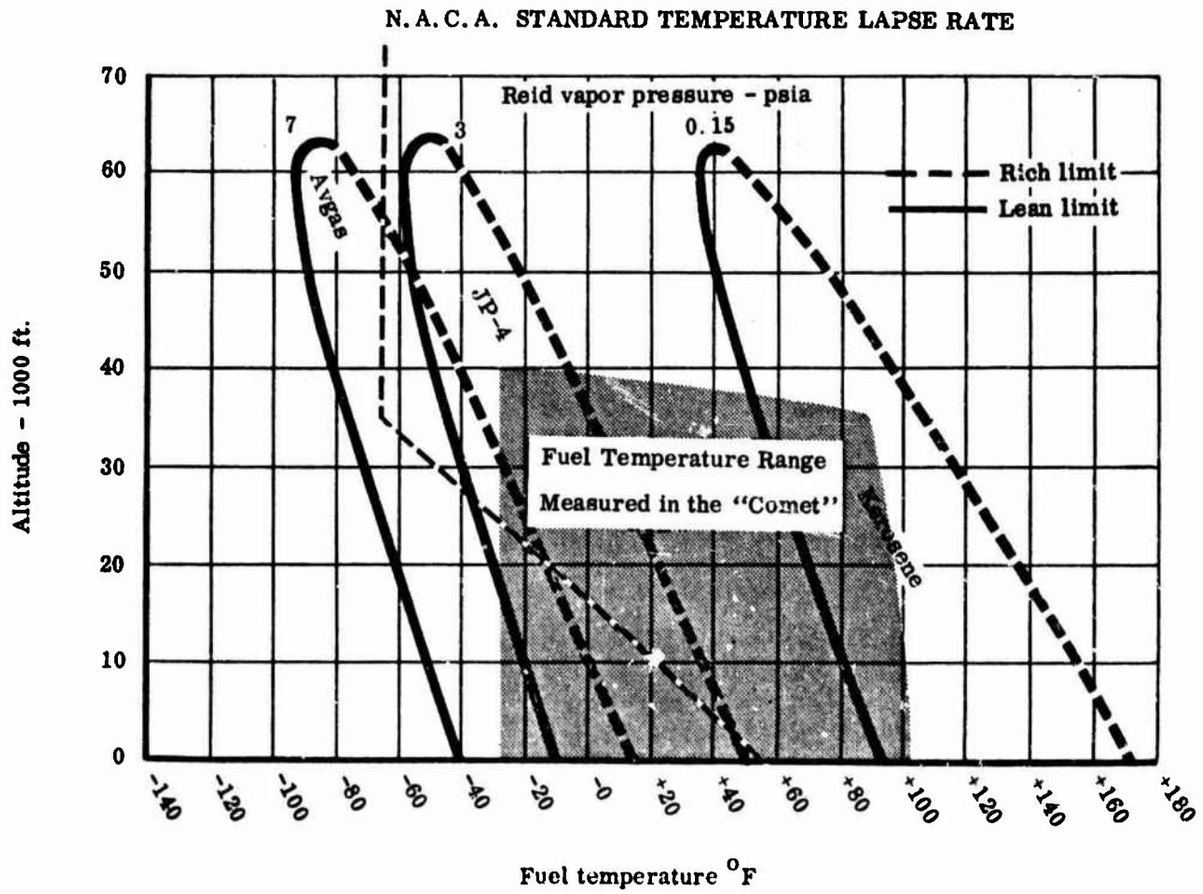

Figure 3. Combustible Range of Fuels as a Function of Altitude and Fuel Temperature (reference 10).

heterogeneous fuel vapor-fuel-mist-air mixture can be present over a wide range of temperatures below and above the flash point.[7] It should be noted that the vent outlet will have fuel-air mixture present during ascent or during rapid decreases in atmospheric pressures, and in level flight just after such pressure changes. During rapid ascent at 3000 ft/min, the maximum effluent velocity through the 707 vent tube is approximately 22 ft/sec. This velocity can purge the vent tube with fuel-air mixtures and, in addition, provide copious quantities of the mixtures at or near the vent outlet.

2.3.3 Flight Environment

It follows from the above that under certain conditions there can be a flammable mixture in the fuel tanks providing a flammable effluent from the fuel vents, and that lightning or other natural electrical activity in and around thunderstorms can provide potential ignition sources. The fact that lightning does strike aircraft is well documented and the frequency of strikes severe enough to show marks on the skin is about once a year per plane. It is also possible for direct strikes to the vicinity of the vent outlets to occur on either a single strike or a swept stroke of a multi-strike lightning discharge. The sweeping action occurs by the plane's forward movement (about 1 ft/msec) into an ionized channel in which discharges are occurring. These discharges may occur for the better part of a second, providing strike points at numerous locations across a wing or fuselage.

The frequency of occurrence of strokes close enough to the 707 vent to ignite the effluent gas has not been determined. In the absence of data showing that such strokes do not occur, it was assumed that there is a hazard to jet aircraft operating in or around thunderstorms due to the possibility of ignition of flammable mixtures in the vent opening which could propagate through the vent system into the fuel tanks, causing a catastrophic explosion. The probability of this sequence occurring must be small. However, with the increasing size of the commercial and military jet fleet the probability of such an accident occurring within a given time span is increasing.

2.3.4 707 Aircraft Vent System

The Boeing 707 aircraft is powered by four turbojet engines. Fuel for commercial turbojet transports within the continental limits of the United States is kerosene (JP-1). The fuel supplied to U. S. commercial aircraft at foreign airports is usually JP-4, a kerosene-type fuel which contains a greater percentage of more volatile components than does kerosene. The fuel, totalling 17,400 gallons, is contained in the 707 aircraft in 7 tanks; a bladder-type center tank in the fuselage and two main and one reserve wet-wing-type tank in each wing. Each wing tank is composed of many chambers since the tanks are sectioned by open ribs spaced every 25 to 30 inches. The tanks are interconnected so that it is possible to operate all engines from one tank or have all tanks feed one or more engines. In addition, each tank is vented directly or indirectly through "hat" shaped channels into surge tanks located at each wing tip. This is shown schematically in Figure 4 obtained from reference 11. Float valves are used in the "hat" sections to minimize liquid fuel transfer during banking maneuvers. The 15-gallon surge tanks are formed by two ribs and two spars and are enclosed by the upper and lower wing skins. Three "hat" vent tubes enter the surge tank from the inboard side and a 3/4-inch diameter drain hole allows fuel carried into the surge tank to return to the reserve tank. A 5-inch diameter duct is comprised of an elbow, with its open end up in the surge tank and the other end flanged to an opening in the outboard rib, and an "S" shaped vent tube which is flanged into a rectangular box-like vent outlet. The peripheral area between the elbow and the surge tank wall is equal to the cross sectional area of the duct. The vent outlet is recessed into the underside of the wing and its opening is located so that air flows across and perpendicular to its larger dimension. Figure 5 shows the underside of the right wing tip of the Pan American 707 aircraft which crashed at Elkton, Maryland. The vent scoop panel is removed showing the location of the vent duct. A rectangular hole was cut in the surge tank during the Civil Aeronautics Board. Figure 6 shows a simulated surge tank and all the individual components.

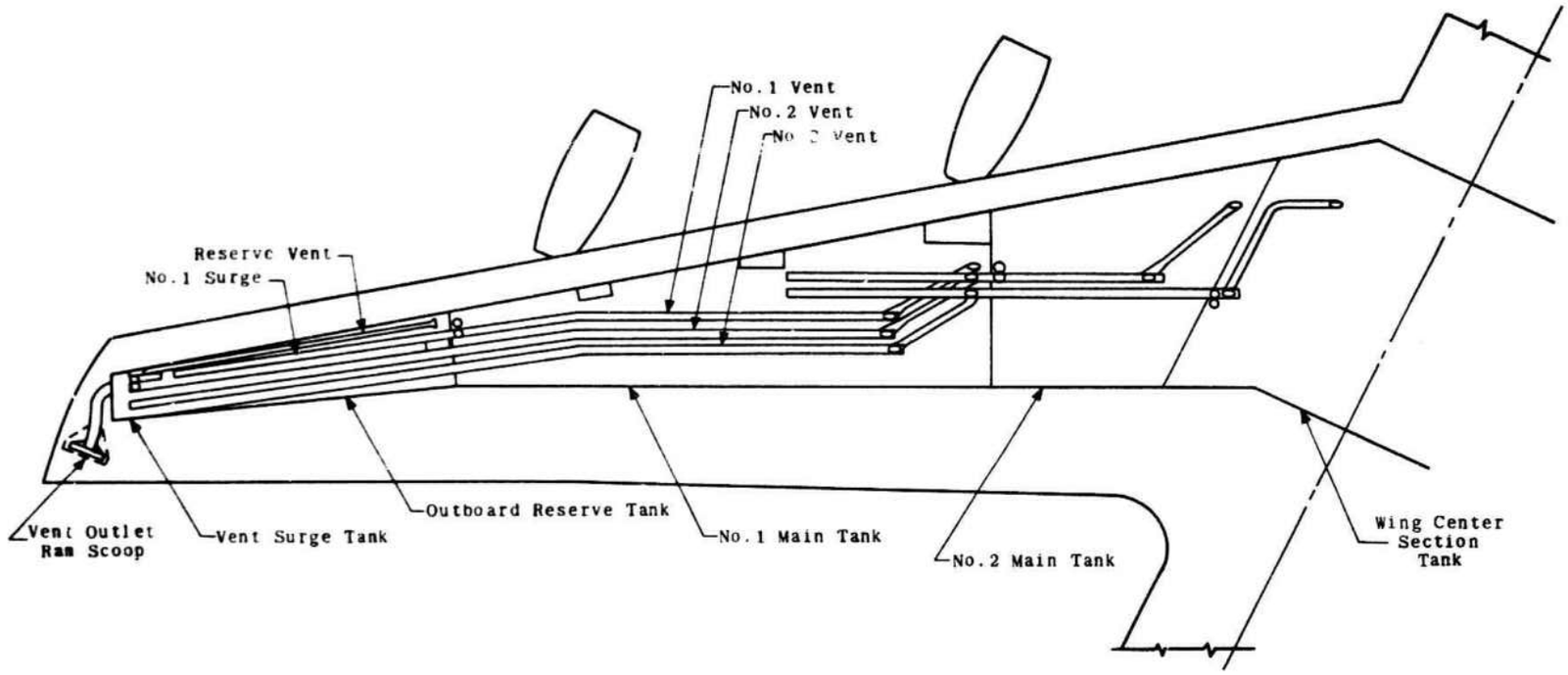

Figure 4. Schematic Diagram of 707 Vent System (Obtained from reference 11).

R 32515

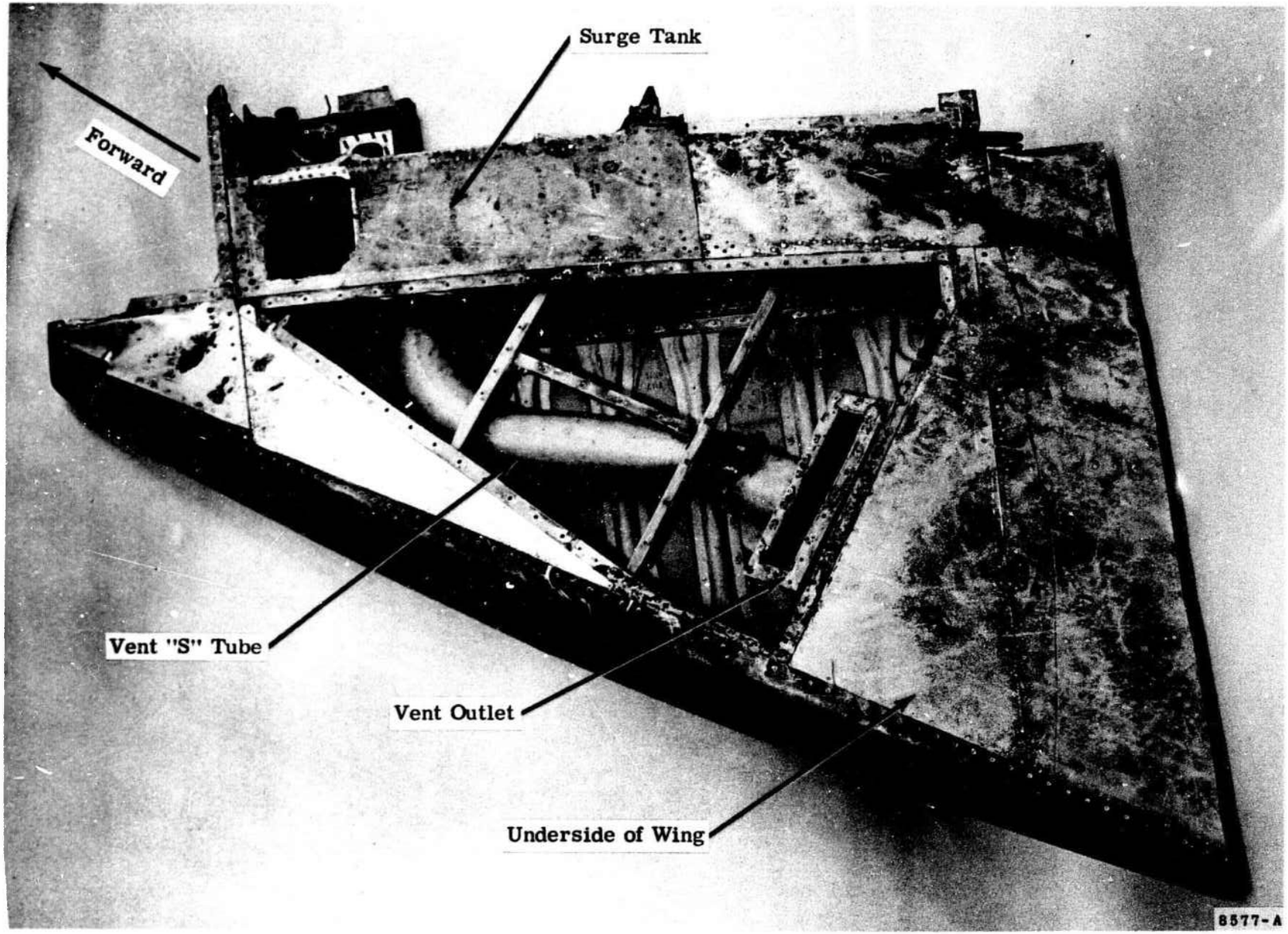

Figure 5. Right Wing Tip of Crashed 707 Aircraft.

603233

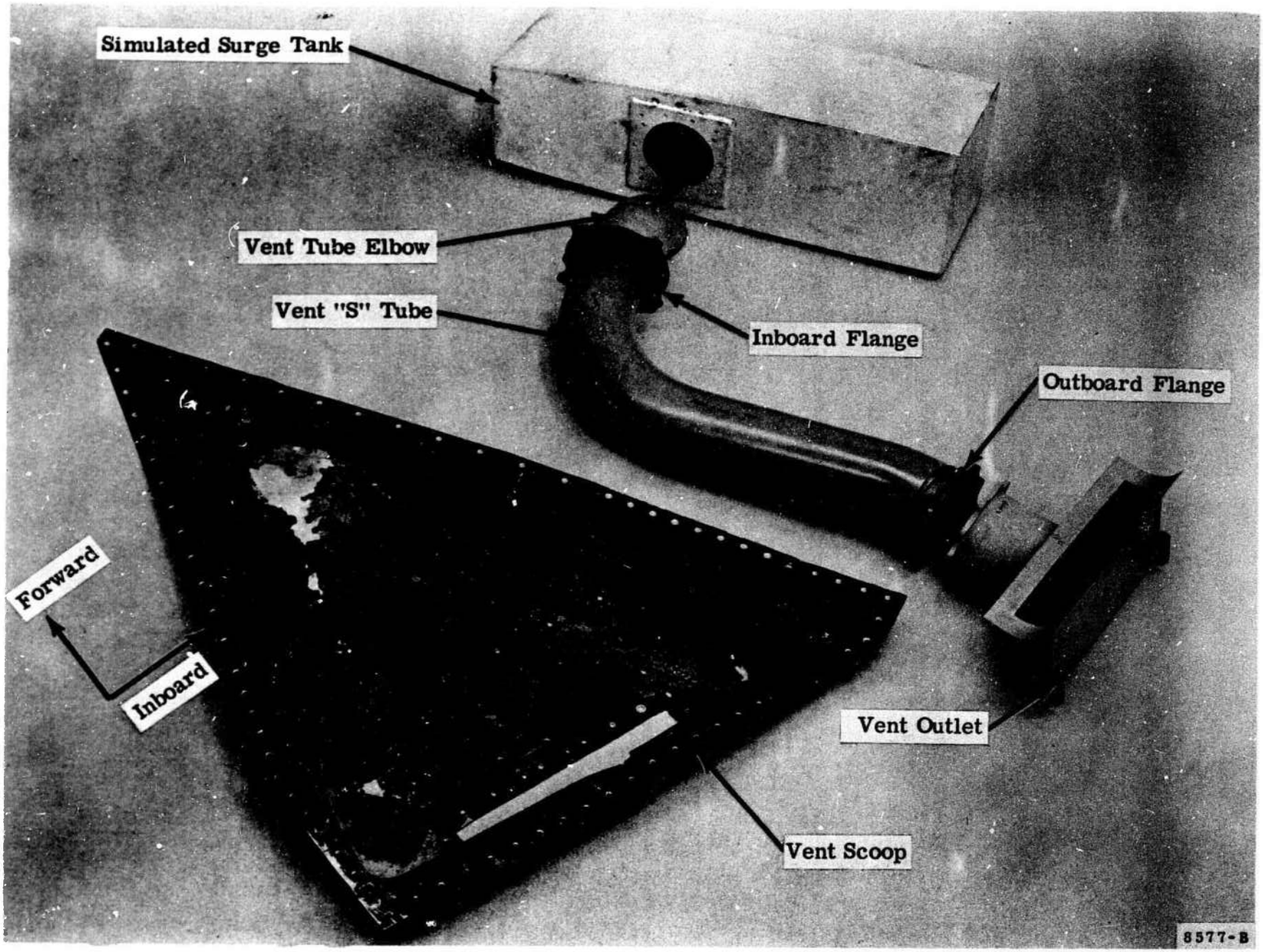

Figure 6. Vent System Components of 707 Aircraft.

In the experimental program conducted by Atlantic Research Corporation all vent components used were actual production aircraft parts supplied by the Boeing Company, except for the surge tanks which were simulated for a large portion of the testing.

3.0 EXPERIMENTAL PROGRAM

3.1 INTRODUCTION

The objectives of the experimental program were twofold. The first phase objective consisted of establishing a test environment which physically simulated conditions in the vent system during a lightning strike in the vicinity of the vent outlet. The second phase objective was to determine by testing the feasibility of two methods by which flame propagation through the vent system could be eliminated, namely flame arresters and explosion suppression. In order to accomplish these objectives, two identical assemblies of experimental apparatus were made using actual 707 vent system components instrumented to detect the presence of a flame front, measure its speed and record the pressure history in the system. One apparatus was set up at Lightning and Transients Research Institute. The tests performed there with high-energy discharges established the range of flame speeds of interest and the effectiveness of selected flame arresters. The other apparatus was used at Atlantic Research Corporation to duplicate the conditions generated by the simulated lightning. These tests increased the knowledge concerning flame propagation through the 707 vent system and the operation of flame arresters and explosion suppression systems in the 707 hardware.

It was assumed throughout the program that a combustible mixture could exist in the vent system during flight operations and that lightning, acting as an ignition source at the vent, could cause a flame to propagate through the vent system into the surge tank. Because of this basic prior assumption no attempt was made to simulate free-stream conditions at the vent outlet. This position is partially justified by earlier work[9] which showed that combustible envelopes exist near vent outlets of various types under simulated free-stream conditions. The interaction of the combustible envelope as determined by the free stream effects with the probabilities of lightning strikes in specific locations in the vicinity of the vent remains to be investigated in detail.

In addition to free stream conditions at the vent outlet, two other properties of the system have major importance in determining its flame propagating

characteristics. They are (a) direction and rate of flow through the vent system prior to ignition, and (b) properties and condition of the fuel-air mixture.

The direction and rate of flow of combustible mixture through the vent is determined by the flight trajectory, fuel tank void volume, and atmospheric conditions. In the present experiments a stagnant system was employed because it represents the most severe venting condition with regard to flame propagation. An outflow through the vent system, during a climb, would impede the progress of a flame propagating toward the surge tank. An inflow through the vent, during a descent, would aid the progress of an inward-propagating flame provided a combustible mixture were present. It is highly improbable that a combustible mixture can exist in the vent tube during an inflow, since free-stream air carries no fuel vapor. There is a possibility that the vent outlet, having been wetted by fuel spray, might constitute a source of combustible vapor during an inflow situation. However, Pan American World Airways conducted tests with 707 aircraft to determine whether fuel wetting of the vent outlet occurred during severe skidding turns. They concluded that no visible discharge of fuel occurred and that there was no evidence of fuel stain near the vent outlet.[12] It follows then that the stagnant system represents the most hazardous state in which flame propagation is possible.

The fuels used in jet aircraft are usually paraffinic hydrocarbons. The nature of the combustion process in the vapor of these compounds is such that their pertinent combustion properties are nearly independent of their molecular weight. For example, the heat of combustion per gram, flame temperature, quenching distance, burning rate, and lean limit of combustion for the various paraffins are nearly equal.[6] For this reason, it is possible to employ any of the higher homologs of the paraffin series. Propane (C_3H_8) is readily available and easily manipulated in the gaseous state and hence was used in this program. Table 3 summarizes the properties of propane.

There is little doubt that conditions do arise in which the various jet fuels will provide combustible atmospheres in the fuel tanks. The choice of fuel may reduce the frequency of occurrence of hazardous conditions but will not eliminate their possibility. Some question exists as to the physical nature of the

Table 3. Combustion Properties of Propane.

Heat of Combustion (298°K), kcal/gm-mole	530.6
Limits of Inflammability in Air (% by volume), per cent	
Lower	2.2
Upper	9.5
Flame Temperature (stoichiometric in air, STP), °C	1925
Quenching Diameter[a], inches	0.11
Minimum Spark Ignition Energy[a], millijoules	0.27
Critical Velocity Gradient for Flashback[a], sec^{-1}	600
Laminar Flame Speed[a], cm/sec	40

NOTE: The combustion of propane and oxygen is written as:

$$C_3 H_8 + 5O_2 \rightarrow 4H_2O + 3CO_2$$

For every mole of propane consumed, 5 moles of oxygen are required for complete combustion with no residual oxygen. Thus, 44.09 gm of propane require $5 \times 32.00 = 160$ gm of oxygen or 691.44 gm of air which is 23.14 per cent by weight oxygen. Hence, the weight of air to weight of propane required for stoichiometric burning (i.e., complete combustion of propane with no excess oxygen) is $\frac{691.44}{44.09} = 15.7$. A 1.15 fraction of stoichiometric mixture of air and propane has an air-to-fuel weight ratio of $\frac{691.44}{1.15 \times 44.09} = 13.7$.

[a] Applicable to 1.1 stoichiometric propane-air at STP.

combustible atmosphere during in-flight conditions. It is possible that fuel may be dispersed as an aerosol or as poorly mixed vapor pockets or stratified layers. This lack of information is of little importance to the present work because the premixed gaseous mixture used for these experiments represents the most stringent fuel condition for flame quenching. That is, the physics of flame propagation in aerosols demands that the quenching distance for a channel be larger than that of a vapor-air mixture of the same proportion and composition. Hence a flame arrester which stops a flame supported in a gaseous mixture can be expected to stop a flame in an aerosol of the same composition.

In order to accomplish the two tasks of the experimental program the work was organized into four major activities:

1. Flame propagation studies
2. Flame arrester tests
3. Flame suppression tests
4. Plasma and blast measurements

Each of these is discussed in turn in the following sections.

3.2 FLAME PROPAGATION STUDIES

3.2.1 General

The purpose of these tests was to measure flame speed and pressure in the Boeing 707 vent system during a simulated lightning strike in the vicinity of the vent outlet. This information was useful in establishing the mechanism of flame propagation through the vent system. Experiments were performed using three types of ignition sources. Two of these sources were simulated lightning strikes furnished by Lightning and Transients Research Institute. The two facilities at Lightning and Transients Research Institute, as described earlier in this report, furnish electrical discharges with peak currents and peak current rates of rise characteristic of severe lightning strokes. These facilities simulate the characteristics and effects of lightning to the best extent available within the state of the art.

In an effort to simulate the results of the tests at Lightning and Transients Research Institute and also to provide a laboratory method to facilitate testing of flame arresters and explosion suppression systems, Atlantic Research Corporation developed a drive-tube assembly with a spark igniter described in Section 3.2.4.

3.2.2 Flame Propagation Studies Using High-Current Facility

3.2.2.1 Apparatus - A schematic diagram of the vent system and surge tank is shown in Figure 7. This diagram shows the locations of the pressure transducers and thermocouples for all testing performed in the program, both at Lightning and Transients Research Institute and Atlantic Research Corporation. The drive tube and "stand-off" sections were used only at Atlantic Research Corporation.

The time responses of the thermocouples are used to estimate flame speed. The chromel-alumel thermocouple junctions are suspended in the vent tube by means of insulating spacers which are attached to sealing glands. The glands are screwed into mounting pads which are welded to the vent tube surface. The outputs of the thermocopules are fed to R-C circuits whose function is to attenuate low-frequency signals. The outputs of these circuits feed galvanometers on a direct recording oscillograph manufactured by Consolidated Electrodynamics. Experimental evidence shows that the thermocouple response time is faster than 8 msec. In order to determine the response time of the thermocouple, the following experiment was performed.

A thermocouple and ion probe were mounted in an insulating spacer as shown in the sketch.

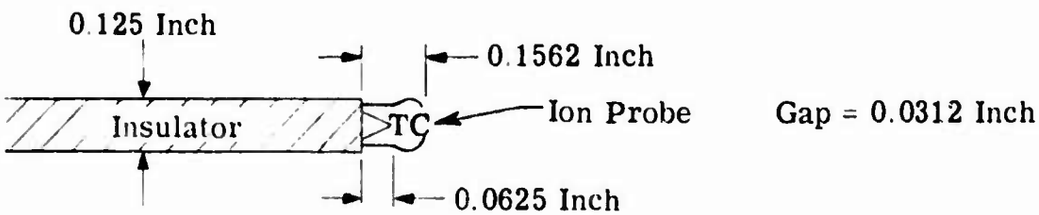

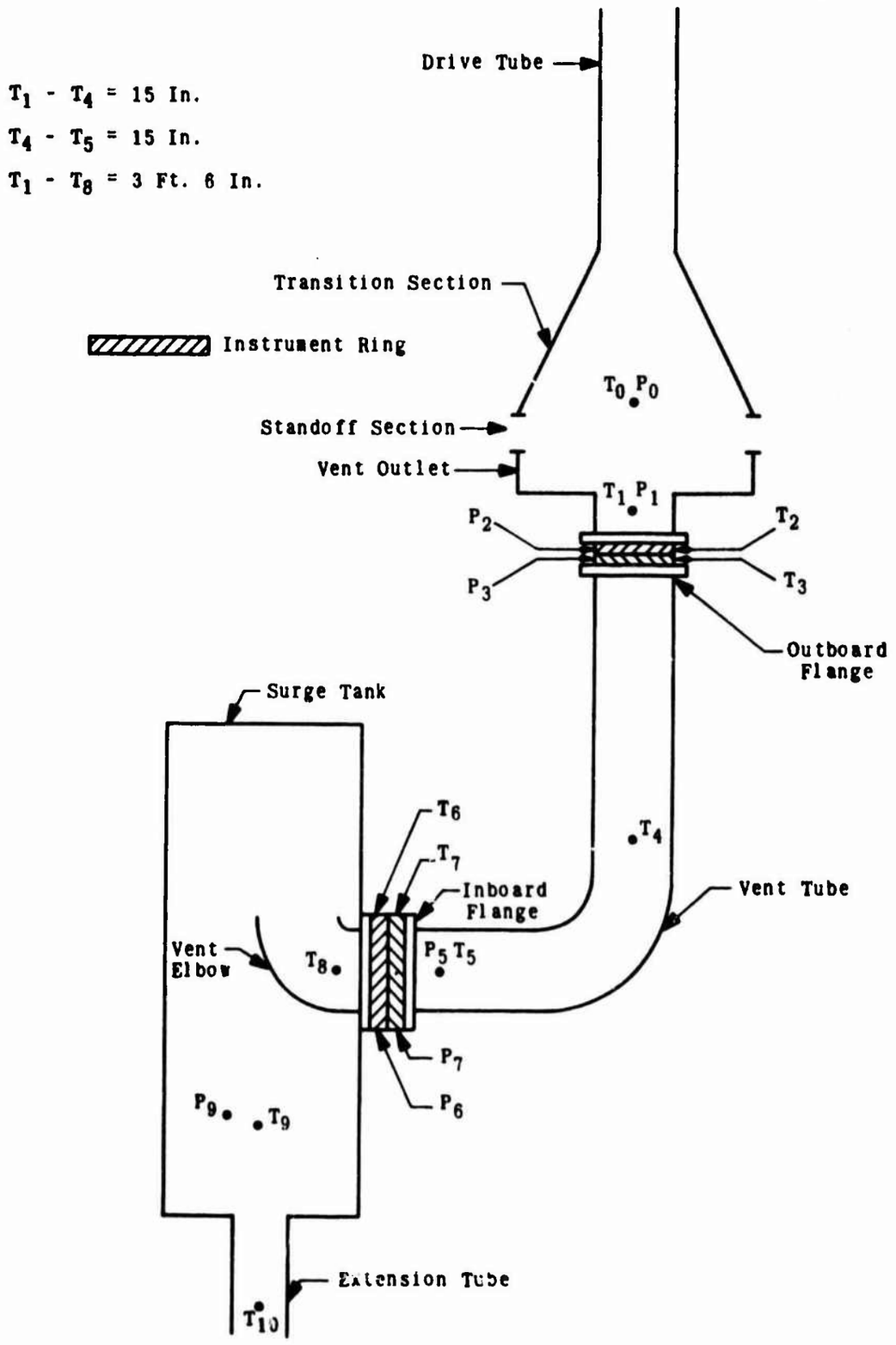

Figure 7.. Schematic Diagram of Test Apparatus Showing Instrument Location.

A 90-volt potential drop across the ion probe was applied. The outputs of the ion probe and thermocouple were fed to two galvanometers on an oscillograph. The ion gauge and thermocouple were then simultaneously bathed in the reaction zone of a propane flame. The estimated velocity range for the propane torch used was 50 to 150 ft/sec. It is important to duplicate the range of interest since the time response of the thermocouple is proportional to $(Re)^{-0.8}$ and the response time will vary for different gas velocities past the thermocouple junction. The average of 8 tests showed that the TC response lagged that of the ion probe by 7.9 msec.

The pressure transducers are temperature-compensated to 250°F and have an operating range of 0-25 psig. The transducers are mounted to the vent tube with flexible tubing in order to reduce mechanical coupling. The outputs from the transducers are amplified by Kintel amplifiers and then fed to the galvanometers of the recording oscillograph. The transducers are calibrated with a standard pressure gauge using compressed air. The excitation voltage for the transducers is supplied by a Video Instrument Inc. power supply. In this system it is estimated that the pressure transducers will faithfully follow a pressure wave whose rise time is greater than 0.15 msec. A schematic diagram of the electrical system is shown in Figure 8.

The fuel-air mixture is supplied from bottles of liquid propane and compressed air. After pressure reduction and metering the propane and air are mixed and led to the vent system. The supply rate was approximately 0 21 ft^3/min as measured by calibrated rotameters. The volume of the vent tube and inlet duct is approximately 0.6 ft^3. The residence time is therefore 3 minutes. The system was purged with the prescribed fuel-air mixture for 20 minutes to ensure that the residual air had been displaced. Figure 9 is a schematic diagram of the fuel-air supply system for Lightning and Transients Research Institute tests.

In order to isolate the vent system during the filling operation the vent inlet was sealed with a commercial brand of transparent wrap. The discharge probe was mounted within the region in which combustible gases were

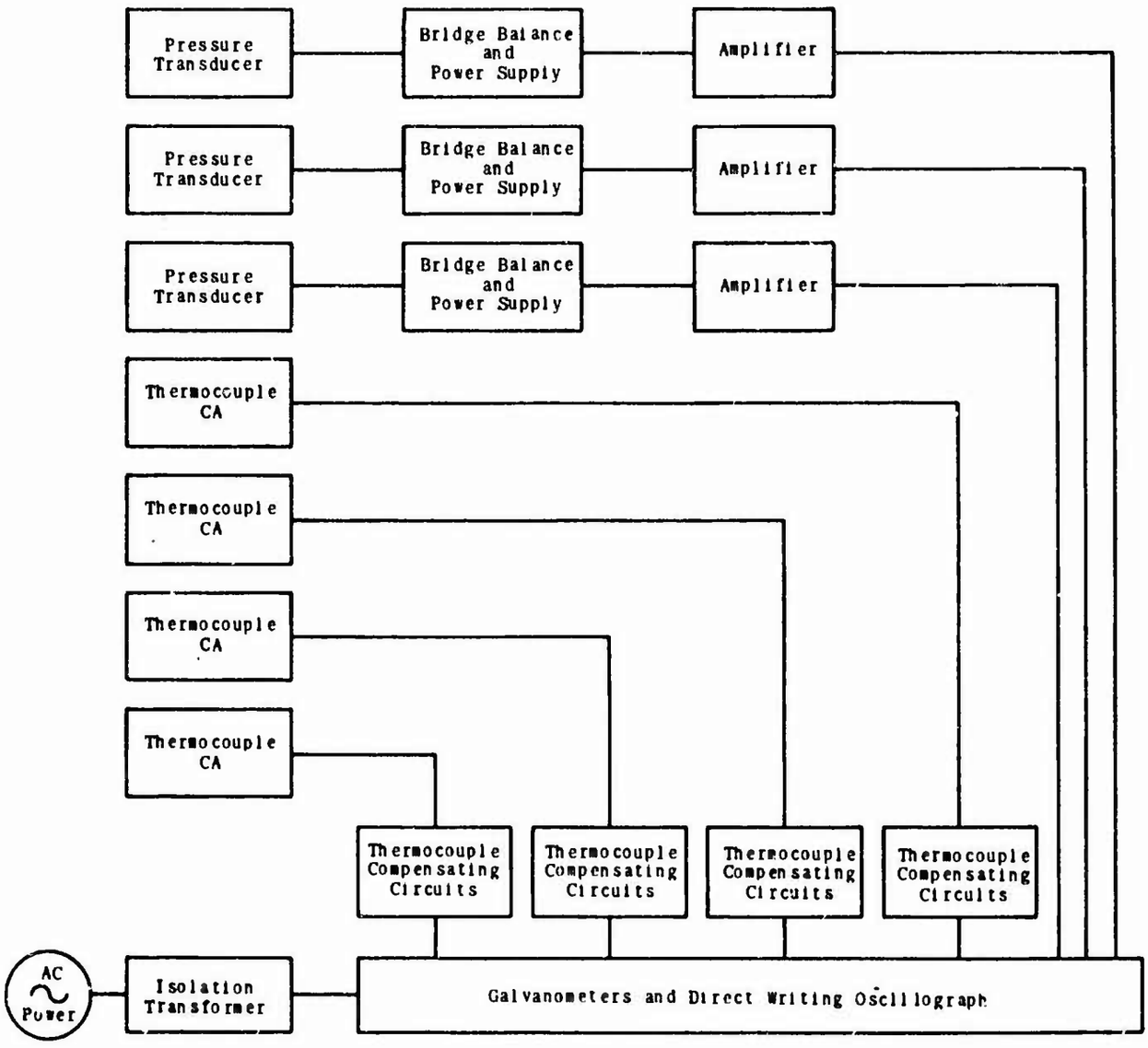

Figure 8. Block Diagram of Electrical Instrumentation.

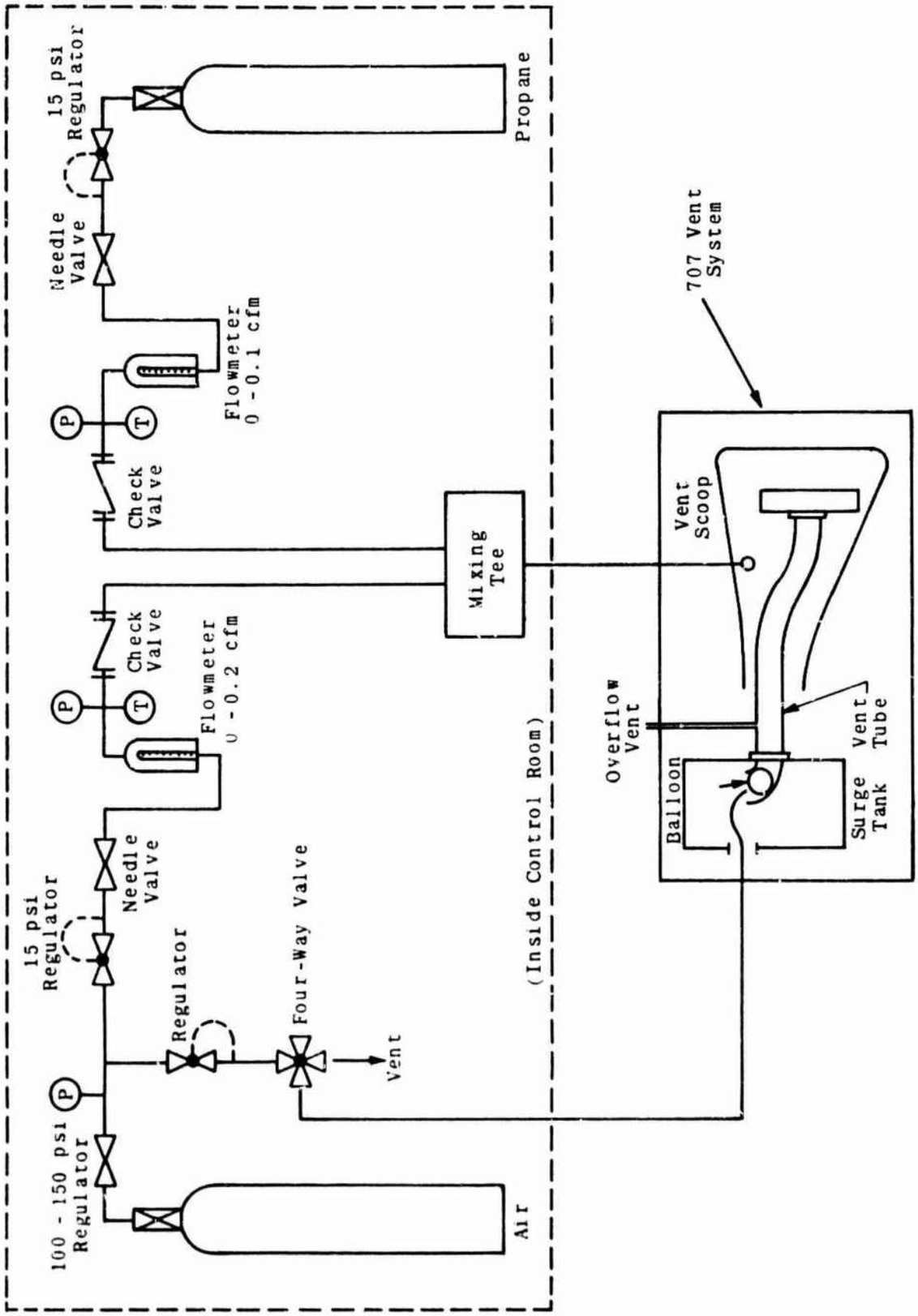

Figure 9. Schematic Diagram of Fuel-Air Supply System for Lightning and Transients Research Institute Tests.

present. The surge tank elbow was blocked with an inflated balloon. Just prior to ignition the balloon was deflated. This allowed simulation of the actual vent and surge tank configuration while limiting the total volume of combustible mixture. The surge tank was vented through an 8-inch diameter hole in the side.

The vent tube, vent outlet, and mock surge tank were installed in a 707 wing tip which had been supplied for test purposes. The wiring and fuel-air supply lines were led through conduit to the control room in which the fuel supply and read-out instrumentation were housed. The entire control room and wing tip section were electrically isolated from ground in order to prevent detrimental effects to instrumentation caused by induced transients from the simulated lightning discharge. Power for the instrumentation was supplied through isolation transformers. Figure 10 is a photograph of the experimental setup at the Lightning and Transients Research Institute High-Current Facility.

The simulated lightning discharge, supplied by Lightning and Transients Research Institute, was obtained by charging a bank of capacitors whose total capacitance was 366 mf. The maximum voltage obtained was 25 kv which gave rise to peak currents of the order of 250,000 amperes and charge transfers of 9 coulombs. A grounding strap terminated with a mounting bracket was placed at the selected point of discharge near the vent outlet. The discharge probe was located near the mounting bracket within a distance smaller than the breakdown distance of air at the prescribed voltage. In some tests, a piece of aluminized tape (4 inches long × 0.375 inch wide × 0.003 inch thick) was stretched from the discharge probe to the grounding bracket. The explosion of the tape provided higher pressures at the vent outlet than direct discharges of equal voltage. To trigger a discharge, the discharge probe was connected to the bank of capacitors by a mechanical switch. In all cases the discharge occurred within the fuel-air envelope. Figure 11 shows the positioning of the elements described above.

3.2.2.2 Results and Discussion - Eighteen tests with the fueled system were executed. The experimental variables were the following:

1. Type of discharge
2. Point of discharge
3. Voltage of discharge
4. Air to fuel ratio

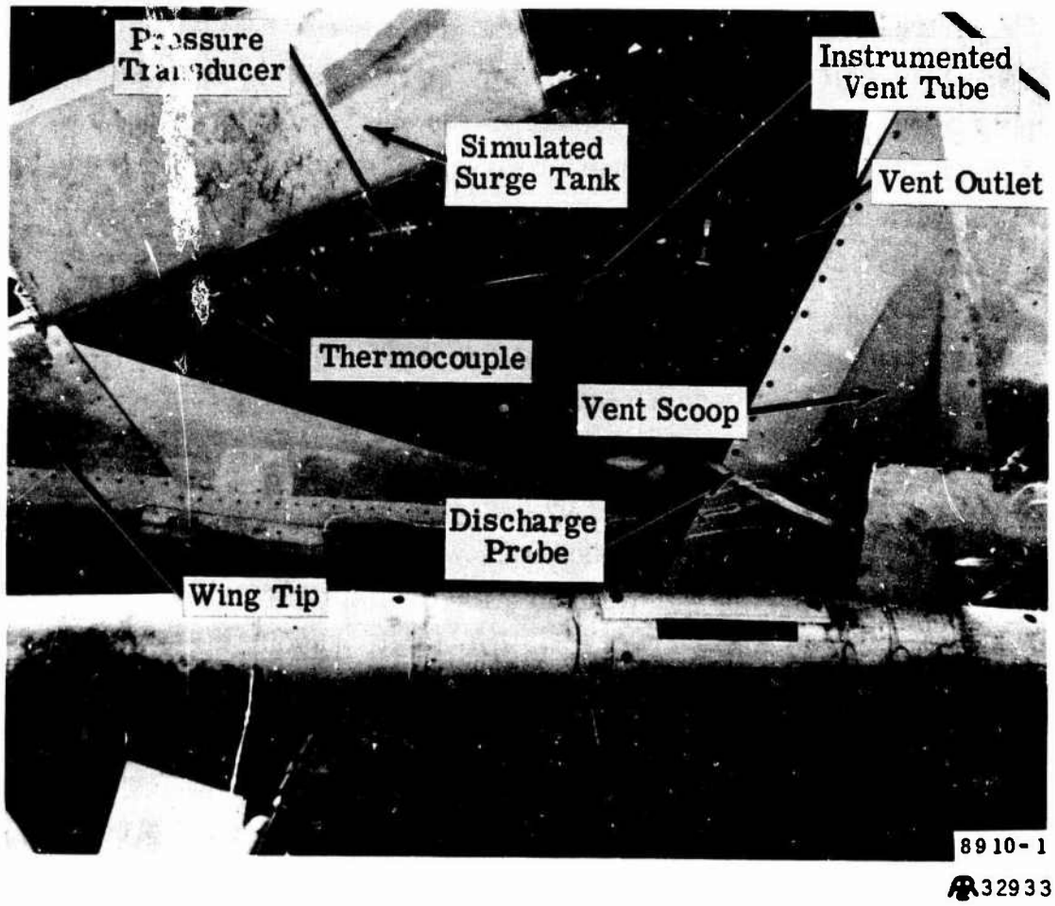

Figure 10. Experimental Apparatus at Lightning and Transients Research Institute High-Current Facility.

603233

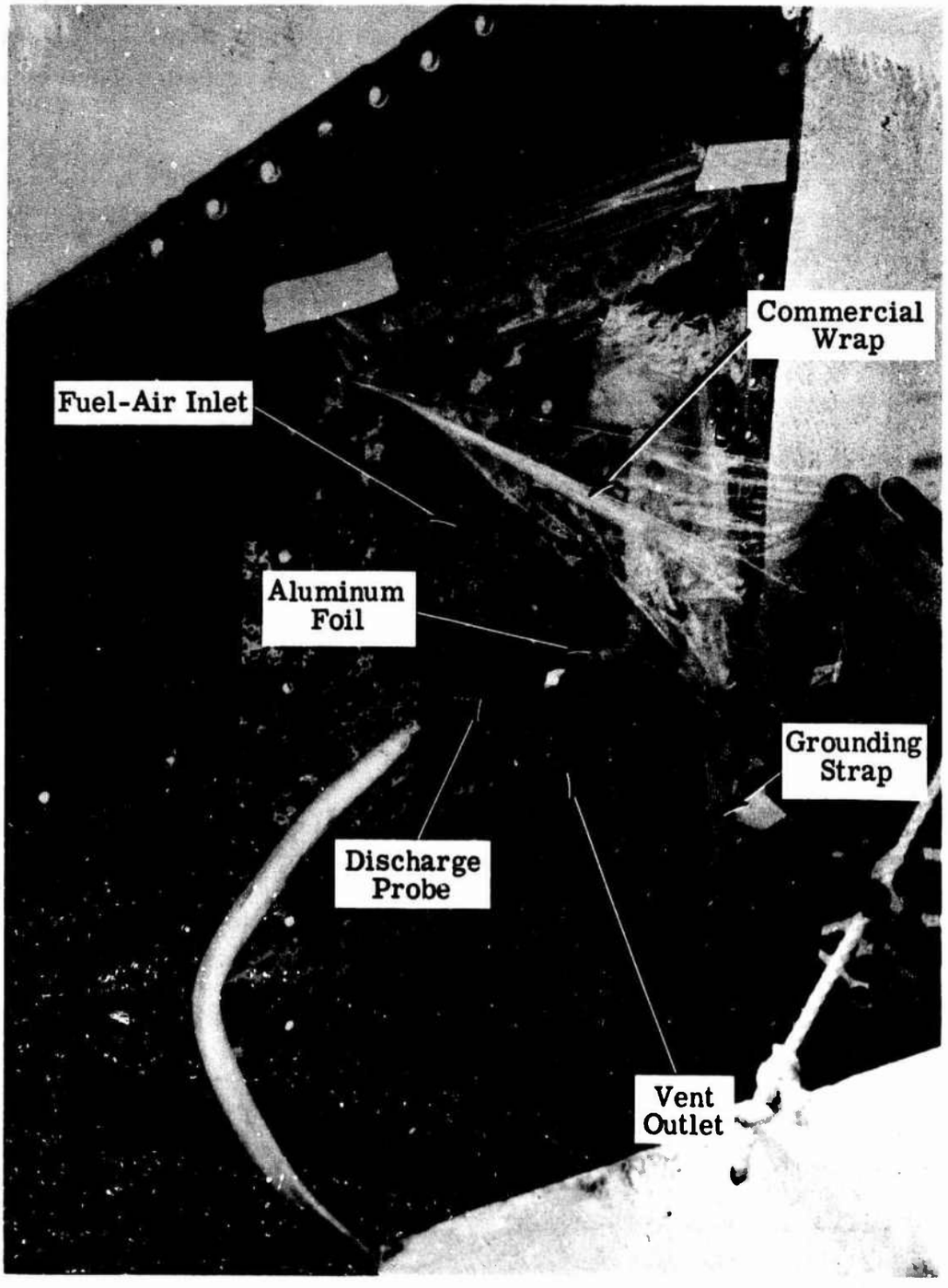

Figure 11. Position of Components for Lightning and Transients Research Institute High-Current Tests.

603233

The discharge was either direct or through the 4-inch aluminized tape. Personnel at Lightning and Transients Research Institute suggested that the tape discharge would provide a closer representation of the pressure wave emanating from a lightning strike.

The position of discharge was located at one of seven positions. Figure 12 shows the various positions (A - G) of discharge. Strikes directed to the edge of the vent outlet should represent the most severe ignition source and driving force. Those directed at the raised portion of the vent scoop should be less severe because of the larger separation from the vent outlet.

The discharge voltage was varied in a range from 5 kv to 25 kv giving peak currents up to 250 kiloamperes. Figure 13 shows the current waveforms of a 15 kv direct discharge and a 15 kv discharge through a 4-inch strip of aluminized tape.

In several tests the fuel-air mixture was varied from 70 per cent of stoichiometric to 150 per cent of stoichiometric based on propane weight. It is known that a slightly fuel-rich mixture (i.e., 115 per cent of stoichiometric) exhibits the minimum quenching distance in tubes. For this reason most tests were conducted using this mixture ratio.

Table 4 summarizes the results of the flame speed and pressure simulated measurements in the vent duct system, and establishes the response to be expected from lightning ignition in the 707 vent.

The following observations may be made:

1. For a given discharge point, an increased voltage results in an increased peak pressure.

2. The tape discharge gives higher pressure peaks and higher flame speeds than a direct discharge of the same voltage and position.

3. The pressures measured "downstream" (i.e., P_5) are larger than those measured "upstream" (i.e., P_1). The pressure measured in the surge tank are relatively small.

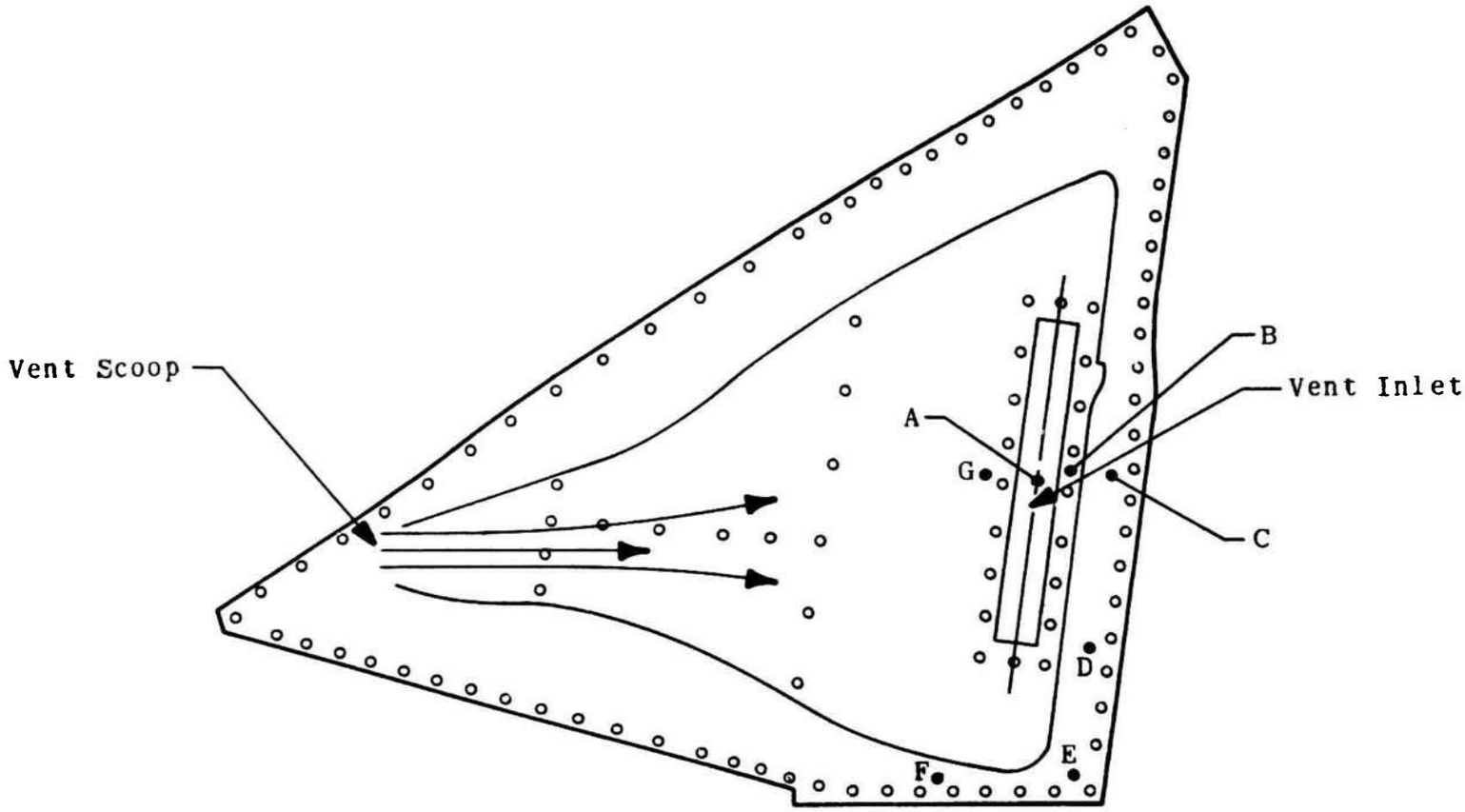

Figure 12. Location of Discharge Point at Lightning and Transients Research Institute High-Current Facility.

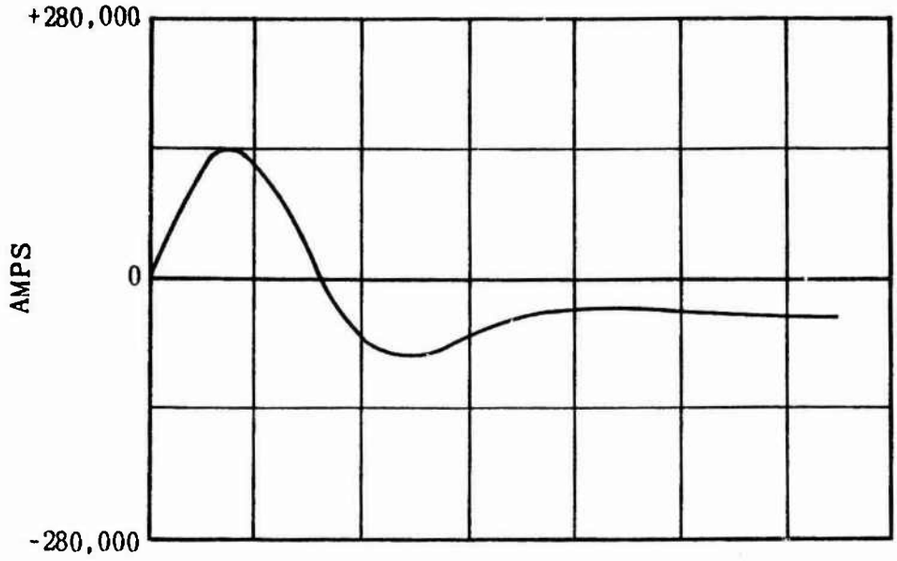

50 MICROSECONDS PER DIVISION

Four-Inch Aluminized Tape Discharge

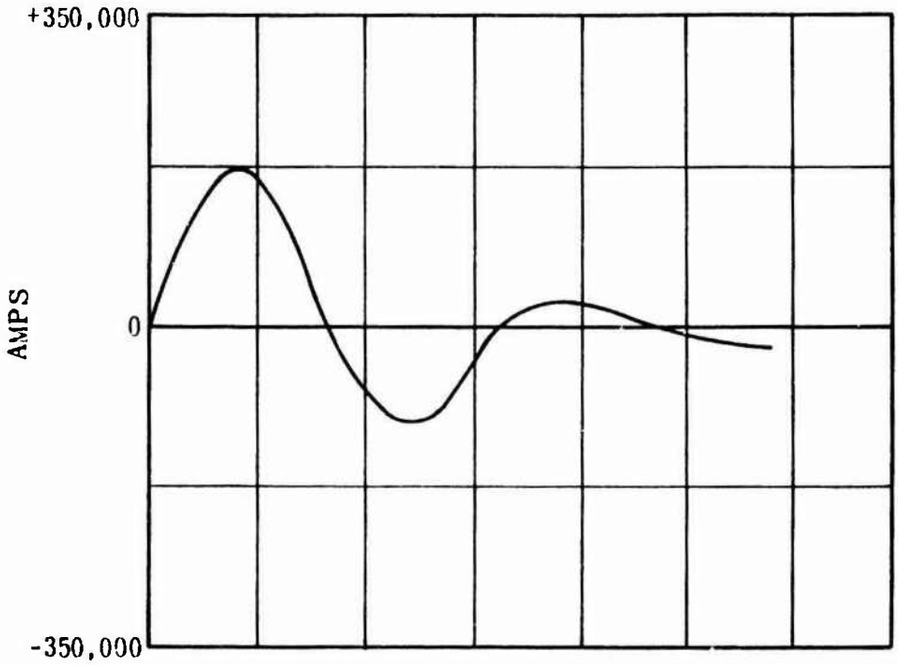

50 MICROSECONDS PER DIVISION

Direct Discharge

Figure 13. Current Waveforms of Lightning and Transients Research Institute 15 kv Discharge.

Table 4. Results of Flame Propagation Studies at High-Current Facility.

Discharge Point	Mixture Fraction of Stoichiometric	Discharge Voltage (kv)	Pressure (psig)			Flame Speed (ft/sec)		
			P_1	P_5	P_9[b]	1st Half	2nd Half	Average
A[a]	1.15	10 (tape)	6.1	6.2	1.0	40	73	52
A	1.15	10 (tape)	6.9	9.3	2.0	96	125	108
B[a]	1.15	5 (tape)	3.7	3.8	1.2	33	26	29
B	1.15	10 (tape)	3.7	6.2	1.2	37	42	40
B	1.15	15 (tape)	5.1	9.4	2.3	54	83	66
B	1.15	20 (tape)	5.0	10.8	2.4	89	156	114
B	1.15	10 (direct)	3.0	2.7	1.0	16	18	17
C	1.15	20 (tape)	5.0	8.1	2.6	37	50	43
C[a]	1.15	25 (tape)	10.6	14.6	2.6	415	83	139
D	1.15	25 (tape)	3.7	15.7	3.1	?[c]	?[c]	?[c]
E	1.15	15 (tape)	3.1	3.7	1.0	13	31	18
E	1.15	25 (tape)	1.8	8.1	1.8	42	62	50
F	1.14	15 (tape)	6.3	2.6	1.1	10	47	16
G	1.15	15 (direct)	5.0	3.4	0.8	18	19	18
G	1.00	15 (direct)	5.0	5.0	1.0	27	37	32
G	0.90	15 (direct)	3.1	3.8	0.9	13	137	24
G	0.80	15 (direct)	5.0	5.0	1.1	14	31	20
G	1.50	15 (direct)	4.9	5.2	1.2	31	18	23

[a] Strip charts for these tests are shown in Figures 14, 15, and 16.

[b] See Figure 7 for location of instrumentation.

[c] Instrumentation was broken.

4. The average flame speeds attained exceed the laminar burning velocity of propane-air mixtures (1.4 ft/sec) by factors up to 100.

5. In most cases the zone of combustion accelerates in the direction of motion.

6. The average flame speed increases with increasing peak pressure and increasing discharge voltage.

7. There is no obvious correlation between peak pressure, flame speed, and discharge location.

8. Variation of the mixture ratio from 0.80 to 1.50 fraction of stoichiometric has little effect on pressure or flame speed.

Figures 14, 15, and 16 are temperature and pressure histories of three typical tests. Figure 17 shows the pressure history of a discharge into an unfueled system. Three general observations can be made concerning the pressure response of the system:

1. The initial pressure disturbance propagates down the vent tube in 3 to 4 msec. This time interval corresponds to sonic velocity.

2. The cyclic variation of the pressure suggests that a standing wave is established which subsequently is damped. The period T of the oscillation is approximately 6 msec. An open-ended organ pipe 2.5 feet long would oscillate with a fundamental frequency of $f = c/2L$, where f = cycles per second, L = effective organ pipe length, and c = velocity of sound.

$$T = \frac{1}{f} = \frac{2L}{c} = \frac{7.0}{1140} = 6.13 \text{ msec}$$

For the tape discharges the pressure P_5 (measured at the inboard flange) is usually greater than P_1 (measured near the vent outlet).

3. The pressure response of the system depends primarily on the characteristics of the discharge, and not on the combustion process.

These observations and data are further discussed in Section 3.4.

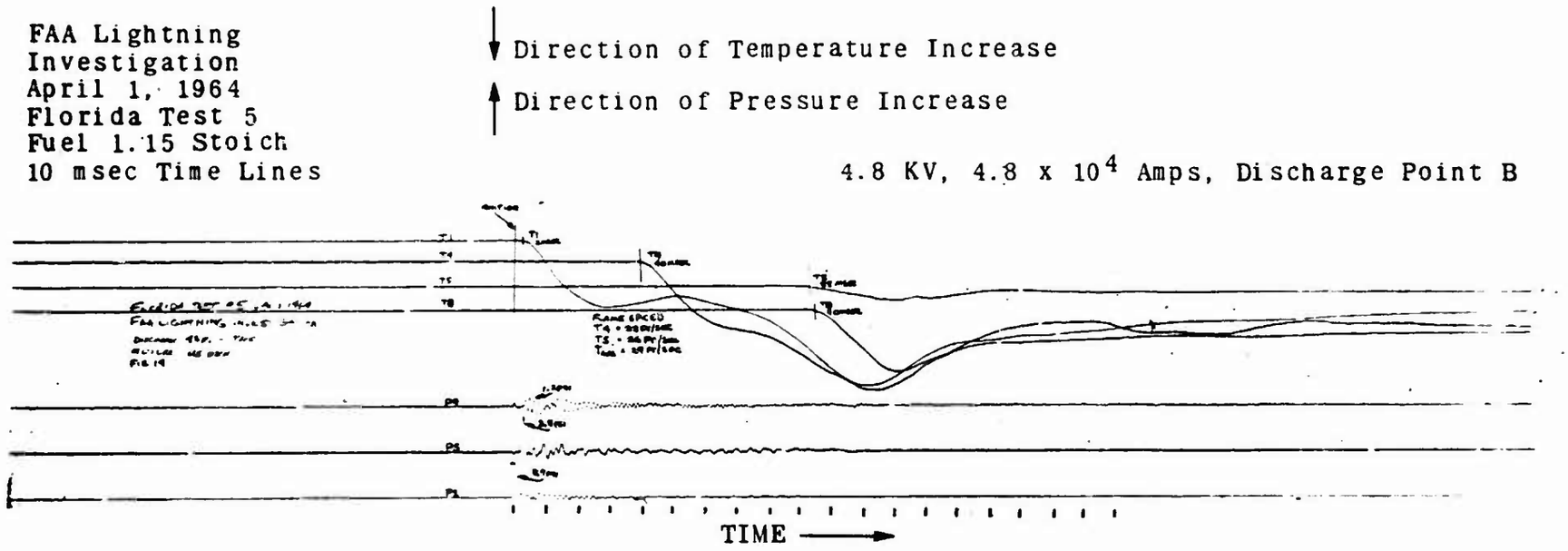

Figure 14. Flame Progagation Test at High-Current Facility.

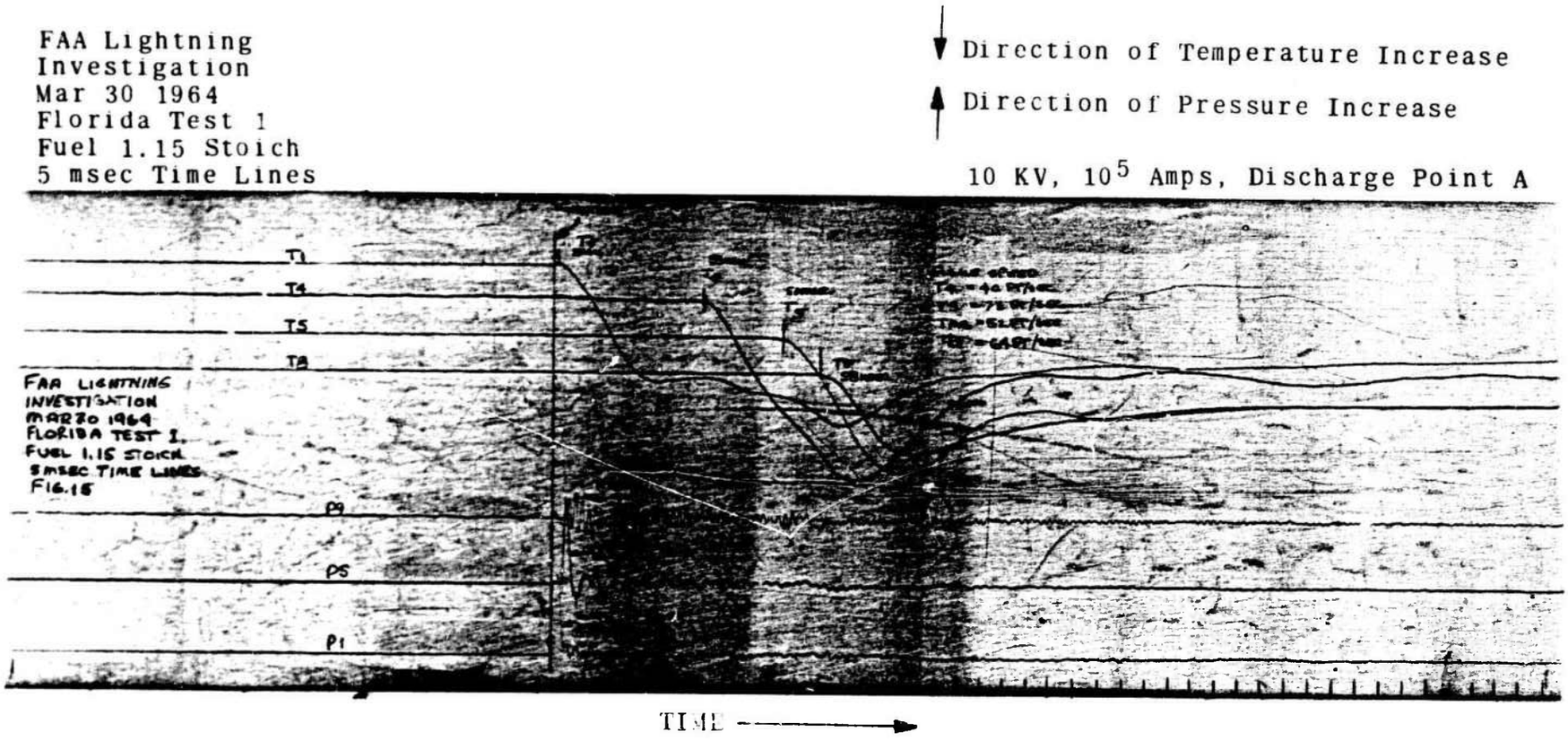

Figure 15. Flame Propagation Test at High-Current Facility.

60233

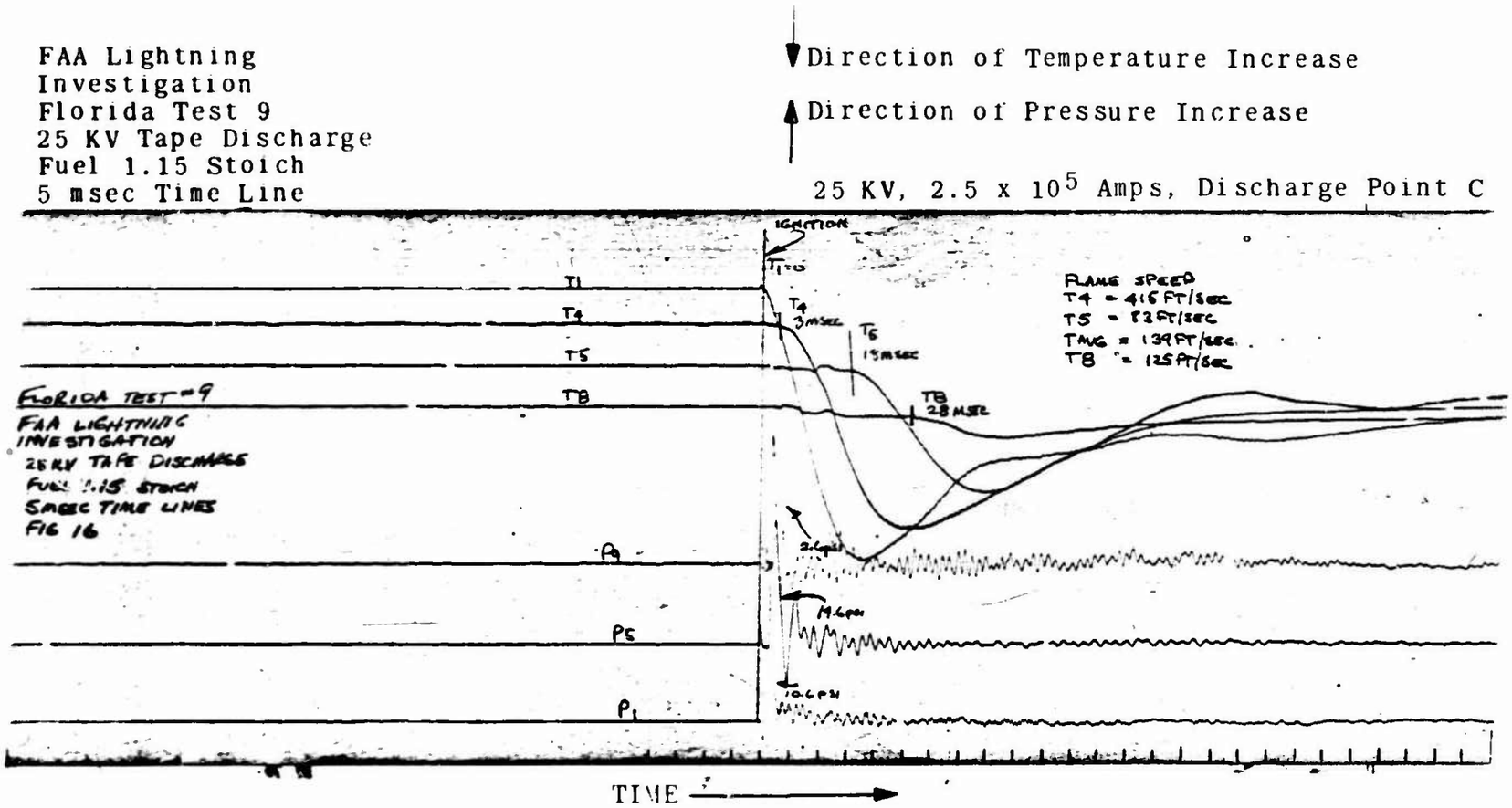

Figure 16. Flame Propagation Test at High-Current Facility.

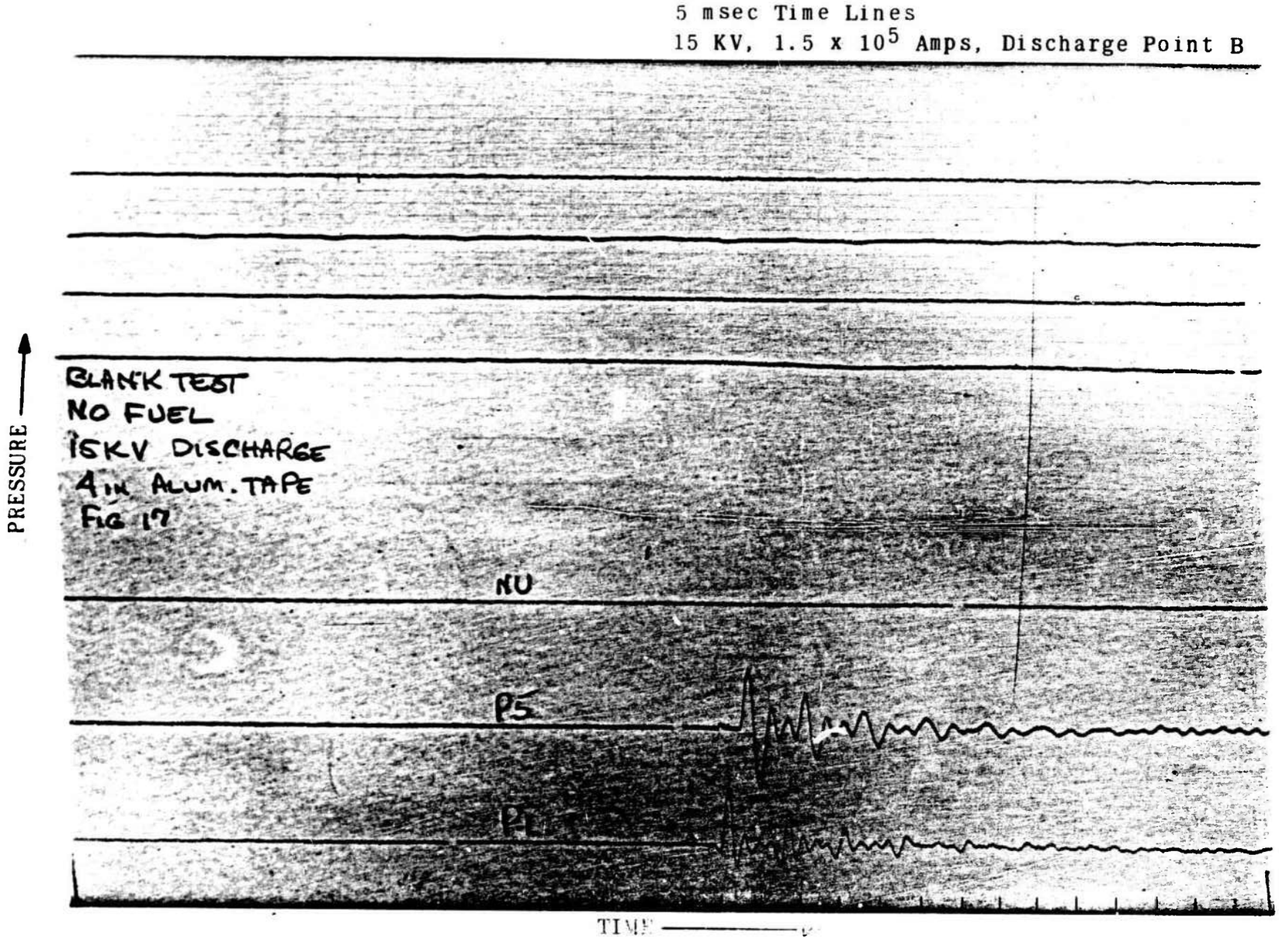

Figure 17. Pressure Response of Unfueled System at High-Current Facility.

AD-A33 33

3.2.3 Flame Propagation Studies Using High-Voltage Facility

3.2.3.1 Apparatus - The high-voltage facility of Lightning and Transients Research Institute is capable of generating potentials of 10 million volts, with peak currents up to 100,000 amperes. The characteristic which distinguishes this facility from the high-current facility is the increased current rate of rise, as discussed earlier in this report. Figure 18 shows the current waveform of a nominal 1,000,000-volt discharge.

The apparatus employed was essentially the same as described earlier, with one exception. The vent tube, surge tank, and air scoop panel were installed in an aluminum box. The box served the same purpose as the wing tip; merely as a support structure and electrostatic shield. Because of the higher voltage available, longer discharge paths could be used. However, the position of the strike could not be predetermined as in the case of the lower voltage facility. For this reason, photographs of the discharge were obtained. The camera was synchronized with the triggering mechanism of the generator. Figures 19 and 20 are photographs of the discharge probe before and during a discharge.

In order to protect the sensitive instrumentation, power was supplied internally from a gasoline-powered 110v - 60 cycle AC generator. Thus, the control room was "floating" at the same potential as the vent tube housing, effectively reducing the amplitude of induced electrical transients.

3.2.3.2 Results and Discussion - Seven tests were conducted using the high-voltage discharge as an ignition source. The distance from the discharge probe to the face of the vent outlet was variable. A 1.15 fraction of stoichiometric mixture was employed. The discharge voltage was nominally 1,000,000 volts.

It is important to realize that although the series capacitance of the Lightning and Transients Research Institute facility may be cascaded to 1,000,000 volts or more, the discharge probe will begin to discharge when the breakdown voltage gradient in air is exceeded. Lightning and Transients Research Institute measurements have shown that the breakdown voltage for their particular probe is approximately 1,000,000 v/m, a value about 1/3 that for sphere gaps under ideal laboratory conditions. The present experiments were performed with gap

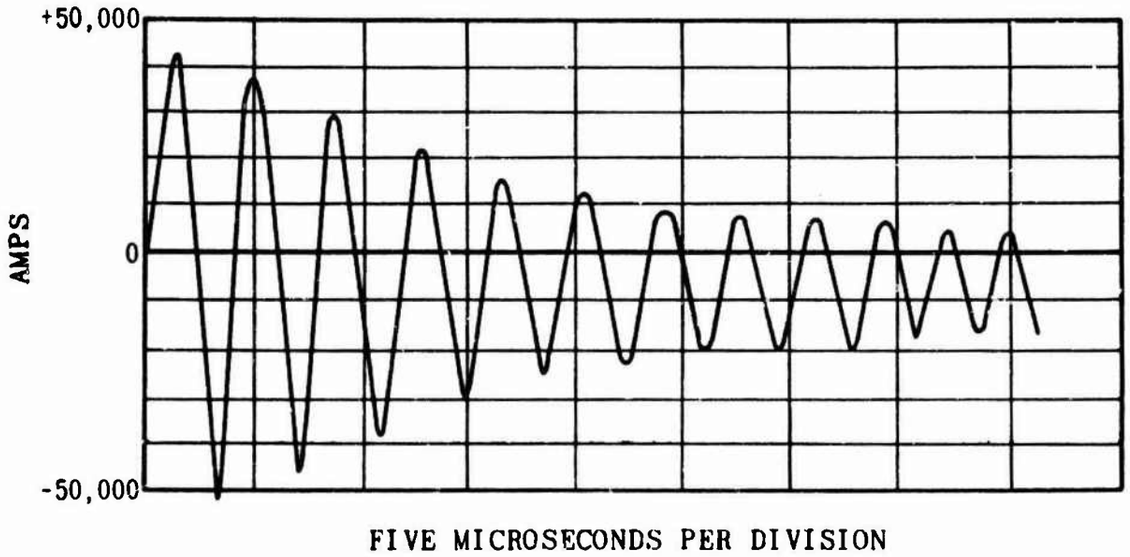

Figure 18. Current Waveform of Nominal 1,000,000-Volt Discharge of High-Voltage Facility.

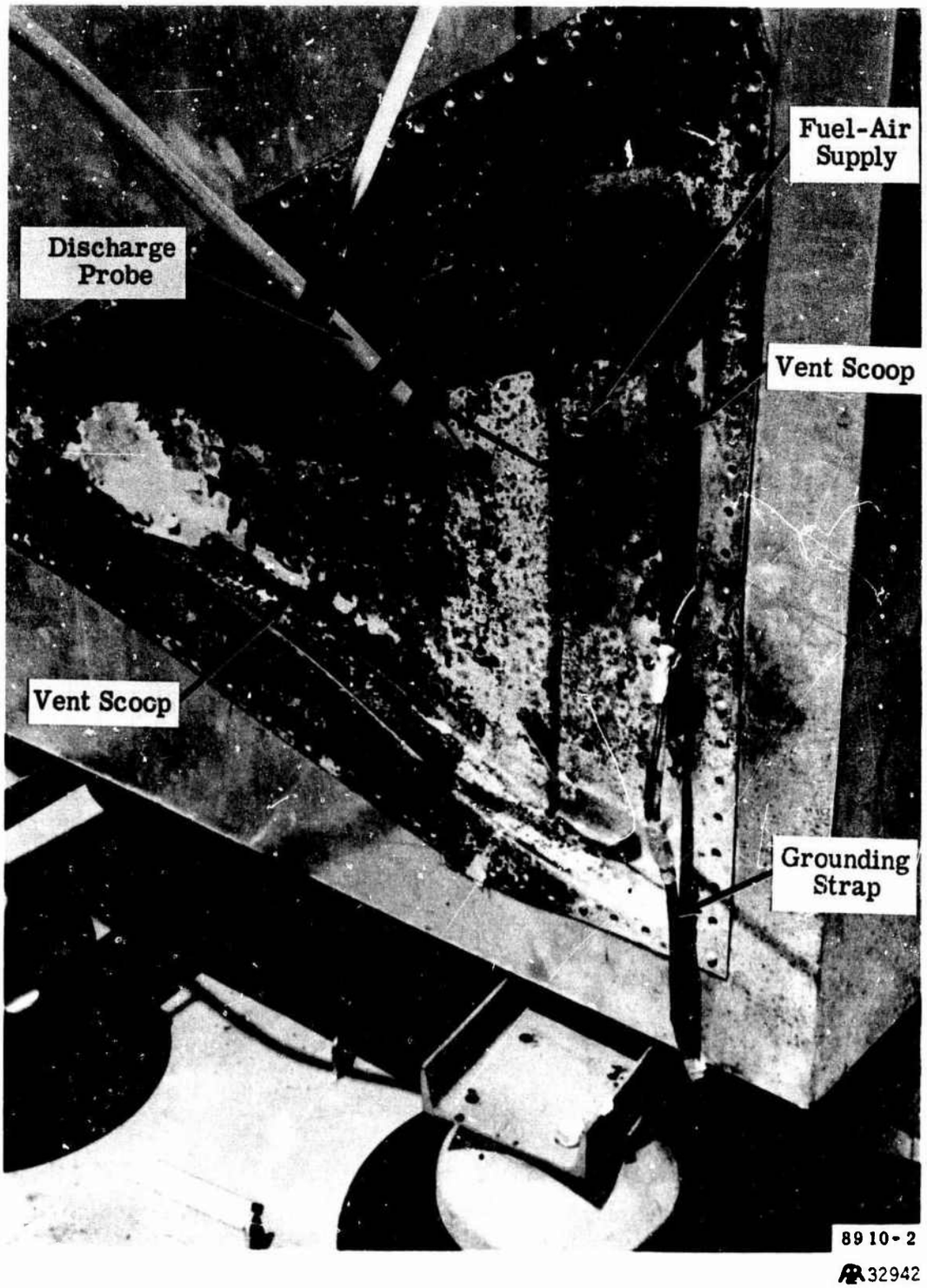

Figure 19. Location of Discharge Probe for High-Voltage Test.

603733

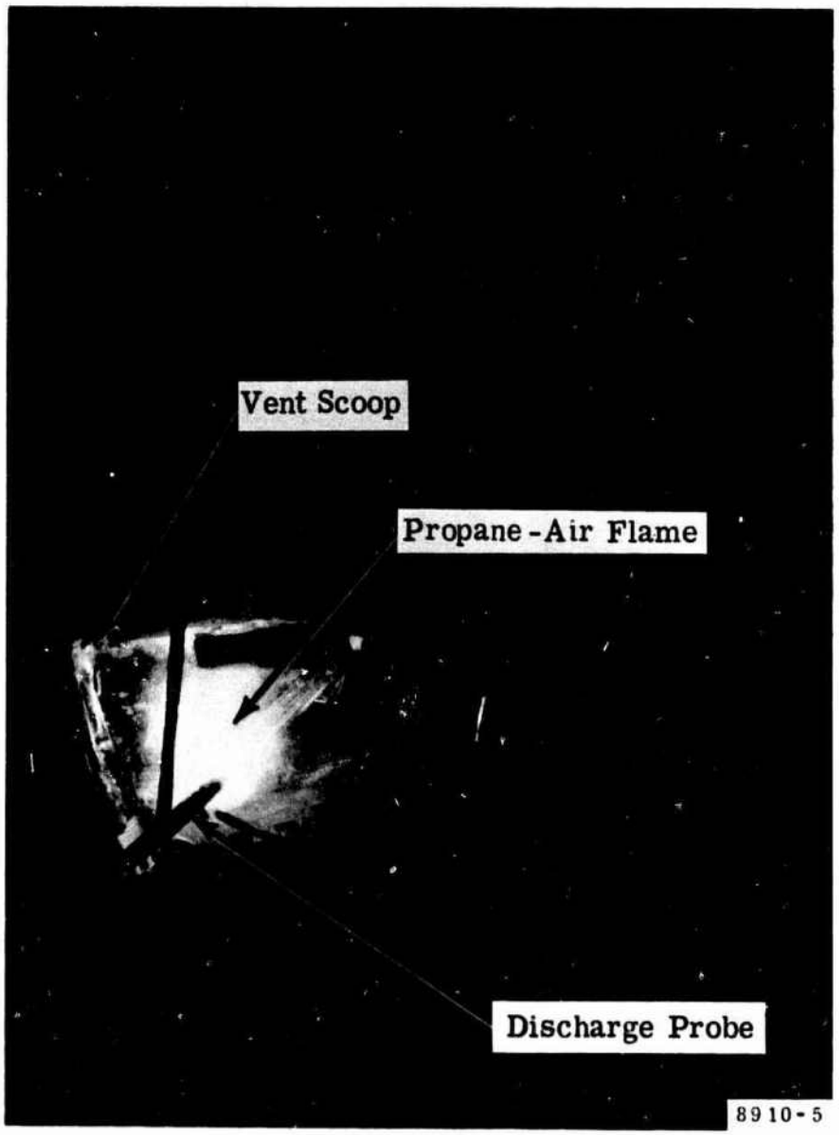

Figure 20. Discharge During High-Voltage Test.

603233

distances of 5 inches or 12 inches. Thus for a 5-inch and 12-inch discharge the peak probe voltages are estimated to be 128,000 volts and 325,000 volts respectively; these values are independent of the capacitance voltage available except for the small effect of voltage overshoot which depends on the initial rate of rise.

In order to actually attain a million volts on the probe, the air gap separation must be a meter or more. With such a large distance one could never be sure whether the strike would be in the vicinity of the vent outlet. Intuitively it is felt that for discharge lengths much greater than the characteristic vent outlet dimensions variation in discharge length should have a relatively small effect on pressure and flame speed. For further discussion of these points see Appendix A.

The results of these high-voltage tests are summarized in Table 5. Figure 21 is a typical time history of the pressure and thermocouple response after a nominal 1,000,000-volt discharge. The following observations may be made:

1. The peak pressures are less than 1 psig, relatively smaller than those measured in the high-current facility.

2. The average flame speeds, being less than 20 ft/sec, are slower than those recorded in the high-current facility.

3. During the time in which flame is propagating through the vent tube the pressure throughout the system is quiescent and equal to ambient pressure.

4. There is a slight increase in average flame speed when the arc length is increased.

5. The presence of combustible mixture in the surge tank has no effect on the pressure and thermocouple response of the system.

It is apparent that the increased rate of rise of the current in the discharge does not adversely affect the rate of flame propagation nor does it increase the peak pressures or mass flows in the vent system.

Table 5. Results of Flame Propagation Tests at High-Voltage Facility.

Nominal Discharge Voltage (volts)	Arc Length (in)	Pressure (psig)		Flame Speed (ft/sec)		
		P_1	P_5[b]	1st Half	2nd Half	Average
1,000,000	5 (center)	~1/2	~1/4	5.2	6.8	5.9
1,000,000[a]	5 (center)	~1/2	~1/4	6.0	7.8	6.7
800,000	5 (center)	~1/2	~1/4	11.6	8.6	9.3
1,000,000	5 (side)	~1/4	~1/8	14.0	10.1	11.8
1,000,000	12 (center)	~1/4	~1/8	15.4	21.6	18.0
1,000,000	7 (center)	~1/4	~1/8	13.5	15.1	14.3
1,000,000	12 (center)	~1/2	~1/4	9.4	57.0	16.3

NOTE: Discharge probe was centered above vent inlet opening unless otherwise noted.

[a] Surge tank filled with propane-air mixture.

[b] See Figure 7 for location of instrumentation.

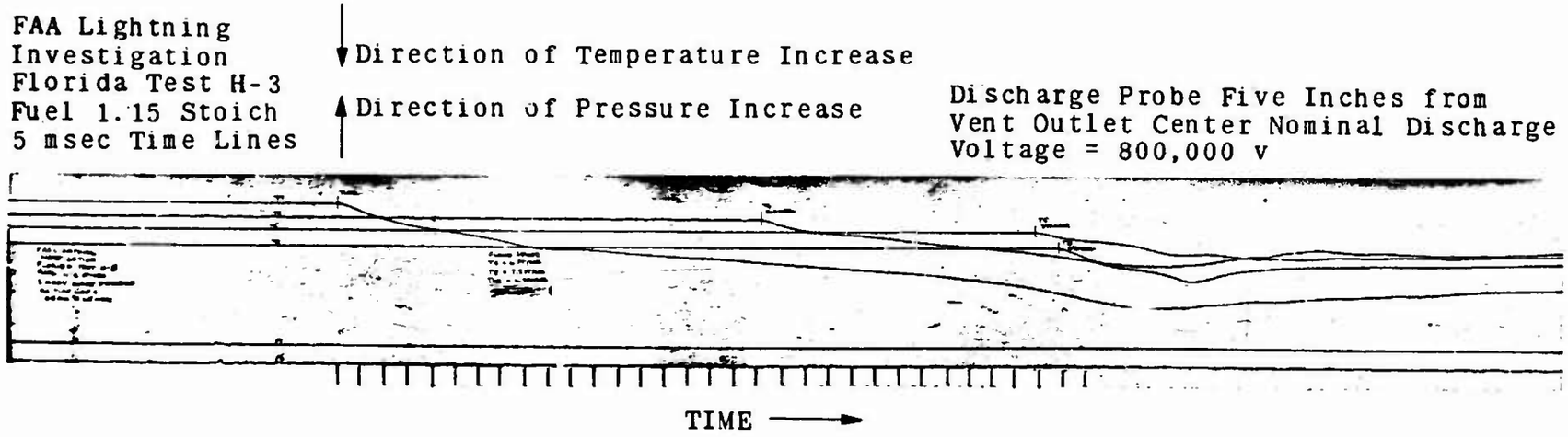

Figure 21. Flame Propagation Test at High-Voltage Facility.

3.2.4 Flame Propagation Studies Using Atlantic Research Corporation Drive Tube Assembly

3.2.4.1 Apparatus - Early in the program, Atlantic Research Corporation constructed a laboratory test facility for the purpose of testing flame arresters. Little was known concerning the pressures and flame speeds that lightning would induce in the vent system. For this reason it was decided that the system should be flexible enough to give a wide range of conditions. As data from the experiments at Lightning and Transients Research Institute facilities were accumulated, modifications were made to better simulate these results.

The facility is best understood by examining the isometric drawing shown as Figure 22. A 3-inch diameter pipe was attached to the existing Boeing 707 vent tube assembly. The length of the pipe (i.e., the drive tube) could be altered by the addition of 1-foot sections fastened with pipe couplings. The "transition section" served to join the pipe to the rectangular face of the vent outlet.

Ignition of the combustible mixture was initiated by an aviation spark plug located in the transition section or in any one of the drive tube sections. An orifice was placed at the end of the drive tube, which provided varying amounts of pressure relief depending upon its diameter. Flame speeds and pressures could be controlled by changing the drive tube length (maximum length of 5 feet), by changing the point of ignition, or by changing the diameter of the drive tube orifice. To seal the system during the filling operation, aluminum foil was placed over the orifice and at the inboard flange. These foils were punctured immediately prior to ignition by compressed-air-operated plungers in order that they offer no restruction to induced flow. The system was filled from the drive tube end and vented near the inboard flange. Fuel-air mixture was bled from the inlet supply and from the vent line. These bleed streams passed through flowmeters to burner tubes. The cone heights and flame color of the two burner flames were compared to ensure that the system was homogeneously filled. Figure 23 is a schematic diagram of the fuel supply and control system. The surge tank was a mock-up of the actual 707 surge tank, which is an integral part of the wing. Fuel could be supplied to the surge tank by an alternate piping system. The surge tank was protected by means of an 8-inch diameter blowout panel,

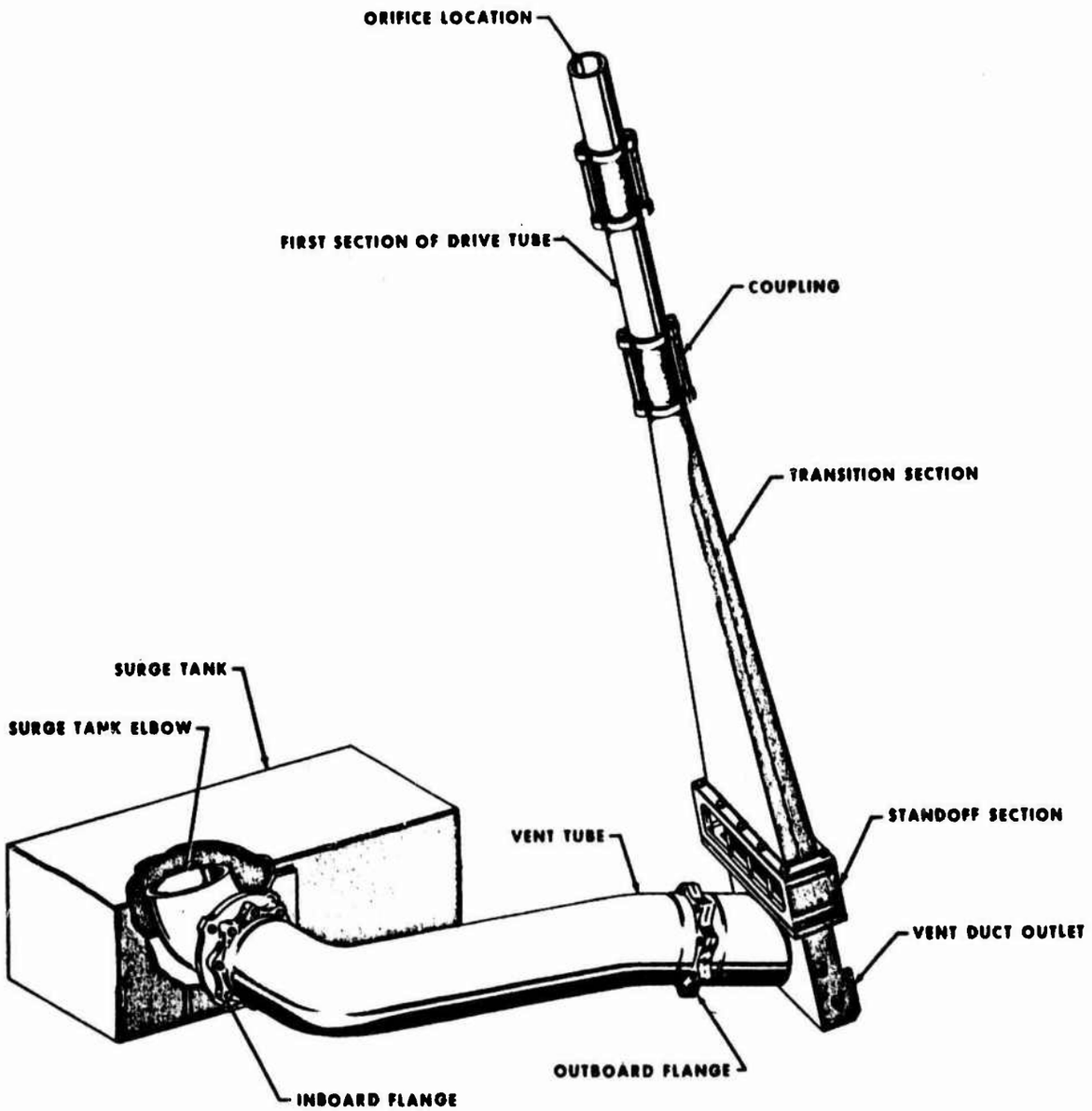

Figure 22. Isometric Drawing of Atlantic Research Test Apparatus.

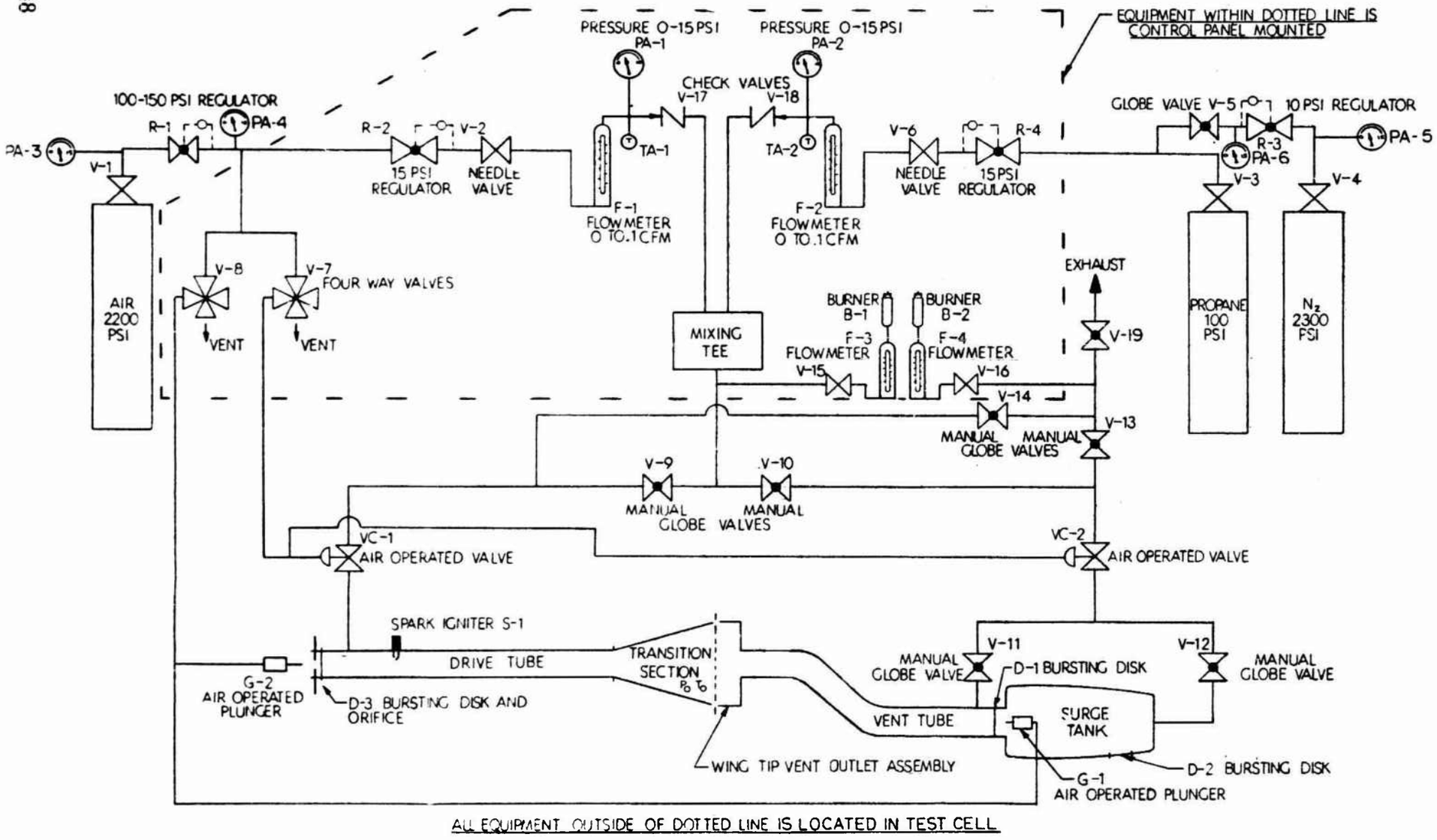

Figure 23. Flow Diagram of Fuel-Air Supply for Atlantic Research Test Facility.

which also served as an access port for assembly of the system. The instrumentation employed was identical to that used in the tests at Lightning and Transients Research Institute. Pressure transducers and thermocouples were placed at various locations in the vent tube as well as in the transition section (see Figure 7). All readout instrumentation and fuel-air supply controls were stationed outside of the test cell which was protected on three sides by heavy concrete walls. Figure 24 is a photograph of the interior of the cell.

3.2.4.2 Results and Discussion - Early tests were conducted without the stand-off section (to be described later). The transition section was bolted directly to the vent outlet. Table 6 summarizes typical values of the flame speeds and pressures obtained for various configurations of the drive tube assembly. Figures 25, 26, and 27 show test curves for three tests. Some general observations are pertinent:

1. A wide range of flame speeds were attained with variations between 5 ft/sec and 400 ft/sec.

2. The pressures and flame speeds are highly sensitive to the orifice diameter and less sensitive to ignition point and drive tube length.

3. There appears to be two relatively stable regimes of flame speeds; those in the range below 10 ft/sec and those with speeds of 300 ft/sec or more.

4. Results of repeated tests show a scatter of data in the intermediate range.

These results show the trends which were expected in the experimental design. Increasing restriction of the burned gases by the orifice induced convective transport of the flame and increased the flame speed. The effect of moving the ignition point and increasing drive tube length are more complex.

The system, in the unmodified form does not adequately simulate the effects of combustion initiated by high-energy electric discharge, as indicated by the differences in the pressure responses between tests at the high-current facility of Lightning and Transients Research Institute and those at Atlantic Research Corporation (compare Figures 15 and 26). For this reason the "stand-off"

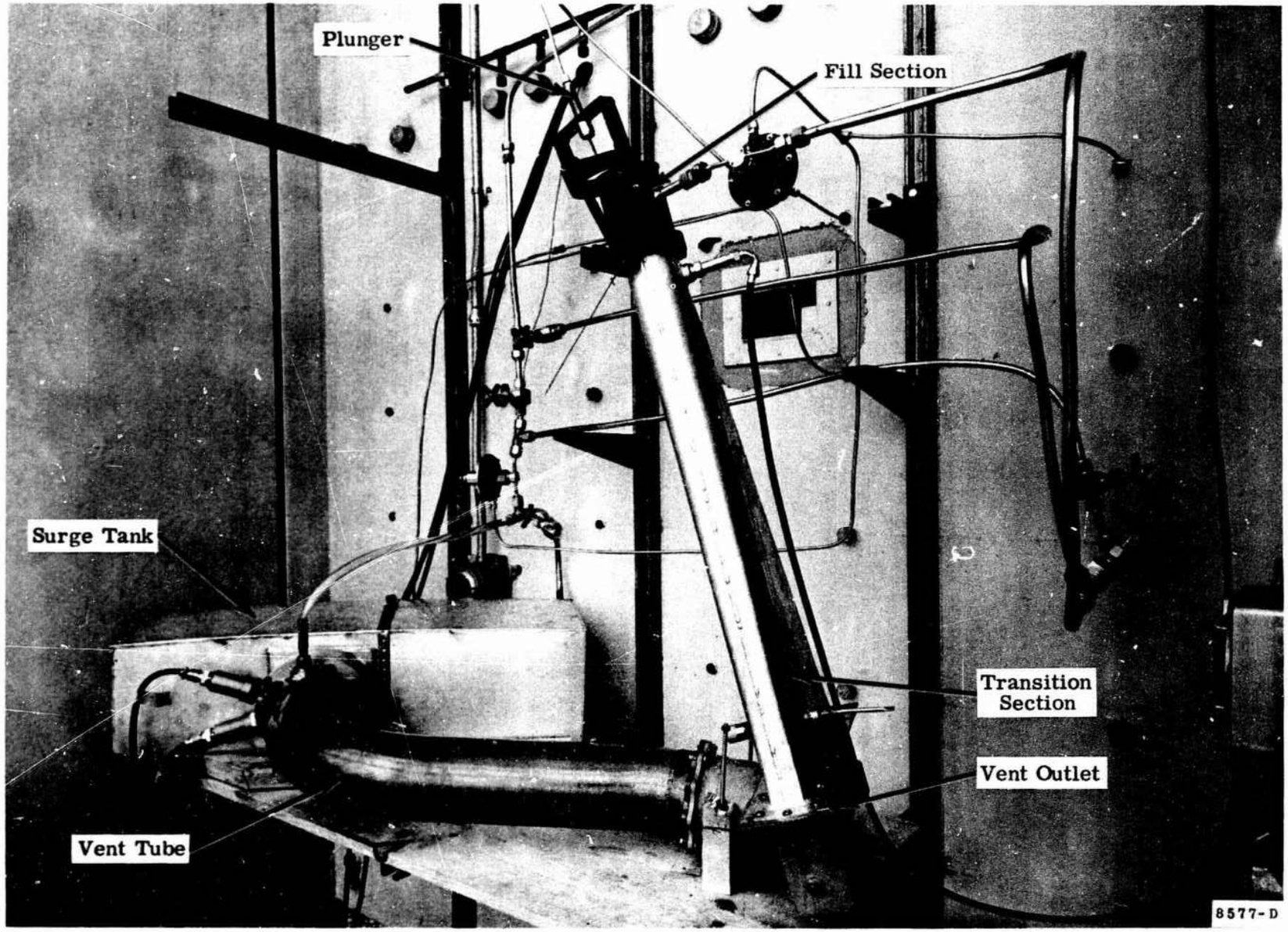

Figure 24. Interior of Atlantic Research Test Cell.

63333

Table 6. Results of Flame Propagation Tests at Original Atlantic Research Corporation Facility.

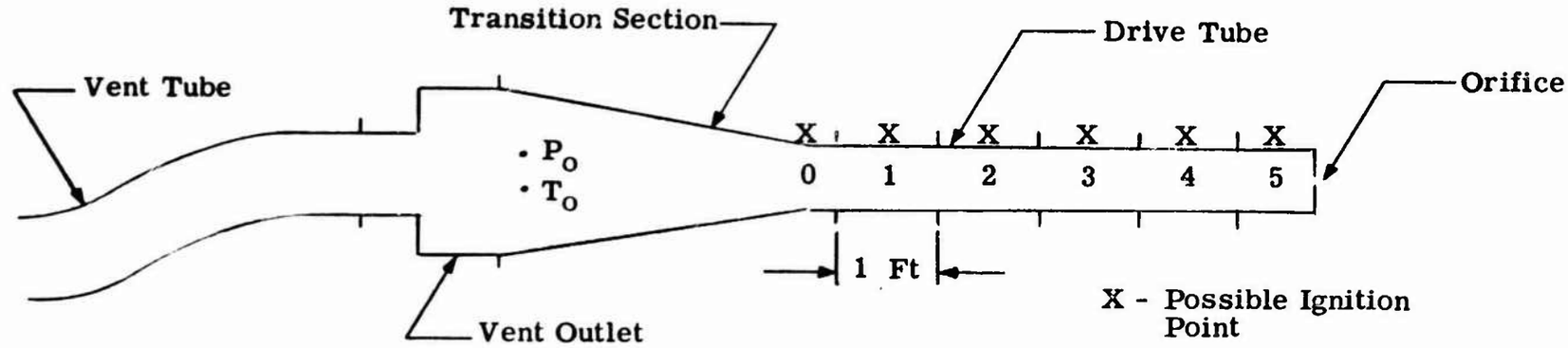

Orifice Diameter~inches~	Drive Tube Length~feet~ 0 (ft/sec)[a]	0 (psig)[b]	1 (ft/sec)[a]	1 (psig)[b]	2 (ft/sec)[a]	2 (psig)[b]	3 (ft/sec)[a]	3 (psig)[b]	4 (ft/sec)[a]	4 (psig)[b]	5 (ft/sec)[a]	5 (psig)[b]
2-3/4	6	1	4	1			8	2			166	7
	5	1	5	1	7	1	27	2	17	3	250	16
			6	1			86	2	300	8	430	19
2-1/2	300	13	—	—	—	—	75	5	—	—	—	—
							100	3				
2-1/4	—	—	—	—	—	—	230	15	—	—	—	—
2	290	11	—	—	—	—	—	—	—	—	—	—
	300	11										

NOTE: Ignition point in transition section for all tests

[a]Flame speeds are averages from T_o to T_5 (see Figure 7)

[b]Pressures measured at P_o

Table 6. (Continued)

Drive Tube Length-feet	Ignition Point 1 (ft/sec)[a]	1 (psig)[b]	2 (ft/sec)[a]	2 (psig)[b]	3 (ft/sec)[a]	3 (psig)[b]	4 (ft/sec)[a]	4 (psig)[b]	5 (ft/sec)[a]	5 (psig)[b]
3	28	2	94 100 100	3 3 1	50 50	1 1	—	—	—	—
4	—	—	83	3	—	—	10	2	—	—
5	17	2	—	—	63	2	—	—	11 5 9	1 1 1

NOTE: No orifice on drive tube for these tests

[a]Flame speeds are averages from T_o to T_5 (see Figure 7)

[b]Pressures measured at P_o

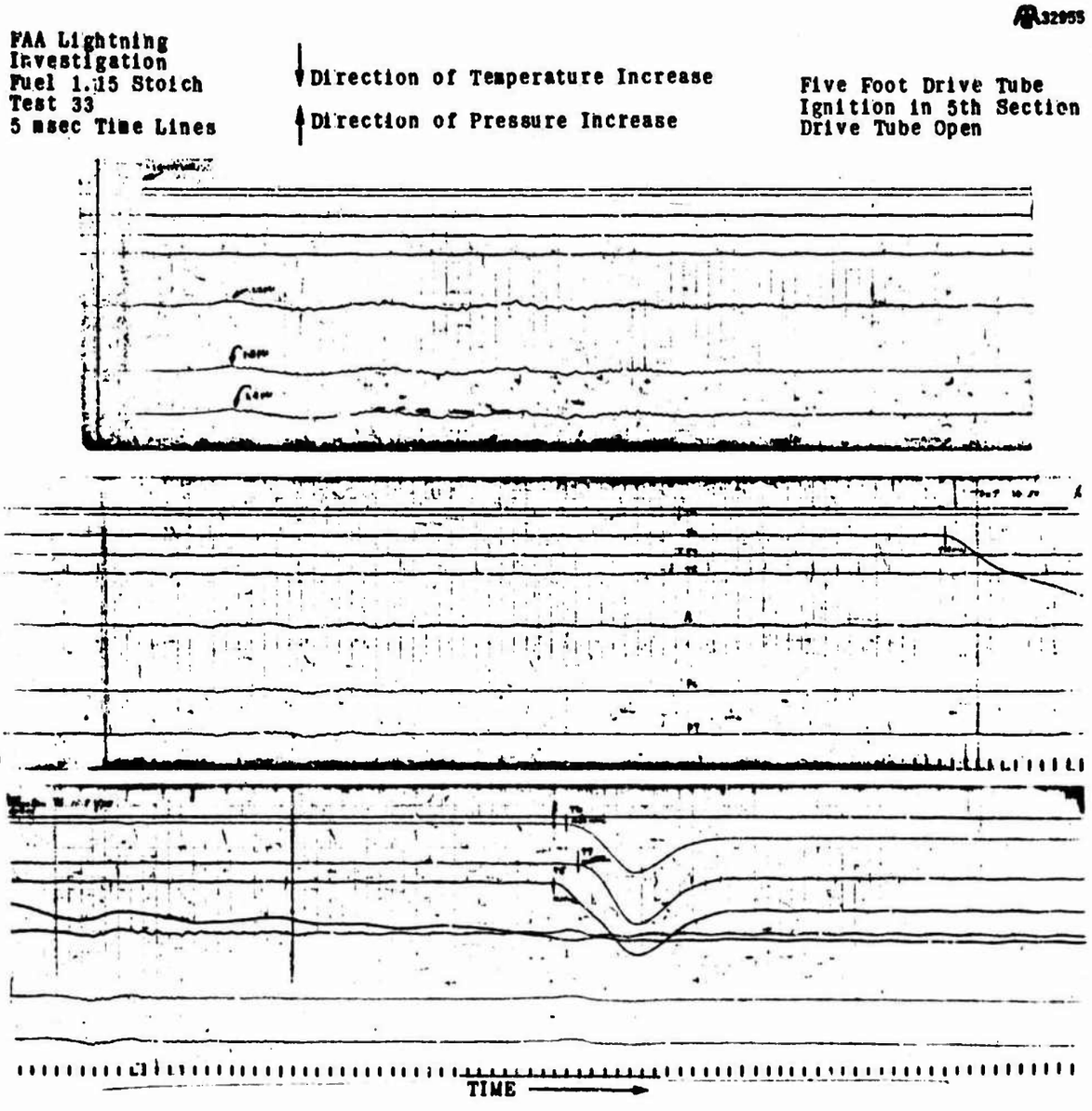

Figure 25. Flame Propagation Test at Original Atlantic Research Facility.

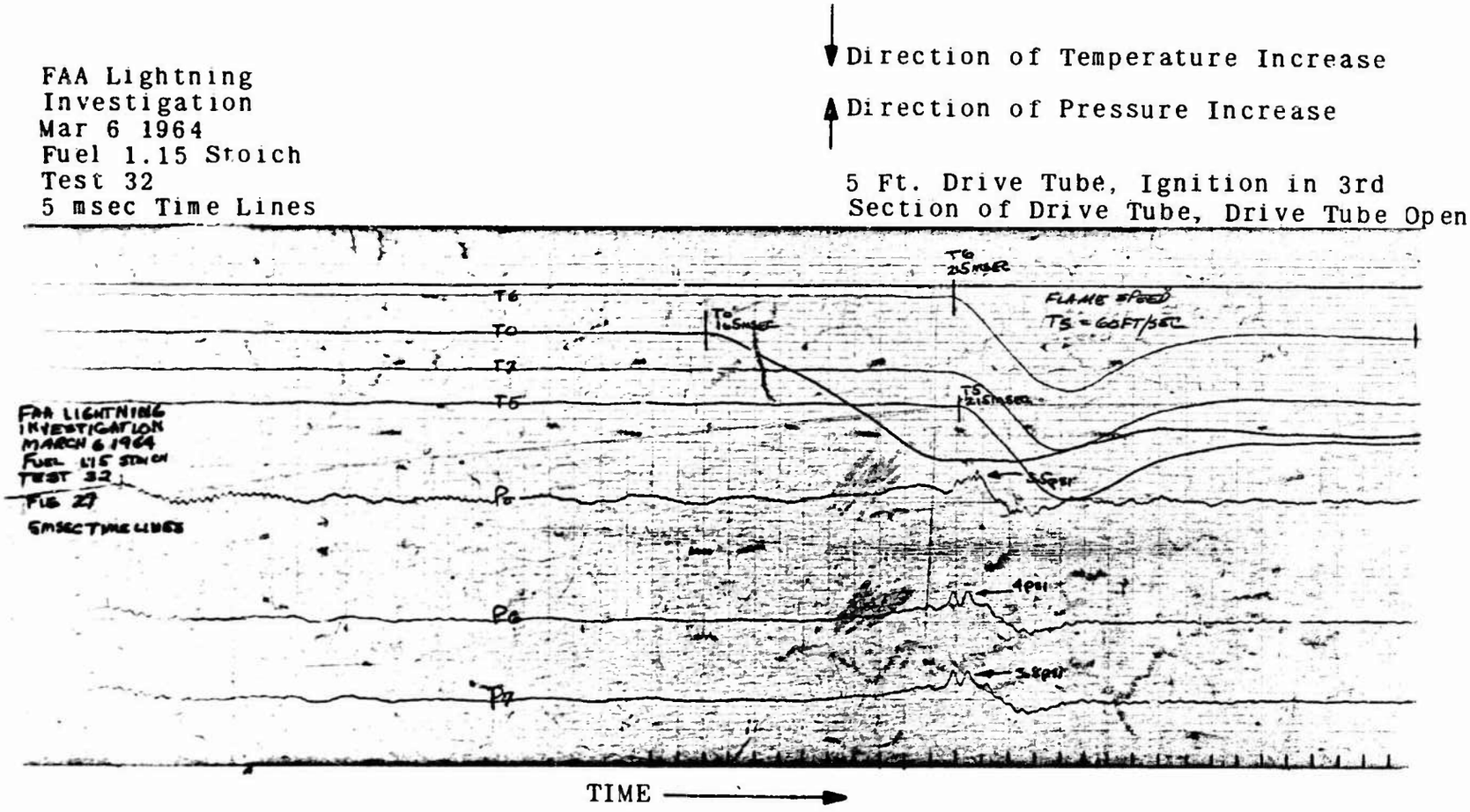

Figure 26. Flame Propagation Test at Original Atlantic Research Facility.

603233

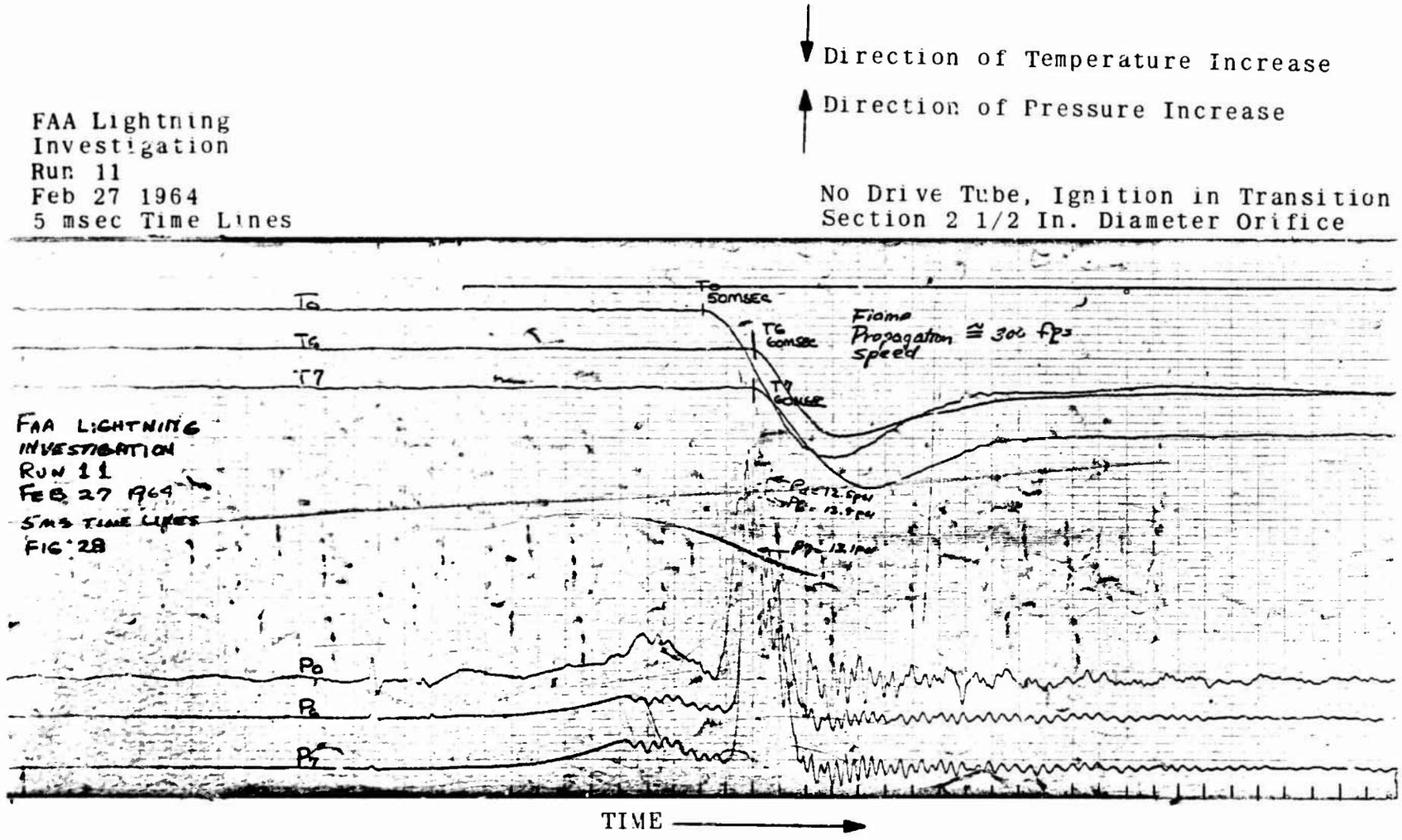

Figure 27. Flame Propagation Test at Original Atlantic Research Facility.

section was added to the system. The stand-off section shown in Figure 28 separated the transition section and drive tube assembly from the face of the vent outlet. This provided a large venting area at the outlet, more closely simulating the physical environment of the open vent. Original tests with the stand-off section and 5-foot drive tube did not yield the flame speeds of interest (they were less than 75 ft/sec); however, the pressure response was quite similar to those measured at Lightning and Transients Research Institute. In order to increase the flame speeds the end of the drive tube was blanked off and two orifices were incorporated in the drive tube. The orifices divided the 5-foot drive tube into two approximately equal chambers. Ignition occurred at the end of the drive tube. Expansion of the burned gas in the first chamber increased the turbulence in the second chamber. The additional turbulence increased the burning rate and hence turbulence in the transition section was augmented. The result was that the initial flame speed was magnified even though a large venting area was available at the vent outlet. Flame speeds up to 250 ft/sec were measured. The flame speeds could be varied by replacing the blanked-off end of the drive tube with various orifices. These tests gave speeds from 120 to 150 ft/sec. One such test is compared with a Lightning and Transients Research Institute high-current test in Figure 29. The results are remarkably similar considering the means by which they were obtained.

The drive tube assembly with stand-off section provides a facility which reasonably simulates the conditions measured at the Lightning and Transients Research Institute high-current facility during combustion initiated by discharge voltages up to 20 kv. It permits rapid, convenient testing of flame propagation in vent systems at low cost.

3.3 FLAME ARRESTER TESTS

3.3.1 General

After a literature search and design analysis, several flame arresters were constructed. These arresters were fabricated from corrugated aluminum, corrugated stainless steel, a ceramic material, and various copper screens. Descriptions of the arresters are given in Appendix B.

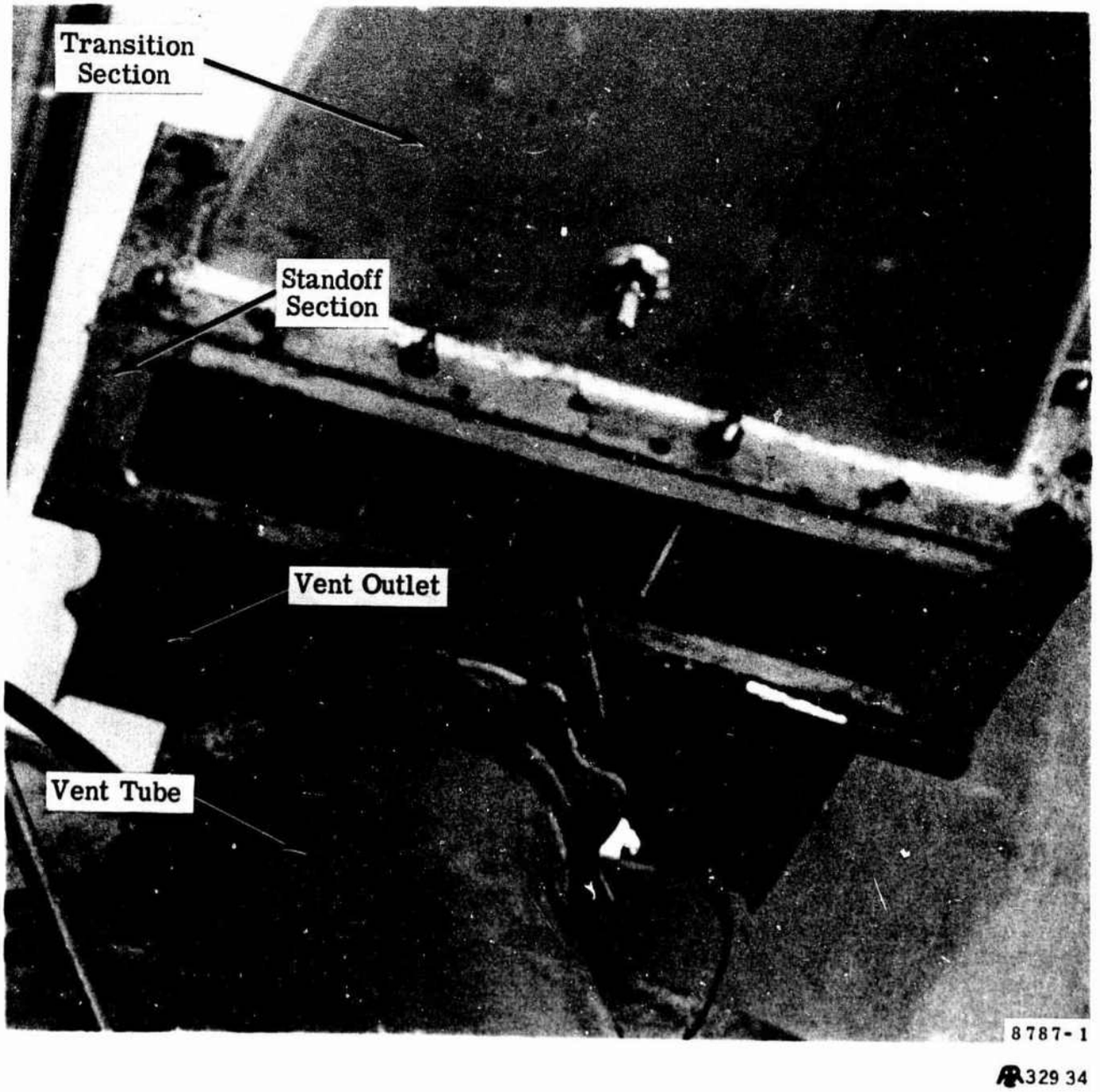

Figure 28. Standoff Section of Modified Atlantic Research Apparatus.

603233

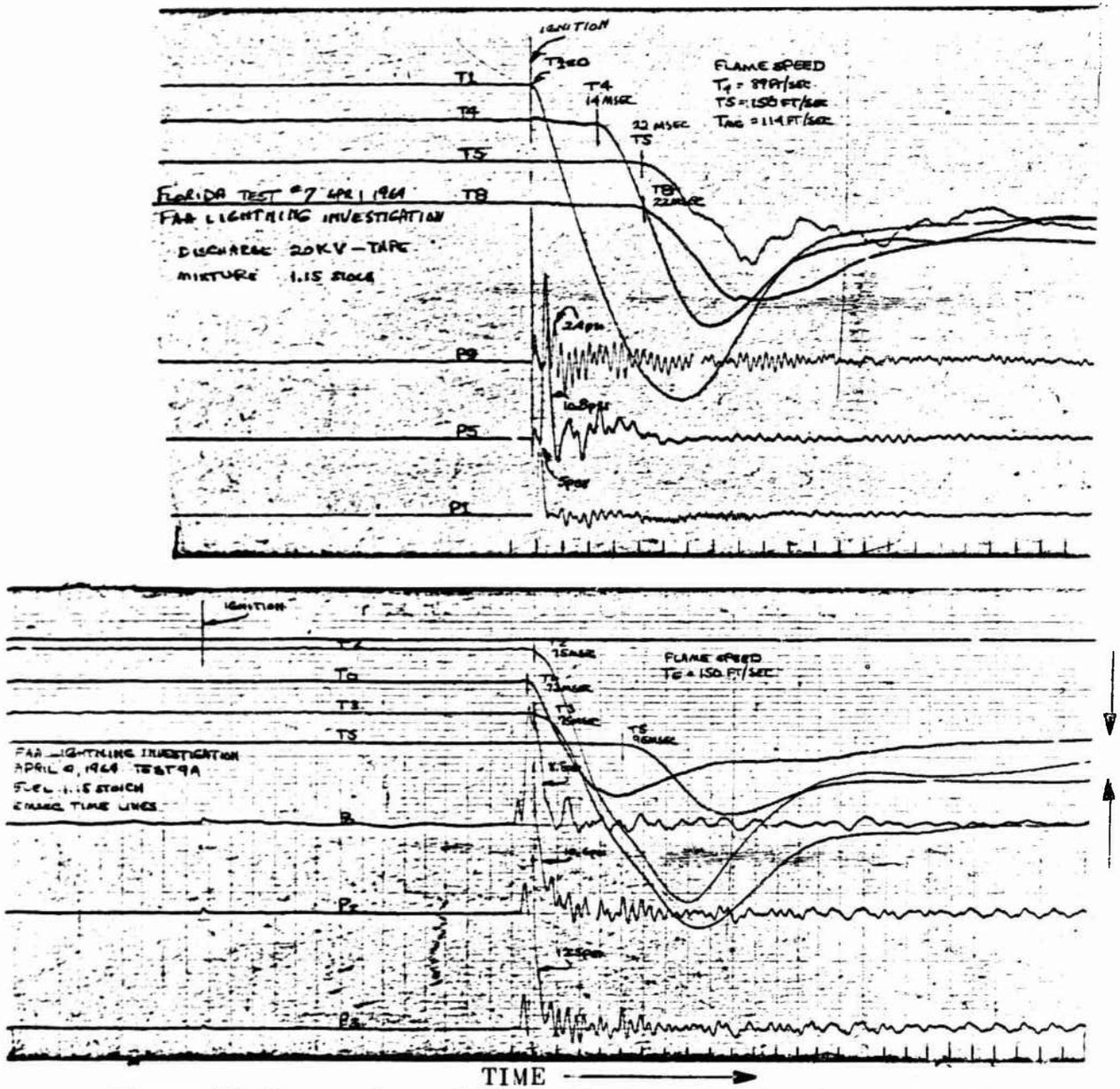

FAA Lightning Investigation
Florida Test 7
April 1 1964
Discharge Point B
20 KV Tape Discharge
Fuel 1.15 Stoich
5 msec Time Lines

ARC Test With Stand-Off Section 9A

Direction of Temperature Increase

Direction of Pressure Increase

Figure 29. Comparison of Flame Propagation Results at High-Current Facility with Modified Atlantic Research Test Apparatus.

603733

The arresters were cemented into retaining rings. The retaining rings could be sealed between two ring flanges which were then incorporated into the vent system at the existing vent tube flanges. Each ring flange (henceforth termed "instrument ring") was fitted with ports for a thermocouple and pressure transducer. Thus it was possible to determine whether flame approached and penetrated the arrester by observing the responses of the "upstream" and "downstream" thermocouples. Any significant pressure drop through the arrester could also be determined. Figure 30 is a drawing of the instrument ring and flame arrester assembly.

Tests with the flame arresters were conducted using the three facilities in which flame propagation experiments were performed.

3.3.2 Flame Arrester Tests Using High-Current Facility

3.3.2.1 Results - Table 7 summarizes the results of these tests. All tests were conducted using a 1.15 stoichiometric mixture and the discharge point was always located at position B (see Figure 12). The discharge was either direct or through a 4-inch strip of aluminized tape. With the arrester positioned at the outboard flange the indicated flame speed is obtained only if flame penetrates the arrester. With the arrester positioned at the inboard flange the indicated flame speed is that approaching the arrester.

3.3.2.2 Discussion - The results show emphatically that flame arresters placed at the outboard flange are ineffectual. Flame penetrated the arresters on all but one test with the arresters at this location. Increasing the depth of the arrester did not stop propagation even for a 5-kv discharge. Flames initiated by direct discharge as well as by tape discharge penetrated the 1-inch × 0.050-inch arrester. These facts are further discussed in Section 3.4 below. Estimates of mass velocities and quenching times are presented which show that the initial mass flow at the vent outlet may carry the flame through the arresters when located at the outboard flange. Pressure response in the vent tube was unaffected by introduction of flame arresters. The same arresters when placed at the inboard flange were successful, indicating that the convective flow in this region had diminished or ceased by the time the flame had propagated the additional distance (approximately

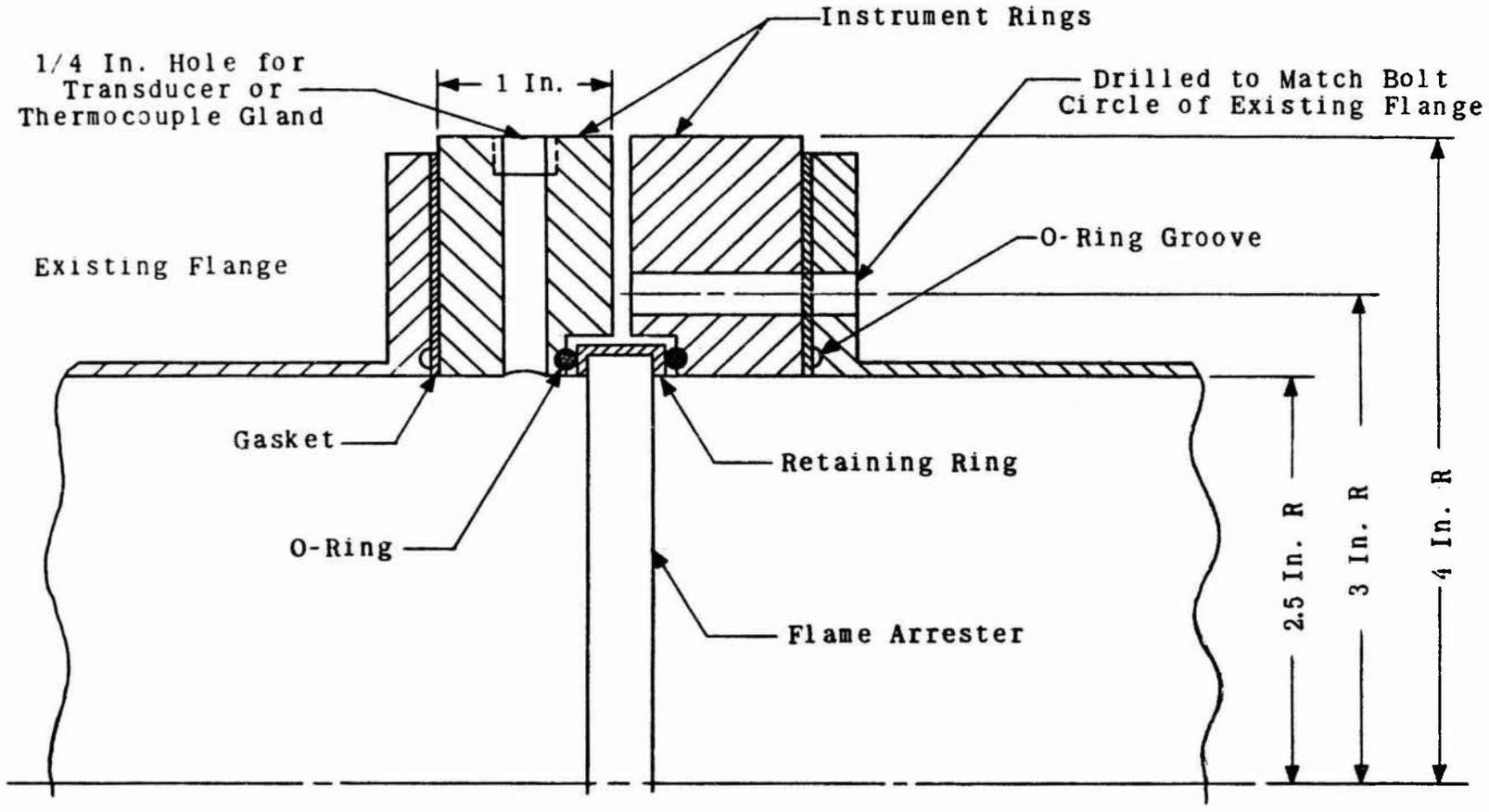

Note: Dimensions are Approximate

AR32521

Figure 30. Sketch of Instrument Ring and Flame Arrester Assembly.

Table 7. Results of Flame Arrester Tests at High-Current Facility.

Arrester Type[a]	Arrester Position	Discharge Voltage (kv)	Pressure (psig) P_1	Pressure (psig) P_5[b]	Flame Speed[c] (ft/sec)	Did Flame Penetrate Arrester?
1/2" × 0.050"	Outboard Flange	5 (tape)	2.9	3.1	41	Yes
		10 (tape)	6.3	6.7	125	Yes
		15 (tape)	8.3	8.8	150	Yes
		20 (tape)	3.8	11.3	125	Yes
1" × 0.050"	Outboard Flange	5 (tape)	2.4	2.5	44	Yes
		5 (tape)	2.9	3.1	49	Yes
		10 (direct)	0.5	1.0	—	No
		15 (direct)	0.6	1.1	10	Yes
		20 (direct)	2.9	3.1	48	Yes
1/2" × 0.050"	Inboard Flange	5 (tape)	2.5	4.5	16	No
		15 (tape)	8.8	10.6	80	No
		20 (tape)	2.5	13.8	75	No
1" × 0.050"	Inboard Flange	5 (tape)	1.6	3.1	19	No
		20 (tape)	15.8	8.7	120	No
		25 (tape)	16.3	23.7	TC's Broken	
0.055" Screen	Inboard Flange	5 (tape)	2.1	4.2	20	Yes
Accordian	Inboard Flange	5 (tape)	0.7	3.5	21	No
		10 (tape)	3.5	11.0	60	Yes

[a] See Appendix B for description.

[b] See Figure 7 for instrumentation location.

[c] Measured between T_1 and T_5.

3 feet) to the inboard flange. The 1-inch × 0.050-inch arrester stopped a flame whose average speed was 120 ft/sec. Another point of interest is that the flame speeds after penetrating the arrester at the outboard flange were somewhat higher than the speeds measured when no arresters were placed at that location. That is, the presence of the arrester effectively increased the average flame speed when the arrester was placed at the outboard flange. This phenomenon is probably caused by the additional turbulence introduced by flow constriction and subsequent expansion near the inboard face of the arrester. This additional turbulence effectively increases the surface area of the flame brush and hence the burning rate, according to the principles discussed in Section 3.4 below.

3.3.3 Flame Arrester Tests Using High-Voltage Facility

3.3.3.1 Results - Using the same apparatus as described earlier for high-voltage tests, flame arresters were tested at both inboard and outboard flanges of the vent tube. The results are tabulated in Table 8.

3.3.3.2 Discussion - The results show that all arresters with the exception of the 0.067-inch screen are capable of stopping flames generated by a nominal 1,000,000-volt discharge. The arresters may be placed at either of the existing vent tube flanges. The measured pressures and flame speeds are relatively low (less than 1/4 psig and 20 ft/sec) compared to those in the low-voltage facility (up to 16 psig and 140 ft/sec), indicating that the mass flows are of a lower magnitude. These data are in accord with the results and discussion presented in Section 3.2.3.2.

3.3.4 Flame Arrester Tests Using Modified Atlantic Research Corporation Apparatus

3.3.4.1 Results - Several flame arresters were tested in the modified Atlantic Research Corporation apparatus (see Section 3.2.4). The purpose of the tests was to check the degree of simulation of these laboratory results with results of flame arrester tests using the high-current simulated lightning facility of Lightning and Transients Research Institute. Additionally, because of the better control of flame speeds afforded by the laboratory apparatus, it was possible to test the

Table 8. Results of Flame Arrester Tests at High-Voltage Facility.

Arrester Type	Arrester Position	Discharge Voltage	Discharge Length[a]	Pressure (psig) P_1	Pressure (psig) P_5[b]	Flame Speed (ft/sec)[c] 1st Half	Flame Speed (ft/sec)[c] 2nd Half	Flame Speed (ft/sec)[c] Average	Did Flame Penetrate Arrester?
1" × 0.050"	Outboard Flange	1,000,000	5"	0	0	—	—	—	No
1" × 0.050"	Outboard Flange	1,000,000	12"	1/4	1/8	—	—	—	No
1/2" × 0.050"	Outboard Flange	1,000,000	5"	1/4	1/8	—	—	—	No
1/2" × 0.050"	Outboard Flange	1,000,000	12"	1/4	1/8	—	—	—	No
1/2" Cercor	Outboard Flange	1,000,000	5"	1/4	1/8	—	—	—	No
1/2" Cercor	Outboard Flange	1,000,000	12"	1/4	1/8	—	—	—	No
0.067" Screen	Outboard Flange	1,000,000	12"	1/4	1/8	10	15	12	Yes
0.067" Screen	Outboard Flange	1,000,000	12"	1/4	1/8	14	33	19	Yes
1/2" Cercor	Inboard Flange	1,000,000	12"	1/4	1/8	6.6	8.3	7.3	No
1/2" × 0.050"	Inboard Flange	1,000,000	12"	1/4	1/8	8.4	6.9	7.6	No
1" × 0.050"	Inboard Flange	1,000,000	12"	1/4	1/8	18.3	15.2	16.7	No

[a]The discharge probe was located above the center of the vent inlet in all tests. Mixture ratio was 1.15 stoichiometric in all tests.

[b]See Figure 7 for location of instrumentation.

[c]First half refers to locations 1 to 4; second half to 4 to 5; average is 1 to 5.

arresters with faster flame speeds than those measured at Lightning and Transients Research Institute. These latter tests helped establish a wider range of flame arrester effectiveness in the vent system under consideration. Flame speeds ranging from 40 ft/sec to greater than 400 ft/sec were attained. Experiments in the high-current facility of Lightning and Transients Research Institute gave flame speeds below 150 ft/sec. The important results of the present tests are listed in Table 9.

3.3.4.2 Discussion - The results show that the 1/2-inch × 0.050-inch arrester was successful when placed at the inboard flange, while flame penetrated it when placed at the outboard flange. This behavior is similar to results of experiments with simulated lightning discharges at the vent outlet and can be explained in the same manner (see Section 3.4). However the 1-inch arrester effectively stopped flames at both inboard and outboard flanges. This result does not duplicate the results of simulated lightning initiated combustion. The laboratory facility may not simulate in every detail and degree the effects of artificial lightning discharges.

As expected screens do not offer protection against flame speeds much in excess of the laminar burning velocity. The 1-inch × 0.050-inch arrester stopped a flame whose speed was in excess of 400 ft/sec indicating that this arrester allows a large margin of safety regarding its arresting properties. The maximum flame speeds measured under conditions characterized as severe lightning strokes were of the order of 150 ft/sec. The 1/2-inch × 0.050-inch arrester did not stop flames of speeds greater than 400 ft/sec though the arrester may have been ruptured prior to arrival of the flame brush. Mechanical damage to the ceramic and 1/2-inch × 0.050-inch arrester was caused by pressure waves associated with the higher flame speeds. Some attention should be devoted to bonding and structural stability of future arresters.

3.4 RELATION OF SYSTEM CONFIGURATION TO FLAME PROPAGATION AND FLAME ARRESTER PERFORMANCE

As pointed out in Section 3.2.2.2, the vent system responds to acoustic oscillations approximately as an organ pipe. In an organ pipe, resonance generates a standing wave with a pressure node at the closed end and an antinode at the open

Table 9. Results of Flame Arrester Tests with Modified Atlantic Research Corporation Facility.

Arrester Type	Location	Did Flame Penetrate Arrester?	Average Flame Speed (ft/sec)[b]
1/2" × 0.050"	Outboard Flange	Yes	166[a]
1/2" × 0.050"	Outboard Flange	Yes (damaged arrester)	190[a]
1" × 0.050"	Outboard Flange	No	—
1/2" × 0.050"	Inboard Flange	No	156
1/2" × 0.050"	Inboard Flange	Yes (damaged arrester)	>400
1" × 0.050"	Inboard Flange	No	40
1" × 0.050"	Inboard Flange	No	100
1" × 0.050"	Inboard Flange	No	114
1" × 0.050"	Inboard Flange	No	>400
0.050" Screen	Inboard Flange	Yes	166
1/2" Ceramic	Inboard Flange	Yes (shattered arrester)	139

NOTE: All tests conducted with 1.15 stoichiometric mixture. Surge tank filled for all tests.

---

[a]Indicated flame speed is that measured after penetration.

[b]Average flame speed measured between T_3 and T_7 (See Figure 7).

end. During an acoustic cycle air flows in to and out of the open end, whereas at the closed end the air is substantially at rest. At the open end, the cyclic variations of the particle velocity attain their maximum amplitude while the pressure remains constant and equal to the ambient; whereas at the closed end the particle velocity remains zero and the pressure oscillates at maximum amplitude. The pressure traces in Figures 12 to 17 show that after the initial lightning-generated pulse the pressure oscillations near the vent duct outlet vanish rapidly, while at the other end, i.e., near the surge tank elbow, the oscillations decay comparatively slowly. Furthermore, as pointed out, the recorded frequency is in substantial agreement with the calculated acoustic frequency. It thus appears that with respect to acoustic resonance the surge tank elbow acts substantially as a closed end and the vent duct outlet as an open end.

The significance of this acoustic response lies in the generation of a fluctuating flow field near the duct outlet where the lightning strikes and the flame enters. The lightning stroke provides the ignition source and the initial acoustic energy. The resulting flow field has two effects: the flow turbulence accelerates the propagation of the entering flame, and the inflow phase of the acoustic particle velocity may defeat a flame arrester by transporting ignited gas through the arrester channels.

Because the subject of interaction between flame and flow is not widely known, a brief description may be helpful. The electric discharge acts principally as a heat source inflaming the affected volume of fuel-air mixture. This initial flame imparts heat to the adjacent layer of unburned gas, which thus inflames and becomes the ignition source for the next layer, and so on, so that flame propagates through successive layers as a wave, the combustion wave. The wave occupies at any instant a layer volume characterized by a steep temperature gradient and a distinct zone of rapid chemical reaction of fuel and oxygen. It overruns successive layers at the rate S_u which is referred to as the burning velocity and is essentially determined by the heat flux into the unburned gas. The wave layer is also subject to displacement by convection. In a turbulent flow field where convection currents are random in direction and velocity, the wave surface becomes correspondingly distorted and wrinkled, so that in a pipe the wave area

exceeds the cross-sectional area of the pipe. The wave is thus forced into a wrinkled and fluctuating configuration which extends over some length of the pipe and is referred to as the flame brush. The flame brush propagates through the pipe at the rate S_u A/a, where A is the time average of the wave area and a is the cross-sectional area of the pipe.

Although the structural details of the flame brush are not essential for the present discussion, we mention here a few features which permit additional visualization of the phenomenon.[6] The flame area shrinks and increases locally in a random manner corresponding to the random eddy movement of turbulent flow. Shrinkage occurs because the propagation of the wave into the unburned gas tends to eliminate the wrinkles of the flame surface, in a manner similar to Huygen's principle of wave propagation from discrete sources. Increase of flame area results from entrance of the wave into local fields of velocity gradients associated with the eddy movement: elements of the wave surface are driven in opposite directions so that the interface between burned and unburned gas increases. Such freshly formed interface ignites and acquires the gradient structure of the combustion wave; however, the process has a time lag which becomes significant when the velocity gradient is large. Depending on the ignition characteristics of the mixture and the turbulence intensity, the wrinkled wave sheet of the flame brush may have numerous transient holes where burned and unburned gas border on each other without combustion reaction. Such holes occur when the local value of the Karlovitz number is considerably larger than unity. The Karlovitz number is $\alpha(dU/dy)/US_u$, where α is thermal diffusivity of the unburned gas, U is the average velocity of the unburned gas relative to the flame brush, and dU/dy is the local velocity gradient. The wrinkles of the wave sheet are sharp-edged toward the burned gas and scalloped toward the unburned gas; this feature is associated with the geometry of wave propagation which causes neighboring indentations of the wave surface to increase in diameter and hence to intersect along sharp-angled ridges.

The wave surface generates mass flow due to the volume increase that occurs when a gas layer is overrun by the combustion wave. This volume increase is about sevenfold for the present test mixture and it occurs at all points of the

wrinkled wave surface essentially normal to the local surface elements. It thus generates random local mass accelerations which increase the turbulence intensity. In addition, the total mass flow generated by the flame brush is contained by the pipe wall, producing pipe-flow turbulence which feeds back into the flame brush to a significant extent. This phenomenon is well-known from experiments on flames propagating toward the closed end of a tube, the other end being open, which is approximately the case in the present system. At small pipe diameters the viscous restraint on the flow preserves a laminar flow pattern and a regular paraboloid shape of the combustion wave. As the diameter is increased the flow increases. When the Reynolds number exceeds 2,000 the laminar flame configuration breaks down and becomes a turbulent flame brush.

The turbulent flame brush is inherently unstable. The feedback of turbulence tends to increase the flame area and hence the propagation rate; on the other hand, as the wrinkles of the bursh become numerous and closely spaced they tend to close up, so that the brush may collapse with consequent sharp reduction of the flame area. Toward the burned-gas side the flame-brush may break up into islands of unburned gas so that the wave sheet is not continuous. The flame configuration is thus random and non-reproducible in experimental tests. Accordingly, the data reported above show a speed-up of flame propagation in the vent tube as a general trend with occasional exceptions. There is a rough correlation of the propagation rate with the energy of the electric discharge; this evidently reflects the level of turbulence which is initially imparted to the flame. The observed values of the propagation rates should be viewed in relation to the laminar burning velocity of 1.4 ft/sec. Very large ratios of propagation rate to burning velocity that are listed in Table 4 are associated with high peak pressures P_2. The latter correspond to very substantial particle displacements at the vent outlet. Thus, during the inflow phase of an oscillation the flame gas sweeps past the first thermocouple to a distance of several times the pipe diameter, and on the rebound "tongues" of unburned gas are deeply pushed into the burned gas according to the principle of Taylor on the instability of interfaces of different densities. In this way one may visualize the rapid generation of extraordinarily large interfaces with correspondingly rapid flame propagation. The absolute values of the propagation rates are not amenable to further analysis.

Flame arresters such as have been used in the present investigation consist of a web of quenching channels. When a combustion wave enters a quenching channel, heat flows from the reaction zone into the channel wall at a rate exceeding the rate of heat generation, so that the temperature decreases and the combustion reaction ceases. This process of heat abstraction and extinction has a time lag; hence the arrester fails if by convection the wave is transported through any of the channels in a time smaller than the residence time required for extinction.

Because of limitations of theoretical and experimental information the required residence time can only be estimated in order-of-magnitude approximation. A length ΔX characteristic of the width of the combustion wave is obtained from the equation

$$\Delta X = \alpha/S_u,$$

where α is the thermal diffusivity of the unburned gas. For a stoichiometric propane-air mixture α is about 0.2 cm^2/sec and S_u is 40 cm/sec, so that ΔX is 0.005 cm. The flame arresters used in the present investigation have channels of approximately triangular cross section with a side length of 0.050 inch or 0.125 cm. An equivalent cylindrical channel has a diameter of about 0.1 cm, so that the distance from the channel center to the wall is about tenfold the characteristic length ΔX. Distances of this order are adequate for quenching purposes if the flame resides in the channel for a sufficient length of time. This time should be comparable to the characteristic time $\tau = \Delta X/S_u$, exceeding τ by a factor of probably less than 10. From S_u = 40 cm/sec one obtains $\tau \sim 0.12$ msec, so that, if the gas is at rest and the propagation rate is correspondingly equal to S_u, a channel length of about 0.05 cm or 0.02 inch is sufficient; that is, in quiescent gas a flame can be arrested by a wire grid. When the gas moves at hundreds of feet per second, the quenching channels require lengths of the order of inches.

Amplitudes of the acoustic particle velocities u near the vent duct outlet may be estimated from the equation[13] (and other acoustic texts)

$$U_{max} = \frac{P_5}{P_{ambient}} \frac{c}{\gamma}$$

where c is the sound velocity of about 1,100 ft/sec; $\gamma \sim 1.4$ is the specific-heat ratio; $P_{ambient}$ is 14.7 psia; and P_5 is the pressure maximum near the inboard

flange in psig-units, as listed in Table 4. The ratios $P_5/P_{ambient}$ range from about 0.2 to unity depending on the discharge voltage. The equation is inaccurate for ratios of the order of unity but remains applicable within the order of magnitude; thus, the velocity amplitudes range approximately from 150 to 800 ft/sec. For the 1-inch channel length that has been used in the present tests, this corresponds to residence times ranging from about 0.6 to 0.1 msec. A residence time of 0.6 msec appears to be marginally sufficient for quenching but a residence time of 0.1 msec is definitely too short; thus, a flame arrester placed at the outboard flange is expected to fail much as shown by the data in Table 7. At the inboard flange the particle velocity is low and the 1-inch flame arrester correspondingly performs well at this position; however, the duct system is not ideally a closed-end pipe, so that the particle velocity is not zero and screen-type arresters fail, as shown in the table.

The foregoing data and analysis point to the surge tank elbow and surge tank vent area as the critical elements of the duct configuration that permit a flame arrester to perform successfully at the inboard position. Furthermore, the result may be generalized as follows. By careful acoustic design of a vent system it would be possible to create locations in the vent system where the efficacy of a flame arrester is enhanced.

3.5 EXPLOSION SUPPRESSION TESTS

3.5.1 General

The evaluation of explosion suppression techniques was performed in conjunction with manufacturers of devices of this type. Specifically, Fenwal, Inc., of Ashland, Massachusetts, supplied engineering assistance and delivered components which were tested in the modified Atlantic Research Corporation surge tank-vent tube test apparatus. The components were of an industrial type, not designed for aircraft, and were tested to demonstrate effectiveness only. Graviner, Inc., of Rockville, Maryland, supplied engineering data and the past and current experience of their system on operational turbojet and turboprop aircraft of the British Royal Air Force and Royal Navy. Details of interest from both these manufacturers are presented in Appendix C.

The suppression system should be designed to prevent propagation of flame through the surge tank, thereby preventing explosions in the fuel tanks.

The suppression system is comprised of three basic elements designed to take advantage of the short time before a destructive pressure is built up in a fuel tank by an explosion:

1. A fast-acting sensor for detection of the presence of a flame.

2. A tubular metal suppressor unit containing a quantity of liquid suppressing agent and an electric detonator for rapid dispersal of the suppressant.

When the detector sees the light emitted by the presence of a flame it passes a pulse to the electric detonator. This ruptures the suppressor tube and disperses the suppressing agent in mist form at a speed of 200 ft/sec. This mist inerts the unburned vapors around the expanding flame front, thus arresting the explosion.

System operation is designed to be complete in a few milliseconds and well before the explosion pressure endangers the tank or aircraft structure. The manufacturers say that the operation of the system will not contaminate the fuel nor affect the engine performance.

Certain characteristics of explosion suppression systems should be considered in the evaluation of this technique for aircraft fuel system protection. Effectiveness, reliability, safety, weight and cost are important aspects to review. Once the system is actuated, the chemical agent will keep the tanks inerted for many minutes depending upon the outflow conditions. Therefore, if the system protects against the first of multiple stroke discharges, it should be effective against further strokes. A back-up system could be designed in which two canisters are mounted in the tanks and the second suppressor would not be actuated until a second flame front in the vent tube initiated the unit. A major problem would be reliability. These systems will be expected to perform in milliseconds after being exposed to the aircraft environment for long periods of time. Power systems could fail; the sensor element could be covered with dirt; switches and detonators might become defective or inadvertent actuation by sunlight or a flashlight beam could cause loss of protection. Check-out instrumentation can be

devised to protect against some of these malfunctions. However, the cost, weight and complexity of a fully developed system will have to be determined. In addition, explosive detonators and toxic and corrosive agents which are inherent in the system will require safety precautions for ground handling and storage. Unless the agent is removed from metal parts, undesirable corrosion may occur. The probability of the canister metal shattering and penetrating wing skins may be low, but it should be considered in any actual application.

3.5.2 Apparatus

The basic test apparatus shown in Figure 21 was modified to test Fenwal industrial-type suppression units. Fenwal installed a surveillance detector in the vent tube 29 inches from the surge tank (see Figure 31). The location was chosen so that the sensor would not "see" bright sunlight or inadvertent floodlight illumination through the vent opening, since the system would react to approximately 0.5-ft-candle light pulse intensity. The control unit is supplied with 30 volts DC by means of six lamp dry cells (see Figure 32). This unit connects to a wire bridge explosive switch which activates the suppression device. The suppression devices tested are 500-cm^3 hemispherical units (Catalog No. 92000-X) containing monobromomonochloromethane (see Figure 33). The data sheet for this unit and the health hazard properties of the bromochloromethane are included in Appendix C.

Since the Fenwal (industrial) system is reported to have a response time of approximately 20 to 25 msec,* a flame traveling at an average speed between 120 and 150 ft/sec will have propagated into the surge tank before the suppressant has completely filled the surge tank volume. The explosion may or may not be prevented depending upon the rate of travel of the flame through the surge tank into the reserve tank. It is therefore of interest to test the system with the surge tank filled with explosive mixture and to have passages simulating those passages between the surge tank and fuel tanks instrumented to detect flame travel out of the surge tank. The equipment was modified to obtain this information for the last eight of the eleven tests (see Figure 34).

*3 to 8 msec to sense and detonate and approximately 15 msec to disseminate agent throughout the surge tank at 200 ft/sec. The time response of the system may improve with the use of kerosene since the spectral characteristics of the detectors are designed for the emission characteristics of kerosene flames.

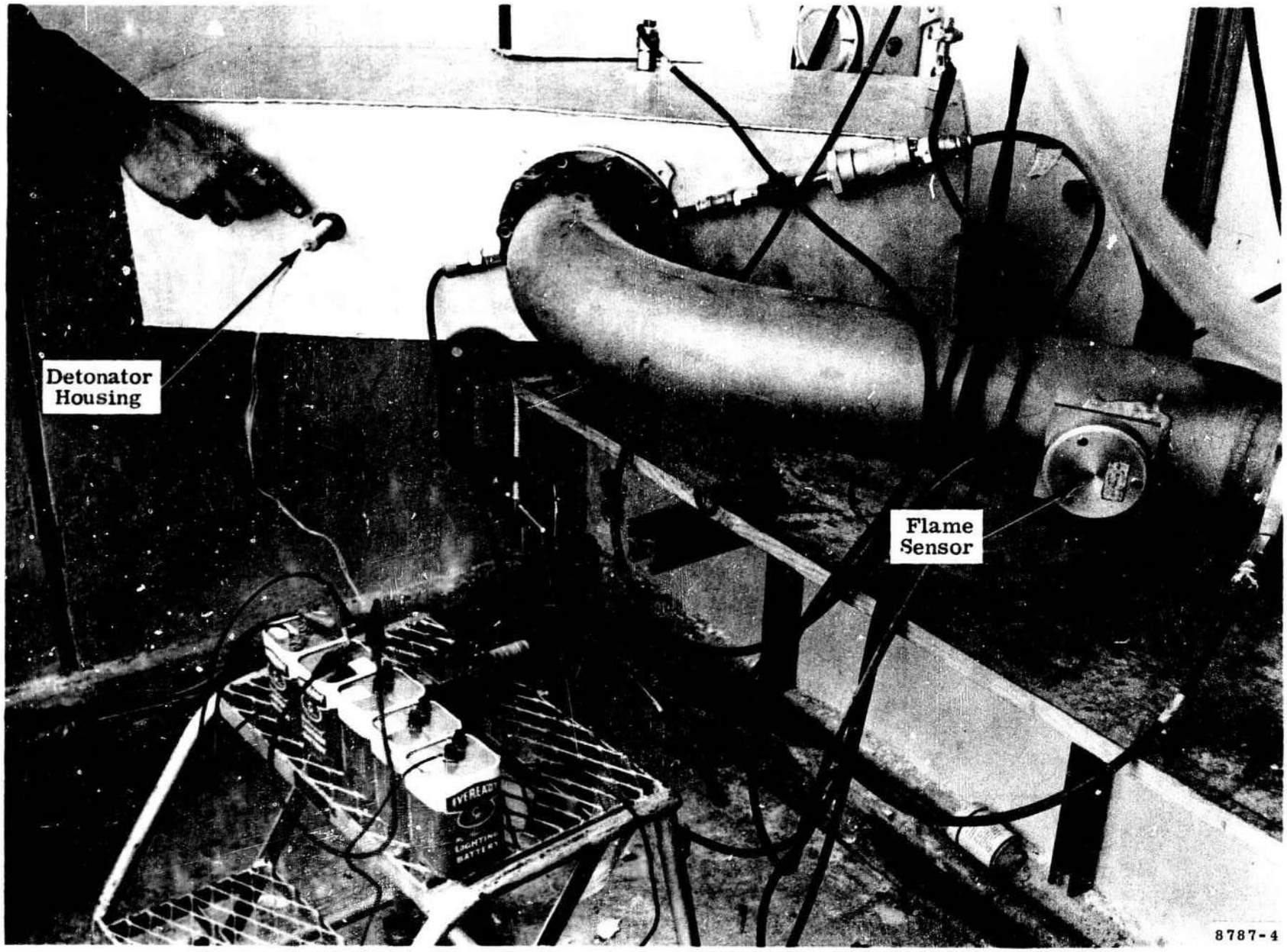

Figure 31. Installation of Explosion Suppression Equipment.

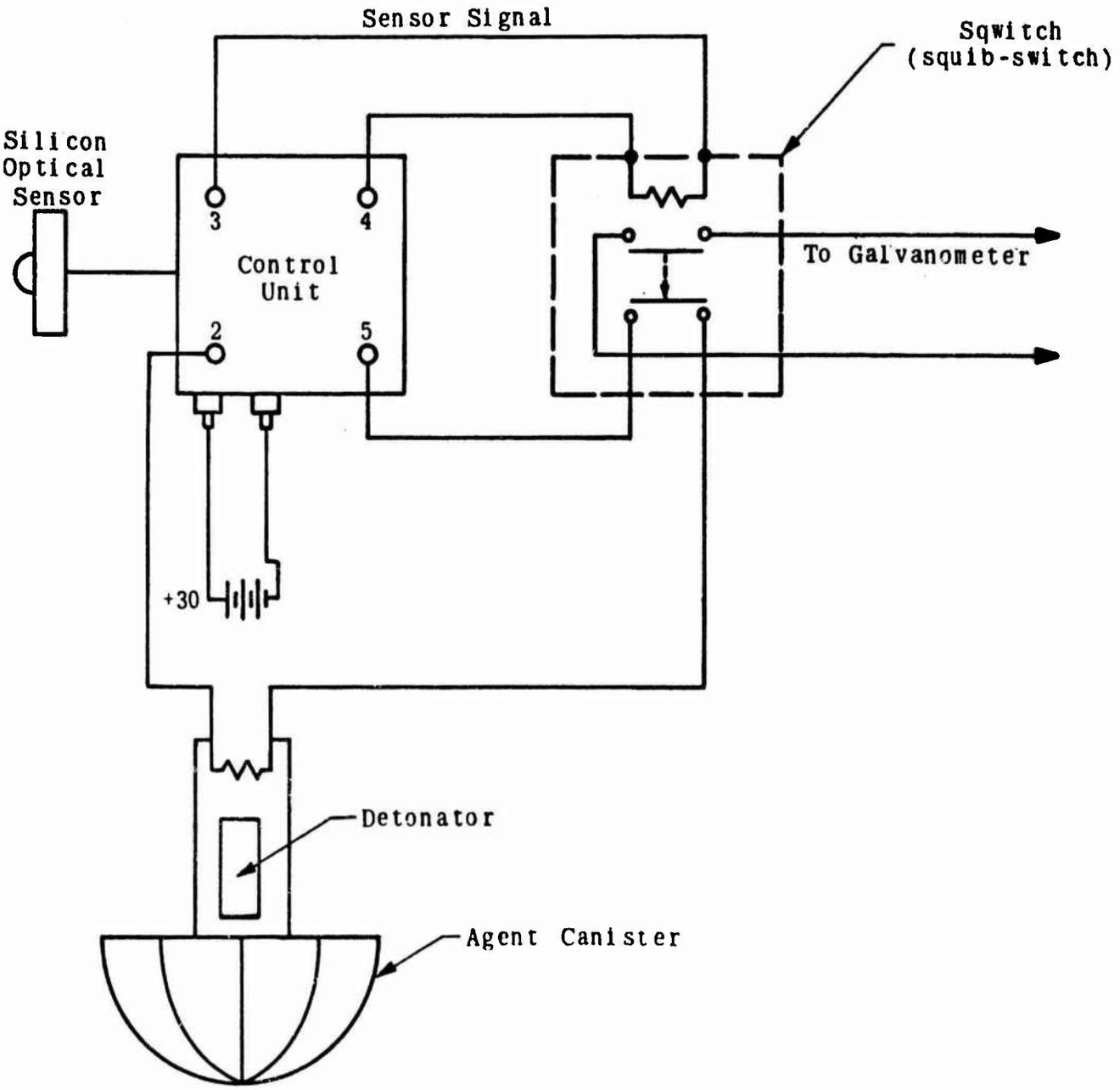

Figure 32. Electrical Schematic Diagram for Suppression Tests.

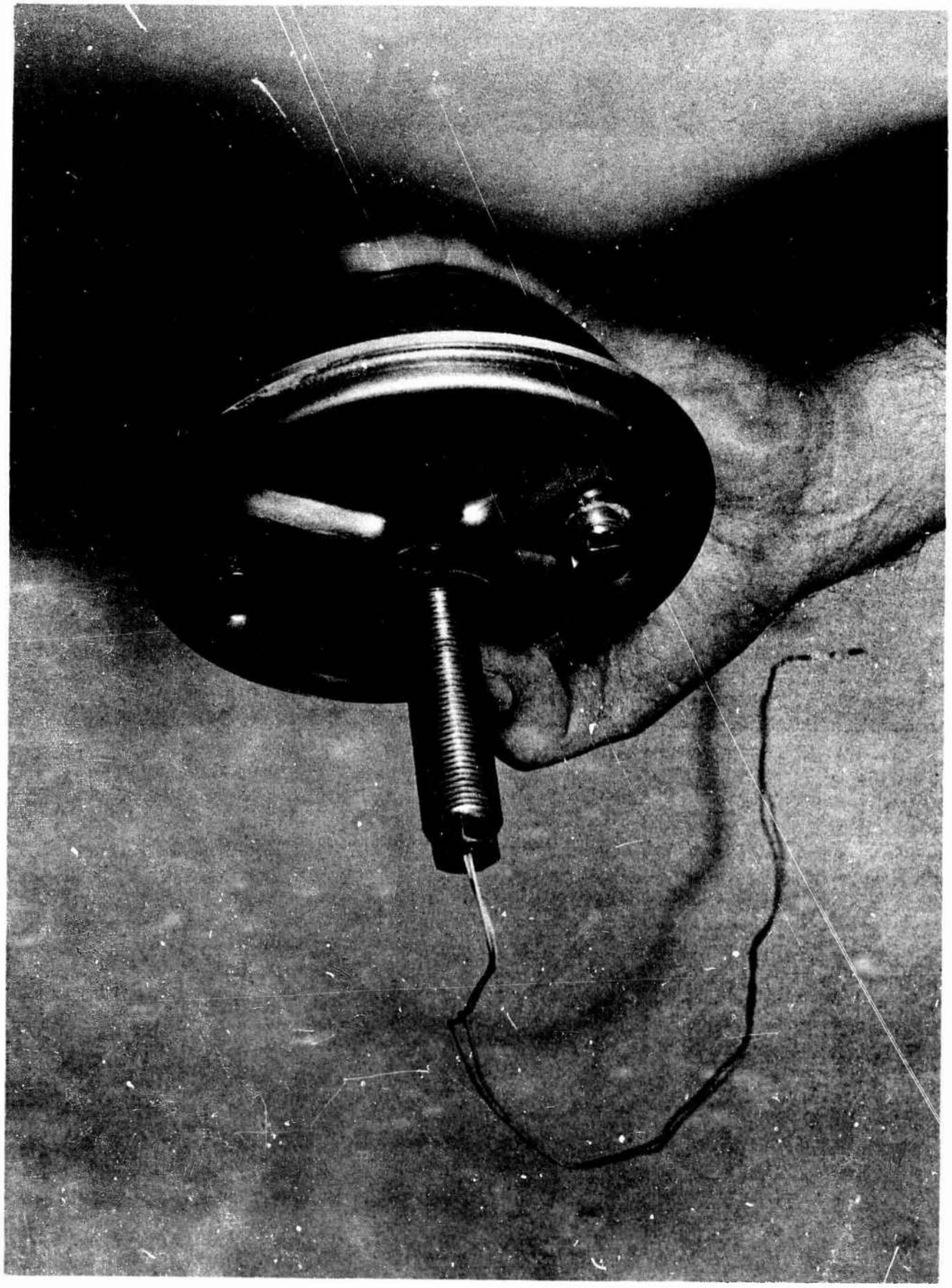

Figure 33. Fenwal Industrial Type Suppression Unit.

60233

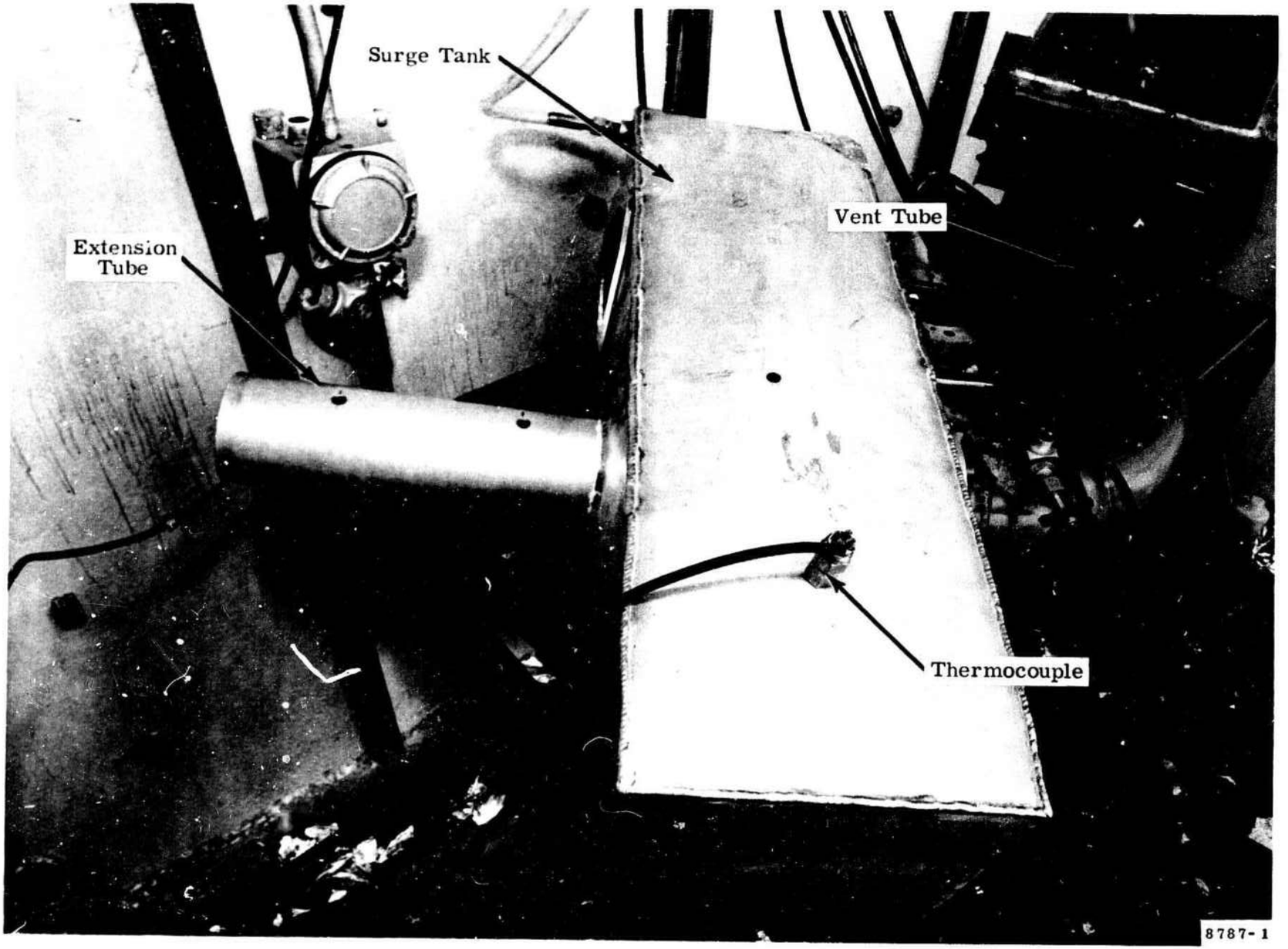

Figure 34. Surge Tank Modified for Explosion Suppression Tests.

60 32 32

Ionization probes were installed for the last six suppression tests; however, the sonic pressure pulses traveling down the tube deflected the probes giving erroneous indications of flame speed.

3.5.3 Results and Discussion

The results of the test are tabulated in Table 10. The flame speed was calculated from the normal system thermocouples located in the vent tube. The suppressor was installed in the surge tank wall nearest the wing tip for the first three tests (G-2, -3, -12) and installed in the aft wall of the surge tank for the last eight tests (G-15 to -42). The latter tests utilized a 4-inch diameter extension tube in the surge tank-reserve tank wall and was instrumented with a thermocouple in the tube.

The results of this rather small sampling of tests provide the following results with standard industrial type explosion suppression units:

1. Flames which traverse the vent tube in times of 18 msec or more (i.e., equivalent to average flame speeds of 140 ft/sec or less) do not propagate through the surge tank.

2. Flames which traverse the vent tube in times of 11 msec or less (i.e., equivalent to average flame speeds of 230 ft/sec or greater) do propagate through the surge tank.

These data indicate that the industrial type explosion suppression system will prevent flames, whose speeds are comparable to the maximum flame speeds measured during simulated lightning experiments, from propagating through the surge tank into the reserve tank. The margin of safety of this particular system is limited since the system may not be effective for somewhat higher flame speeds.

The actuation of the suppressor canister in the surge tank apparently caused a decrease in flame speed through the vent tube for those tests where the initial flame speed was approximately 100 ft/sec or less. This may be due to a slight increase in back pressure caused by the detonation of the canister or by dispersal of the agent into the vent tube. At higher initial flame speeds, there was no evidence that the suppressor actuation caused a decrease in the flame speed in the vent tube.

Table 10. Results of Flame Suppression Tests.

Test No.	Flame Speed (ft/sec)[a]	Suppressor Installed?	Comment
G-6	312 (8 msec)	No	—
G-2	312 (8 msec)	Yes	Not effective[b]
G-3	312 (8 msec)	Yes	Not effective[b]
G-28	250 (10 msec)	Yes	Not effective[b]
G-1	230 (11 msec)	No	—
G-15	230 (11 msec)	Yes	Not effective[b]
G-41	140 (18 msec)	Yes	Effective[d]
G-36	90 (28 msec)	Yes	Effective[d]
G-19	55 (45 msec)	Yes	Effective[c]
G-12	45 (55 msec)	Yes	Effective[d]
G-27	34 (73 msec)	Yes	Effective[d]
G-26	17 (150 msec)	Yes	Effective[d]
G-23	11 (230 msec)	Yes	Effective[d]

[a] Flame speed measured between T_2 and T_6. Propagation time between T_2 and T_6 is shown in parentheses

[b] Not effective - surge tank TC (T_9) and extension tube TC (T_{10}) responded.

[c] Effective - surge tank TC (T_9) responded but extension tube TC (T_{10}) did not respond.

[d] Effective - surge tank TC (T_9) and extension tube TC (T_{10}) did not respond.

Another important observation was made during this series of tests. In order to keep the volume of combustible mixture low in the early propagation and flame arresting tests, it was decided to keep the surge tank filled with air and fuel only the vent tube and vent outlet. There was no reason to suspect that flame speeds through the vent duct would be different if the surge tank were filled with flammable mixture or air. It was planned that a test to demonstrate this would be performed near the end of the program. Since the explosion suppression tests required a flammable mixture in the surge tank, tests were made with apparatus conditions the same as those previously tested, except for fuel in the surge tank. These conditions had previously given reproducible results in the 5 ft/sec range and in the 100 to 150 ft/sec range. With the surge tank fueled, however, erratic results were obtained with flame speeds ranging from 5 ft/sec to 500 ft/sec for the same test conditions.

These observations cannot be quantitatively explained at this time. However, since the original system acted like an organ pipe, the presence of a diaphragm between the surge tank and the vent tube could have a drastic effect on the frequency and amplitude of the pulsating flow in the duct. The transient turbulence generated by these flows could substantially affect the flame speed.

Since this observation has some effect on the tests performed with simulated lightning, tests were repeated at Lightning and Transients Research Institute with the surge tank filled with flammable mixture. There was no difference in the results between the fueled surge tank and the air-filled surge tank. This can be explained by comparing the Lightning and Transients Research Institute tests with those performed in the combustion laboratory. The simulated lightning tests (described in Section 3.2) used an inflated balloon to seal the vent tube before the surge tank. Prior to ignition, the balloon was deflated. Therefore, this system was not perturbed by the presence of the diaphragm. The combustion laboratory tests did use an aluminum foil diaphragm between the vent tube and surge tank, and even when the diaphragm was perforated, the system was still perturbed by its presence. Small geometrical effects, such as the elbow clearance in the surge tank could have been responsible for the high, unstable flow speeds measured with the surge tank fueled. This indicates a requirement for more exact hydrodynamic simulation of the surge tank in any future work than had been thought necessary heretofore.

3.6 PLASMA AND BLAST TESTS

3.6.1 General

Two phenomena, reported in earlier studies,[9] concerned the possibility of plasma being generated which could penetrate long tubes and the possibility of very high pressure peaks, as large as 10 to 100 atmospheres, occurring a considerable distance away from the core of a lightning stroke. It has been stated in the previous study by Lockheed that "flame arresters of normal design appear to offer no protection if the plasma-like discharge occurs," and "the plasma generated by a high-energy discharge is capable of igniting a flammable mixture at a considerable distance from the source of discharge." The experimental investigations have also indicated pressure and temperature ratios of less than two in regions beyond one foot from experimental discharges.

Since both these phenomena are of direct concern to an understanding of ignition and flame propagation through the aircraft vent, a series of experiments was performed to determine the presence of plasma and, if the plasma exists, to obtain information on its velocity and effective length of penetration into the actual vent duct hardware. Another series of tests was conducted to determine if large blast waves propagate inside the 707 vent assembly and vent duct when directly struck by simulated lightning discharge energies of two of three orders of magnitude larger than those previously studied.

3.6.2 Apparatus

3.6.2.1 Plasma Detectors - This plasma investigation was conducted by Atlantic Research Corporation with the aid of simulated lightning strikes by Lightning and Transients Research Institute to vent ducts which had been instrumented to measure velocity and effective penetration length of plasma.

The instrumentation takes advantage of the high level of ionization present in a plasma, rather than temperature, luminosity, or other properties which could be confused with other phenomena associated with lightning and combustion. The instrumentation consisted of a 90-volt battery, a series resistor and two spark-plug mounted probes installed through insulators into the duct. A four-beam oscillograph was mounted across the resistor. The schematic drawing of the instrumentation is shown in Figure 35.

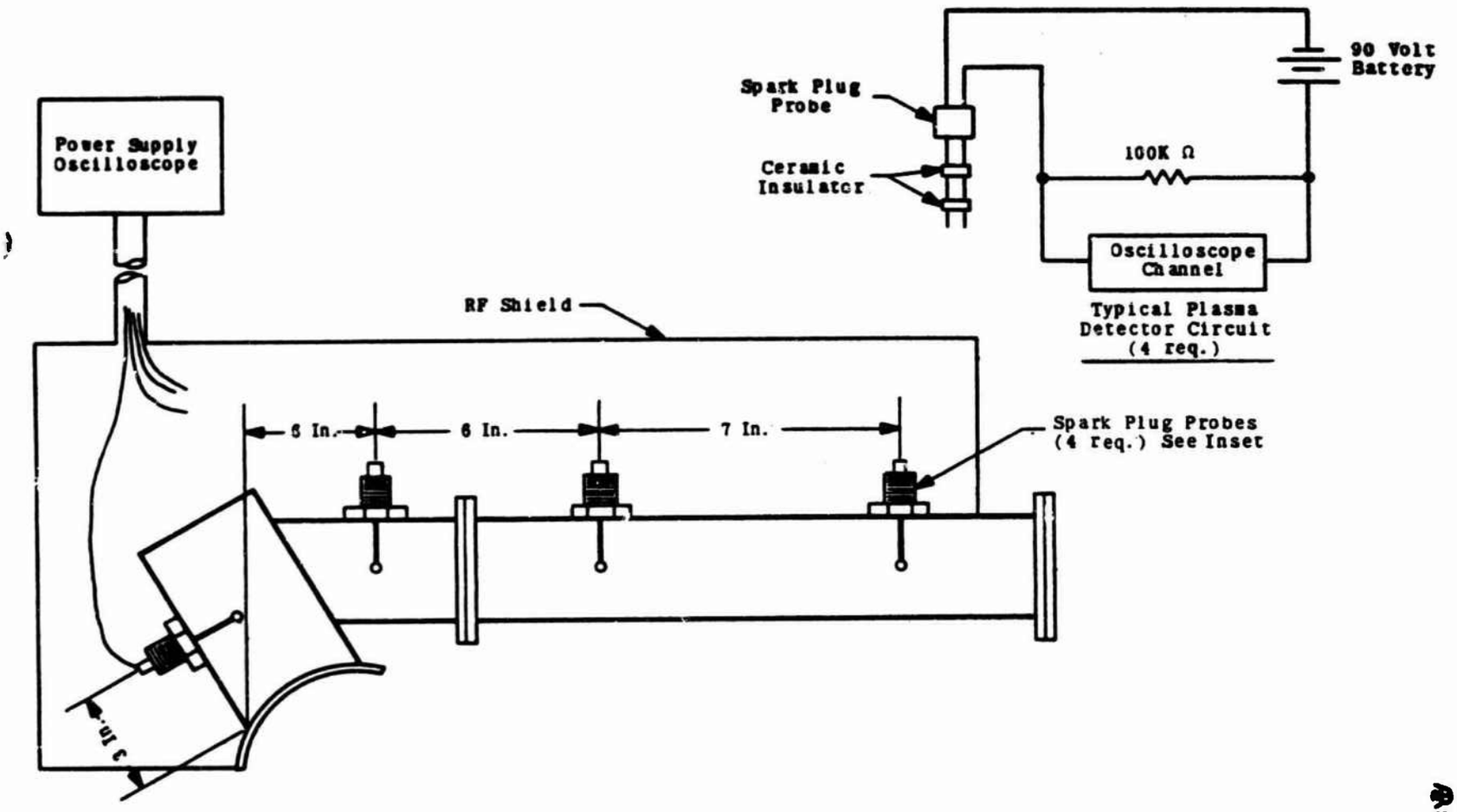

Figure 35. Plasma Detector Locations and Electrical Schematic Diagram.

As ions pass between the probes, current flows across the gap and the series resistor, registering on the oscilloscope. The effectiveness of this device was demonstrated by passing an acetylene-air flame past the probes, which indicated the presence of the relatively small number of ions in the flame.

Four sets of plasma detectors were installed in the vent outlet and vent tube as shown in Figure 35. The leads to the probes were shielded with an aluminum housing to minimize the effect of electromagnetic radiations from the arc. The output of the four detectors was fed into one four-beam oscilloscope so that plasma velocity could be determined. Triggering of one or more probes would establish effective distance of penetration. It was possible to move the probes to investigate effective penetration lengths ranging from several inches to several feet.

It was planned to undertake the initial tests with simulated lightning strikes at Lightning and Transients Research Institute without fuel in the vent. These tests did not detect plasma at any point in the tube, so a planned test series with an explosive mixture in the vent duct was omitted from the program.

3.6.2.2 Blast Measurements - Blast measurements were performed using an Atlantic Research Corporation LC-13 blast probe. The probe was mounted in the center of the vent duct at the outboard flange by means of a Plexiglas cross, and the vent duct was installed in the simulated aluminum wing tip. (See Figure 36.) The probe was vibration and shock insulated with 1/8-inch thick foam rubber, but since this was insufficient high-voltage electrical insulation, the simulated wing tip was insulated from ground with sheets of Plexiglas. The output from the probe went to an oscilloscope with a Polaroid photographic attachment.

3.6.3 Results and Discussion

3.6.3.1 Plasma Tests - All plasma tests were conducted at the high-current facility of Lightning and Transients Research Institute using a tape discharge at 5 kv. The first test employed all bare probes while, in the remaining tests, one or two probes were isolated from any ionization effects. This was done by placing an aluminum sheet metal baffle across the tube at the outboard flange to isolate a pair of probes. The removal of a single probe from the vent tube and

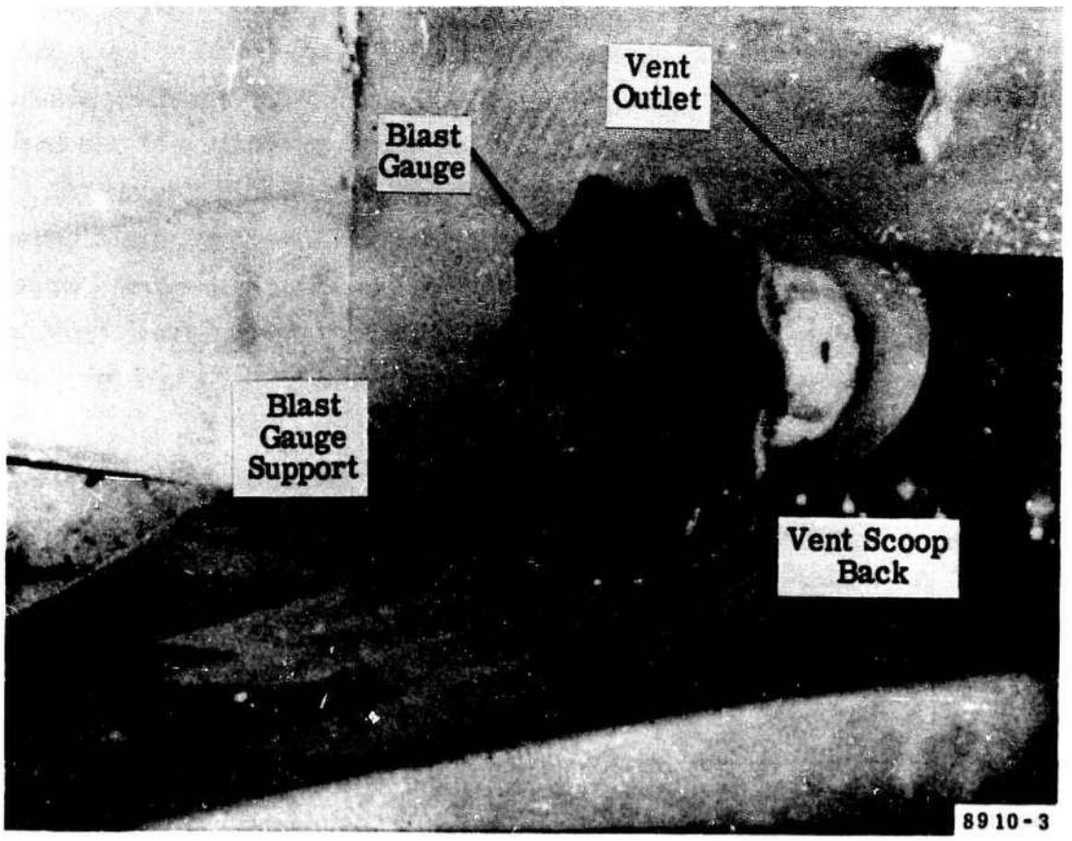

Figure 36. Blast Gauge Location in Vent Tube.

603233

electrically isolating it from the system (while it remained in the housing) provided the additional information needed to interpret the plasma test results.

In the first series of tests all the beams on the oscilloscope triggered. This result was suspect, since the four beams were triggered simultaneously and all had the same frequency and amplitude characteristics. Varying the scope sweep rate and sensitivity did not change the characteristics among any of the four sweeps. Similar results were observed on all four probes when the vent tube was baffled and two inboard probes were isolated in the tube as well as when one probe was physically and electrically isolated from the vent tube. Evidently, the instrumentation responded to the high level of electromagnetic radiation present around the test facility. However, the data can still be of use in determining if plasma were present. Plasma, if present, would trigger the probes giving oscilloscope traces which would be different in form and time sequence from those of electromagnetic actuation. Since the same waveforms were generated simultaneously from detectors in the vent tube and from isolated detectors and no other signals were detected, it could well be that no plasma was ever present.

There remains the possibility that plasma was generated in these tests but that the overriding signal strength produced by the high level of the electromagnetic radiation in the test area prevented its detection. Time was too short in this limited program to explore this possibility, and the question of plasma should be taken up again in a long-range program.

3.6.3.2 Blast Measurements - The results of the blast tests are shown in Table 11. Tests were made in the high-current facility with tape discharges both parallel and perpendicular to the vent opening at voltages from 5 kv to 20 kv.

Since Lightning and Transients Research Institute has experimentally measured pressures of 7 to 8 psig at 6 inches to 18 inches from a discharge (see Figures 37 and 38), it would appear that pressures of up to 14 psig measured in the duct are due to reflection and reinforcement of the pressure waves as they propagate into the tube.

Table 11. Results of Blast Measurements.

Discharge Voltage (kv)[b]	Pressure (psig)		Pulse Duration (μsec)
	Peak	Average	
5	4	2	500
5	4	2	400
5	6	2	500
5[a]	9	4	600
5[a]	10	4	500
10	10	5	500
10	2	1.5	500
10[a]	12	6	500
10[a]	14	6	500
15	9	4	400
15[c]	3	2	500

[a]Blast probe electrically insulated from vent tube and discharge tape was perpendicular to and centered in the vent opening.

[b]All discharges were through aluminized tape placed parallel to the vent duct opening unless otherwise noted.

[c]Discharge location at side of vent opening.

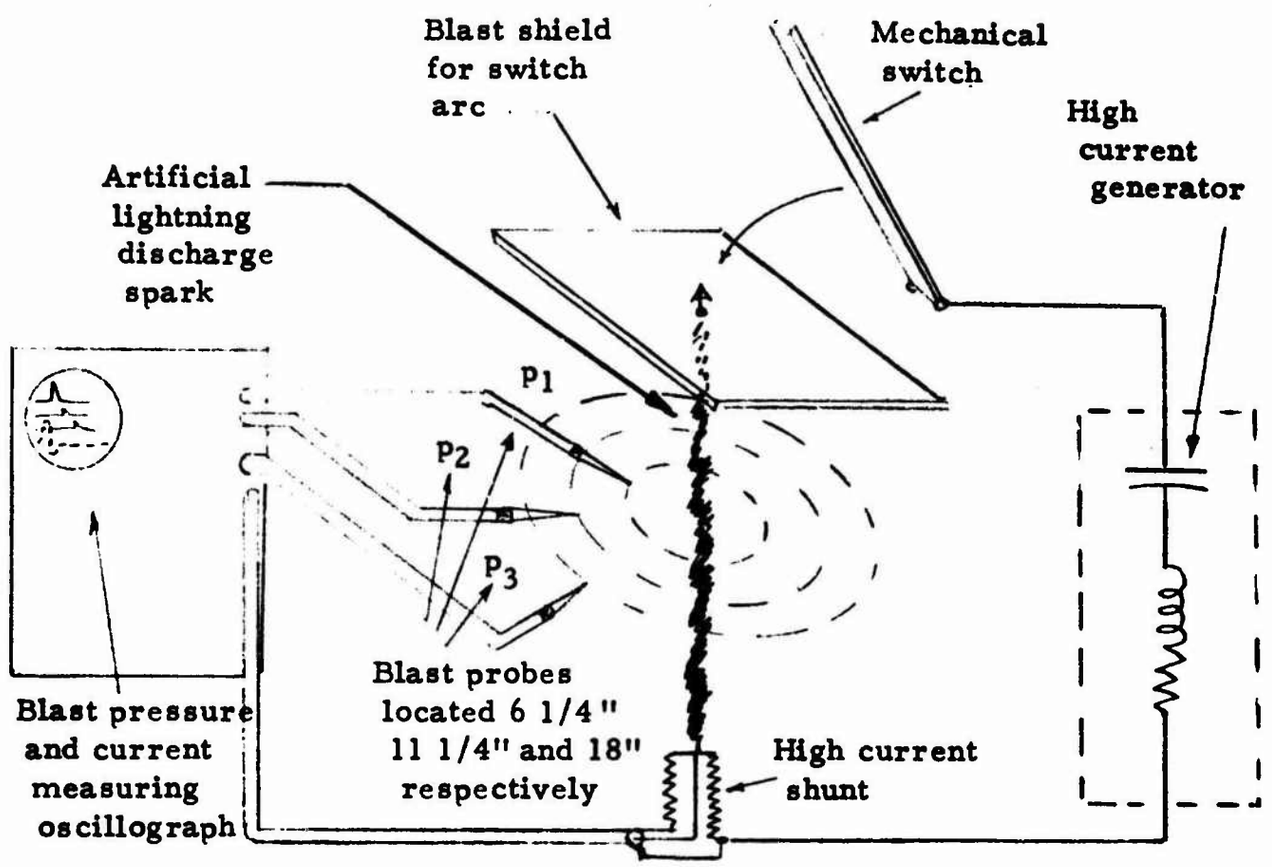

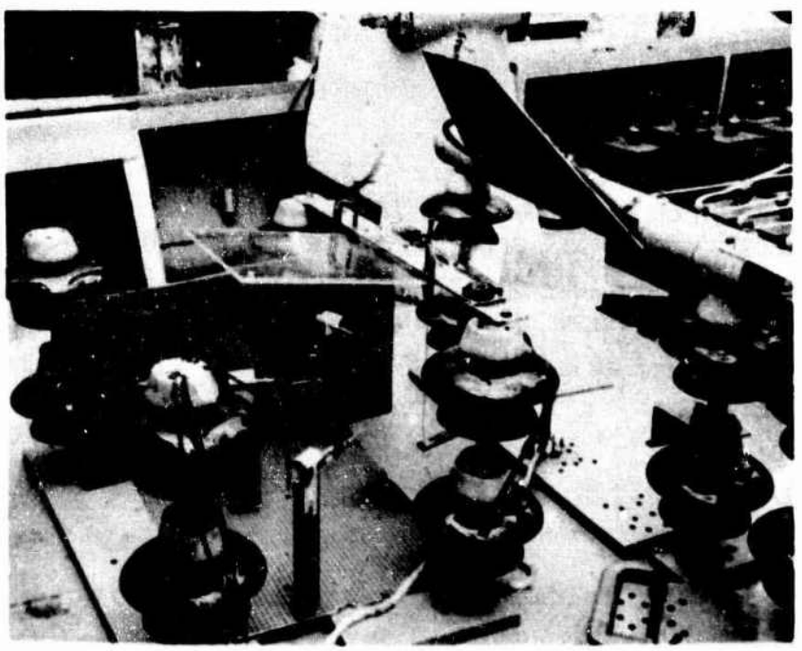

32486

Figure 37. Apparatus for Blast Measurement Performed by Lightning and Transients Research Institute.

603233

All pressures - 9 psi/div. , currents - 30,000 amps/div, sweeps-200 usec/div.

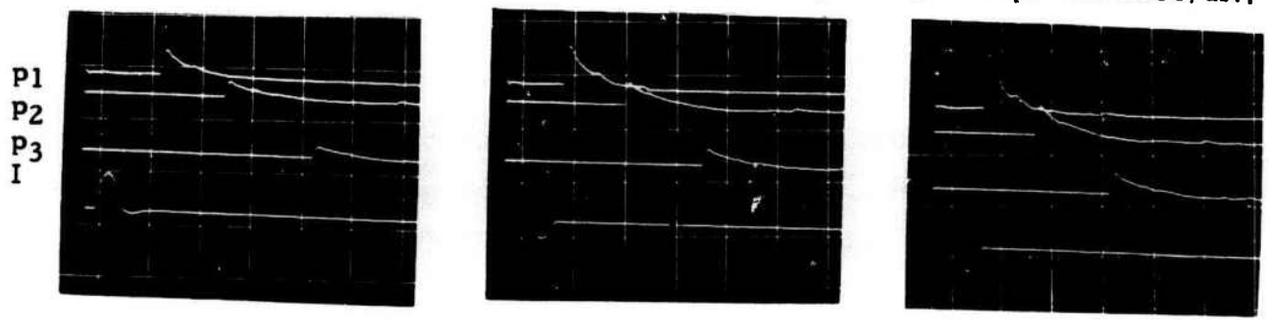

Pressure wave variation with discharge current--
0.003"x0.375" aluminum foil strip used to initiate discharge

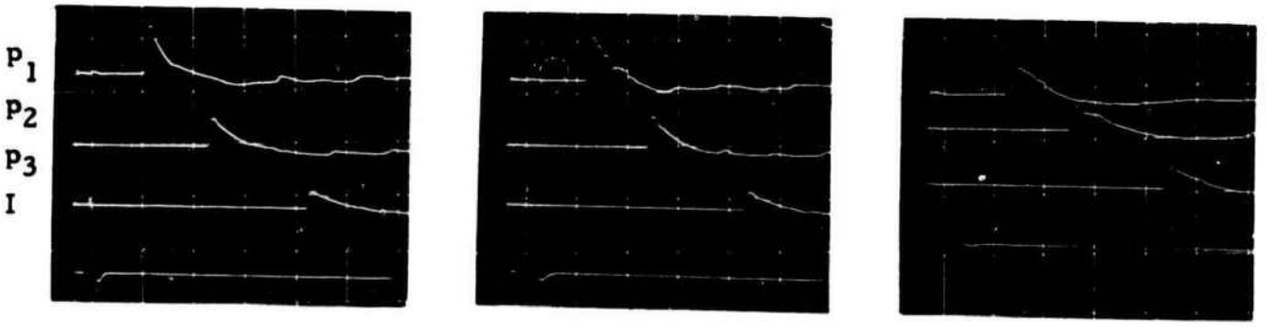

Pressure wave variation with current rate of rise

32485

Figure 38. Results of Blast Tests Performed by Lightning and Transients Research Institute.

603233

There was no evidence of any large magnitude pressure pulses at these distances from the probe. If any were present they would have to be of such short duration (less than 1 μsec) that they would not be picked up by the blast instrumentation.

3.7 CONCLUSIONS FROM EXPERIMENTAL PROGRAM

3.7.1 Flame Propagation

1. Simulated lightning strikes to the vent outlet can initiate flames which will propagate through the 707 vent system into the fuel tanks when a flammable mixture is present.

2. Flames initiated by simulated lightning will propagate through the vent duct at speeds up to 150 ft/sec and generate pressures up to 15 psig. The flame speed and pressure generated appear to be dependent upon the total energy deposited in the vicinity of the vent outlet by the discharge and are not strongly dependent upon the current rate of rise.

3. The 707 vent duct and surge tank act as an organ pipe and provide flame speeds greater than the usual turbulent burning velocities due to large pulsing mass flows in the duct.

4. A simple laboratory apparatus has been developed which duplicates the range of flame speeds and pressures in a duct generated by large energy discharges.

3.7.2 Flame Arresters

1. Flame arresters located in the vent duct will prevent simulated lightning initiated flames from propagating through the duct into the surge tank and fuel tanks.

2. The flame arrester openings should have characteristic cell dimensions of the order of 0.050 inch. Stainless steel honeycomb or rolled corrugated strip with cell depths of 1 inch are satisfactory.

3. Flame arresters located in the 707 vent duct near the vent outlet are ineffective due to the inward mass flow developed in the duct by the simulated lightning discharge. Flame arresters located near the surge tank are effective.

4. Screens and wire gauzes are ineffective against the high-velocity flame fronts.

3.7.3 Explosion Suppression

1. Flames which traverse the vent tube in times of 18 msec or more (i.e., equivalent to average flame speeds of 140 ft/sec or less) do not propagate through the surge tank.

2. Flames which traverse the vent tube in times of 11 msec or less (i.e., equivalent to average flame speeds of 230 ft/sec or greater) do propagate through the surge tank.

3.7.4 Plasma Tests

There was no evidence of plasma (i.e., high ion concentration) penetration into the vent outlet and vent tube from simulated lightning strikes directly to the vent outlet.

3.7.5 Blast Tests

There was no evidence of pressure ratios exceeding 2 generated in the vent tube by simulated strikes directly to the vent outlet. There is evidence that pressure waves are reflected and reinforced as they propagate down the vent tube.

4.0 ANALYTICAL PROGRAM

4.1 FLAME ARRESTERS

The quenching of premixed laminar flames by relatively cold solid surfaces has been explored by several workers.[13,14] This work was conducted using stagnant or low-flow-velocity systems in which the residence time (see Section 3.4) was large compared to the critical residence time required for extinction. There are no data on critical residence times in the literature, so that presently their magnitudes can only be estimated as shown in Section 3.4. The quenching distances as measured by the quoted investigators are inapplicable to the present case in which large flow velocities of unburned gas may occur. However, these measurements do serve as a guide in establishing criterion for flame arrester design. Harris et al.[13] found that the quenching diameter in tubes for a 1.1 stoichiometric propane-air mixture at standard temperature and pressure is 0.110 inch. The corresponding quenching distance for flat plates is 0.073 inch as reported by Friedman and Johnston.[14] It should be noted that the quenching distance increases with decreasing pressure. Hence arresters effective at standard pressure are automatically effective at lower pressures (i.e., higher altitudes).

Due to the lack of measurements in flowing systems, arresters in this program were chosen to have cell sizes ranging from approximately 0.050 inch to about 0.010 inch.

The geometry of the flame arrester cell plays a role in determining its effectiveness, as evidenced by differences in quenching distances for tubes and flat plates. The geometries of the arresters in this program were dictated by availability rather than purely technical considerations.

The composition of the flame arrester material does not affect the quenching distance* in stagnant systems,[15] though the heat capacity of the material is of importance in determining the flame resistance characteristics

*This is attributable to the fact that the controlling heat transfer rate is determined by the thermal diffusivity and temperature gradient in the burned gas, and not by the thermal resistance of the wall material.

of the arrester. That is, if the total heat capacity of the arrester is small, then the temperature of the arrester will increase rapidly to a value where the arrester fails. A flame initially stabilized on the flame arrester surface or a continuous flow of hot burning gases could heat a normally quenching channel to a temperature where the flame can penetrate. This problem may be analyzed as follows.

Using a heat balance it is possible to derive a relation between the channel dimensions and the length of hot gases that can be quenched by the channel. Assume a rectangular, honeycomb-type flame arrester of depth "a" in a constant-diameter duct. A mass of hot, freshly burned and still-burning turbulent gases of length "b" is propelled through the arrester by a pressure gradient caused by combustion and/or ohmic heating by lightning. Assume the openings, of width "δ", in the flame arrester are smaller than the quencing distance. Assume also that only a relatively small cross section of the duct is blocked by the material (of thickness "t") of the honeycomb.

Clearly, the depth "a" of the flame arrester must be as small as possible to minimize viscous pressure drop, but the heat capacity of the arrester must be high enough so that the arrester maintains its quenching effectiveness. Yet the thickness "t" of the metal cannot be very great without producing unwanted pressure drop. One wishes to find an expression relating a, b, δ, t for the just effective arrester.

Assume that the heat transfer coefficient from gas to arrester is adequate when "δ" is smaller than the quenching distance. Then, a heat balance gives

$$a\,(4\delta)\left(\frac{t}{2}\right)\rho_m\,C_m\,(T_c - T_o) = b\,(\delta + t)^2\,\rho_g\,C_g\,(T_f - T_c)$$

Here ρ_m and C_m are density and heat capacity of the metal and ρ_g and C_g the corresponding properties of the hot gas. T_o is initial arrester temperature, T_f is flame temperature, and T_c is the critical temperature at which the arrester becomes ineffective.

If $\delta >> t$, the relation simplifies and, on rearranging,

$$\frac{b}{a} = 2\frac{t}{\delta}\frac{\rho_m C_m}{\rho_g C_g}\left(\frac{T_c - T_o}{T_f - T_c}\right)$$

As a rough estimate, $(T_f - T_c) \simeq 2 (T_c - T_o)$. Using this, the equation reduces to:

$$\frac{b}{a} \simeq \frac{t}{\delta}\frac{\rho_m C_m}{\rho_m C_g}$$

Introducing some numerical values, $\rho_g = 0.0002$ gm/cc, $\rho_m = 2.7$ gm/cc (aluminum), $C_g = 0.3$ cal/gm-°C, and $C_m = 0.2$ cal/gm-°C (aluminum). Accordingly,

$$\frac{b}{a} = 10^4 \frac{t}{\delta}$$

Thus, if $t = 0.001$ inch, $\delta = 0.01$ inch, and $a = 0.5$ inch, then $b = 500$ inches.

Actual performance will always be less than this because of finite transfer rates. However, a reasonable design by this principle is seen to be possible.

4.2 INCREASED VENT VELOCITIES

One method that has been considered as a means of preventing flame propagation through the vent tube of the Boeing 707 is increasing the velocity of the effluent vent gases to a point where the critical flow for flame flashback is exceeded. This could be accomplished by addition of free stream air or engine bleed air to the vent system. In order to determine the flow required for flashback, use is made of the fact that flashback will occur if the wall velocity gradient is less than a critical value.[6] Conceptually, a flame eating its way back against an adverse velocity will advance fastest near the wall where the boundary layer has slowed the adverse flow. As the flow rate increases, the gradient at the wall steepens and the point at which the flame

can advance approaches the wall. At some critical velocity gradient the flame is so close to the wall that the flame is quenched and can no longer propagate upstream.

The value of this critical velocity gradient depends on the composition and pressure of the mixture. It is independent of tube diameter for tubes whose diameters substantially exceed the quenching diameter. The values of these critical velocity gradients have been determined experimentally.

It is possible to calculate the wall velocity for pipe flow using the following analysis:

The shear stress at the wall is μg, μ is the viscosity, g is the wall velocity gradient. By definition,[16]

$$\mu g = f \frac{\rho (\bar{v})^2}{2}$$

where f is the friction factor and $\bar{v}$ the bulk fluid velocity. Experimentally, it has been found that,

for laminar flow $f = \frac{16}{Re}$; $Re < 2000$ in smooth pipes

for turbulent flow $f = \frac{0.046}{Re^{0.2}}$; $Re > 5000$

thus

$$g = 8\, Re \frac{\nu}{D^2} \quad \text{for } Re < 2000$$

$$g = 0.023\, Re^{1.8} \frac{\nu}{D^2} \quad \text{for } Re > 5000$$

Figure 39 is a plot of g versus Re for various values of tube diameter using a value of the kinematic viscosity, $\nu = 13.5 \times 10^{-5}$ ft^2/sec for air at 1 atm and 0°C.

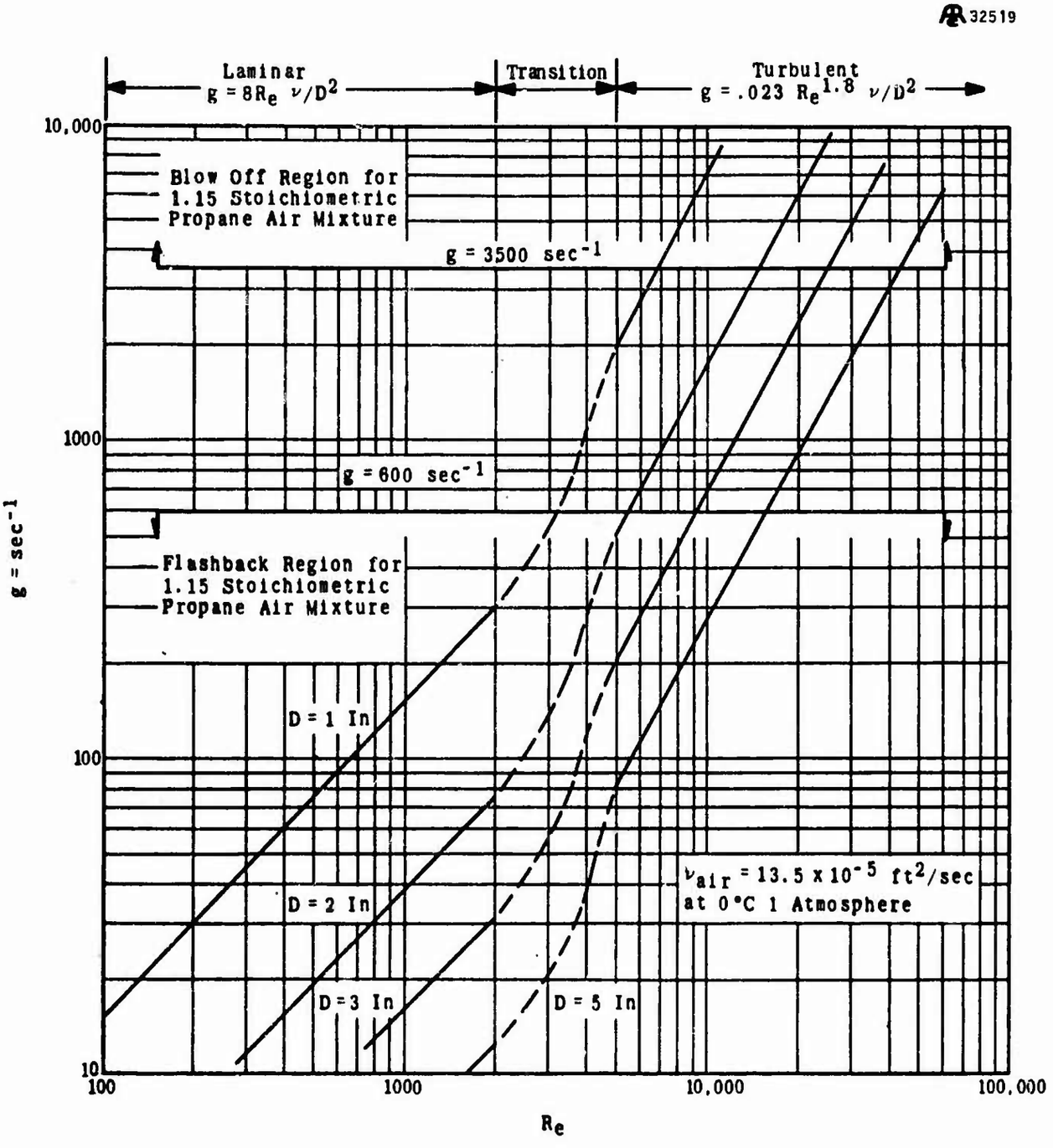

Figure 39. Wall Velocity Gradients Versus Reynolds Number for Various Tube Diameters.

The critical velocity gradient for flashback for propane-air mixture is 600 sec^{-1}; this value occurs for a mixture fraction of 1.15 times stoichiometric.[16]

The value 600 sec^{-1} is drawn as a straight line in Figure 39. It is assumed that the fuel-air mixture in the tube is the 1.15 stoichiometric mixture. Any other mixture exhibits a lower critical velocity gradient for flashback. Hence the value of 600 sec^{-1} represents the most severe case.

Using Figure 39, it is possible to determine the flow velocity and volumetric flow rate necessary to prevent wall flashback. The results are summarized in Table 12

Though wall quenching will occur if the bulk flow velocity exceeds those given in Table 12, a turbulent flame might propagate through the core of the flow. To investigate this phenomenon a correlation relating turbulent burning speed to flow velocity is required. Such a correlation is given by Williams and Bollinger.[17]

$$U_T = 0.1761\, S_L\, D^{0.2564}\, Re^{0.238}$$

U_T = Turbulent burning velocity in cm/sec

S_L = Laminar burning velocity in cm/sec

D = Tube diameter in cm

Re = Reynolds number of pipe flow

The correlation was established experimentally, for ranges of $3000 < Re < 35{,}000$, $1/4$ inch $< D <$ $9/8$ inch, and for fuels acetylene, ethylene, and propane.

Figure 40 is a plot of U_T versus Re for various tube diameters. Figure 41 plots U_T versus $\bar{V}$ (the bulk flow velocity) for various tube diameters. If U_T exceeds $\bar{V}$ one would expect flashback through the core of the flow. Regions to the right of the line $U_T = \bar{V}$ are considered safe with regard to core flashback. Also plotted in Figure 41 is the broken line which is the limit of wall flashback. To the right of the broken line the wall velocity gradient is greater than the critical value of 600 sec^{-1} and wall flashback

Table 12. Flow Velocities Required to Prevent Wall Flashbacks.

Tube Diameter (in)	Bulk Flow Velocity (ft/sec)	Flow Rate (ft^3/min)
5	5	40.9
3	4.8	14.1
2	4.4	5.8
1	5.2	1.7

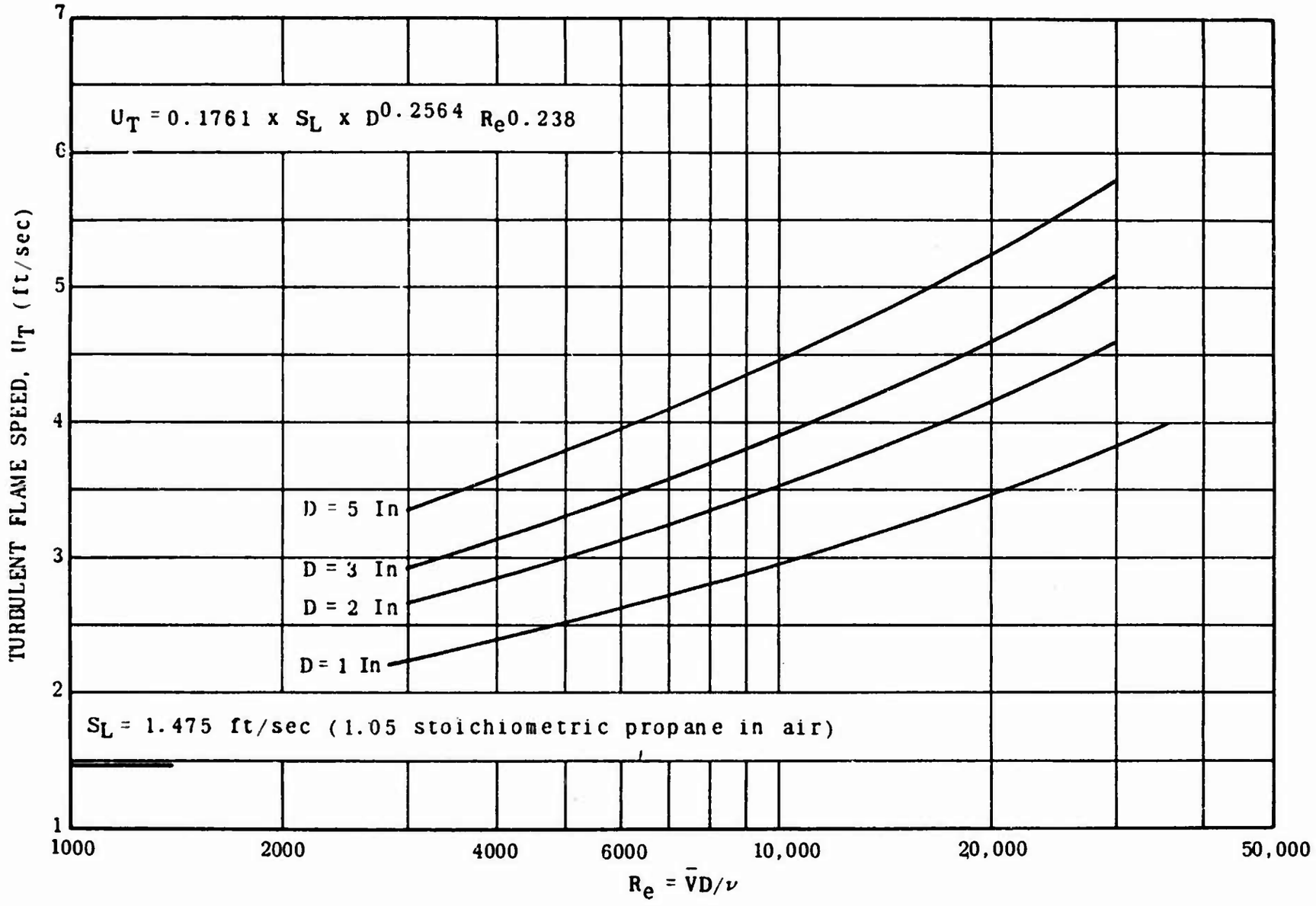

AR 32528

Figure 40. Turbulent Flame Speed Versus Reynolds Number for Various Tube Diameters.

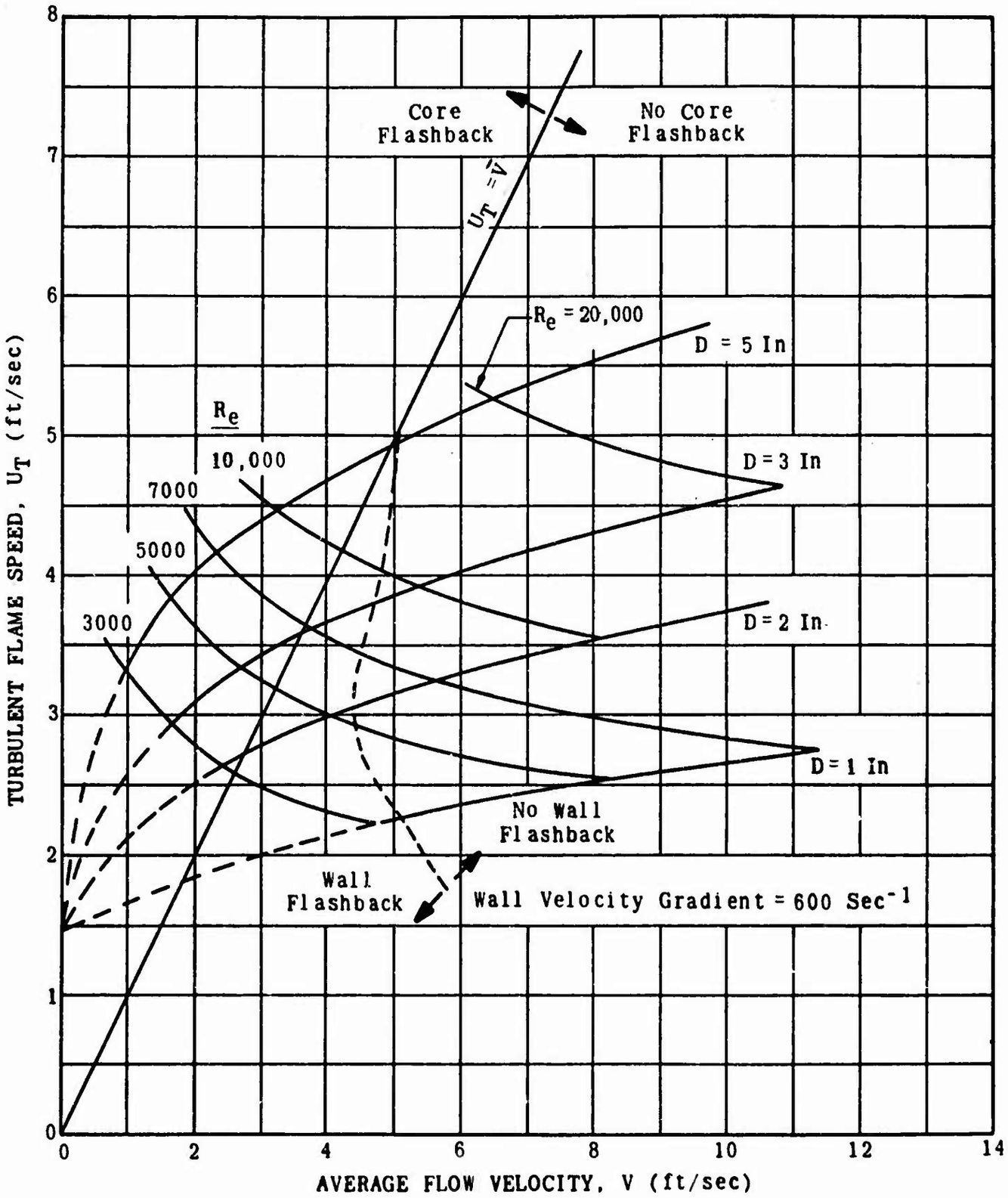

Figure 41. Turbulent Flame Speed Versus Bulk Velocity for Various Tube Diameters.

will not occur. It should be remembered that these curves are based on extrapolation of correlations outside the range of their verification. Experiments should be performed to check these results.

Considering the above limitation, this analysis shows that in a 5 inch duct a continuous net outflow velocity of 5 ft/sec or more should prevent flame propagation through the duct. However, as described in Section 4.4, simulated lightning strikes in the vicinity of the vent outlet induce large convective mass flows into the vent system. Instantaneous flow reversal would make this method inadequate for preventing flame propagation if the flow reversal was of sufficient duration. Measurements have shown that flame speeds of the order of 150 ft/sec are caused by artificial lightning discharges near the vent outlet (see Section 3.2.2) and according to the postulated mechanism (see Section 3.4) thesespeeds are associated with mass flow velocities of comparable magnitude. Hence it appears that outflow velocities of the same order would be needed to prevent the transient flow reversal that is responsible for rapid flame propagation. However, if the transient is of sufficiently short duration these high flow velocities may not be necessary. Further experimental work must be undertaken to determine the merit of this approach. This brief study shows that the idea is feasible.

4.3 OTHER PROTECTIVE TECHNIQUES

4.3.1 General

In addition to evaluating flame and explosion protection of the aircraft vent system offered by flame arresters, explosion suppression systems, and high-velocity discharge of vapors to the atmosphere, several other protection techniques have been examined briefly. These techniques, which are inherently more complex, include the use of mechanical valves in the vent duct to prevent flame propagation through the duct, the use of bladders or other separating devices to isolate the fuel vapor in the tanks from atmospheric oxygen, and the use of nonreactive gases introduced independently into the vent system to prevent an explosive mixture from forming. These three methods have been examined qualitatively to determine their advantages and

disadvantages. No attempt has been made in this study to provide detailed design criteria; however, in the case of inerting systems, other test programs* are in progress which may provide the desired information.

4.3.2 Mechanical Valves

There are two methods in which mechanical valves might be used in the vent system in an attempt to prevent flame propagation through the vent duct to the surge and reserve tanks. These are shown schematically in Figure 42. The first technique would use a parallel duct system to provide vapor flow to the atmosphere through a check valve in one duct. When flow direction reverses, e.g., on aircraft descent, the first check valve closes and a second check valve opens in the parallel duct allowing the tanks to pressurize with air. An independent vent exit and vent inlet would be desirable. The second technique would use a pair of valves in series in the vent duct to provide an "air lock" in the vent system. One valve would always be closed thereby preventing flame propagation through the system. When the first valve is closed and the second is open, pressures in the surge tank and "air lock" would equalize. Then when the second valve closed fully, a servo control would open the first valve allowing the "air lock" to come to ambient pressure. The advantages and disadvantages of both of these systems are described below.

A casual evaluation might indicate that the parallel-duct, check-valve system, has several advantageous characteristics in that it allows fuel vapor to vent from one opening, and if the vapor was ignited, the flame would have to propagate against the flow. In addition, the check valves would be strictly mechanical, operating on pressure differential and not requiring complex and heavy pneumatic, hydraulic, or electric actuators and controls. However, in view of the experimental evidence discussed in Section 3.2 on flame propagation, flame speeds up to 150 ft/sec are probable, which would allow flame propagation through the open check valve in the exhaust vent duct during aircraft ascent.

---

*Pan American World Airways to evaluate inerting systems.

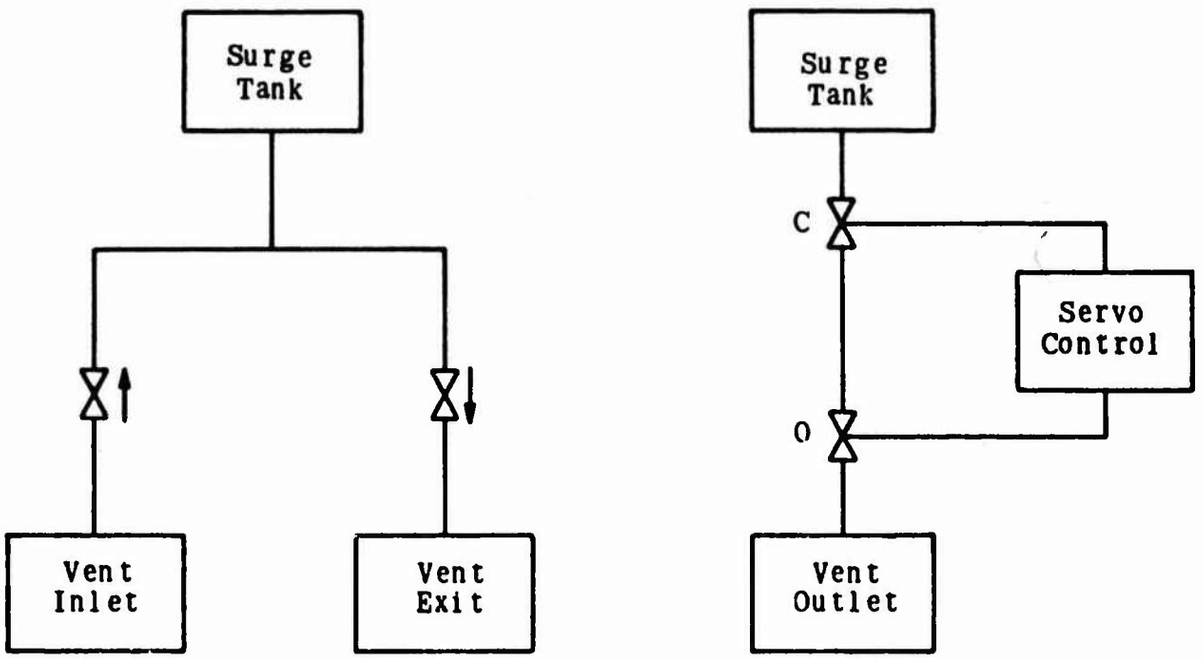

Figure 42. Schematic Diagram of Mechanical Valve Systems.

The failure of this technique to provide protection against flame propagation precludes a discussion of additional disadvantages such as icing, malfunction, size, weight, and pressure drop, some of which could present formidable additional hazards.

The "air lock" series valve system appears, in concept, to provide protection against flame propagation through the vent duct. Two methods could be used; the valves could be normally open and then, at pilot option, the system could be activated to cycle at a given frequency with one valve opening while the other is closed or the system could be designed to cycle at all times during aircraft operation. For valves spaced 3 feet apart, the "air lock" should be sealed for at least one second to prevent the slowest moving flame fronts, i.e., 3 ft/sec, from passing into the surge tank.

Some of the disadvantages of this system are obvious while others are more subtle. The system is complex, requiring a servo control unit with pneumatic, hydraulic, or electronic actuation. The oscillatory operation with moving parts will cause wear of seats, poppets, seals, etc. and increase the probability of malfunction. If either valve failed, disaster from adverse pressure conditions could be averted only by additional protection such as blowout panels to equalize pressure between the fuel tanks and the atmosphere. Valves for the 5-inch diameter ducts of the 707 aircraft would be large, heavy, and might provide excessive pressure drop during ground overfueling conditions. In addition to the above, the system would have to be designed with a large volume between the valves. This volume is necessary since in emergency descent (see Section 5.3) 1470 ft^3 would have to pass through the "air lock". If the volume between the valves was 1/10 that of the void volume in the tanks and the "air lock" equalized pressure with the tanks in ten 15-second cycles (i.e., as the ambient pressure increased per cycle in one psi increments), the differential pressure between the tank volume and ambient would exceed 3 psi by the fourth cycle. For the same volume relationship and twice the cycle frequency the pressure differential would exceed 2 psi within 10 cycles. Less than 2 psi differential pressure would be attained for an "air lock" volume of 1/2 the tank void volume and a 15-second cycle time. These large volumes are prohibitive and in addition, they would compromise the series-valve concept as a flame arresting technique.

4.3.3 Bladders

Bladder tanks (i.e., those which contain fuel only as distinguished from tanks with liners which contain air and fuel) can be used as a protective technique. This system has many operational advantages; however, it is obvious that existing wet-wing aircraft would require extensive modification to incorporate the bladders, in addition to developing a serious weight penalty. Furthermore, bladders may not provide 100 per cent protection on preventing an explosion hazard. Bladder materials such as Buna-N can be used for this application but they must be reinforced with synthetic woven fiber mats. As such they are permeable, to some extent, to hydrocarbon fuels. This phenomenon, or pin-hole leaks and large tears, would provide fuel liquid and/or vapor in the air space surrounding the bladder. Depending upon the amount of air available around the bladder, there may or may not be an explosive mixture present.

The use of bladders can also cause additional hazard as kerosene-type fuels develop a static charge when sloshing inside insulating materials.[13,18] A discharge could have sufficient energy and energy density to ignite the fuel if any air accumulated in the bladder.

4.3.4 Inerting Systems

Although the evaluation of inerting systems was not a part of this short-range study, a review is presented to provide a more complete summary of the possible protective methods against inadvertent fuel combustion.

There are two general schemes which have been proposed. If protective devices cannot be devised to prevent sparking inside of fuel tanks after direct lightning strikes to fuel caps, access ports, etc., then an inerting system could be used to blanket the vapor space in each and every fuel tank. However, if it is desirable to inert only the vent system, then a purge directly into the surge tank or vent tube might provide protection against flame propagation through the vent system. Either scheme could be designed for continuous operation or intermittent operation at the command of the pilot when the aircraft approaches a thunderstorm.

A number of inerting agents can be used including Freons, nitrogen, combustion gases, carbon dioxide, methylbromide, etc. A suitable Freon can be stored as a liquid and would not require high-pressure bottles as would gas storage, but the Freon must vaporize at a low temperature to be effective. Long lines containing liquid or gaseous Freon would be required. Nitrogen can be stored in heavy, high-pressure bottles as a gas or in cryogenic Dewars as a liquid. The gas can be stored indefinitely but the liquid at -320°F would boil off and have to be replaced regularly.

A large storage capacity and large flow rates would be required even for vent system inerting. At maximum climb rates, vapors leave the vent at about 12 ft/sec (100 CFM) and if the mixture was to be decreased from the rich limit (2.2 times stoichiometric) to a mixture which would not ignite at any fuel-air ratio, about 1 additional volume of nitrogen would be needed. One hundred ft^3/min of nitrogen is a sizable flow considering that a standard 2000 psi, 240 SCF bottle would be depleted in several minutes. In addition, special regulators, controls and readout devices would have to be developed for this operation, particularly considering the range of temperatures and pressures to which the supply system might be exposed. If a Freon were used, smaller quantities would be required since, in addition to diluting the fuel-air composition, it would also chemically inhibit combustion.

Another method of inerting would be to supply cooled combustion gases to the vent system either from the main combustion chambers or from small auxiliary engines. The oxygen-poor gases could be easily cooled in a finned tube, filtered and then piped into the vent tube or through the main tanks. The main difficulty with this technique is that CO_2 from the combustion gases readily dissolves in the fuel, generating a "soda water" like fluid. This and the extra water vapor could cause many other problems. If inerting appears desirable, a relatively simple and practical system could be evolved based on this concept. The main problem will revolve about the integration of the system into the aircraft.

5.0 ANALYSIS OF HAZARDS INTRODUCED BY FLAME ARRESTERS

5.1 PRESSURE DROP THROUGH FLAME ARRESTER

As part of the hazards analysis the pressure drops through two arresters for various flows of water were determined. The flow rates were selected to give Reynolds numbers through the arrester cells comparable to to those that would occur in the vent tube during a fueling mishap. The fueling mishap would occur if the fuel shut-off valves failed to operate during filling, thereby forcing the fuel out through the vent system.

If the pressure drop through the vent system is too large, overpressures will develop within the tanks possibly causing structural damage. For this reason Boeing has performed pressure drop measurements on the vent system and specified maximum allowable fueling rates for filling through each tank. If a flame arrester is incorporated in the vent tube, an additional pressure drop will accrue and result in lower permissible fueling rates. Table 13 gives the pressure drops for various flow rates of water through the 1/2-inch × 0.050-inch and 1-inch × 0.050-inch flame arresters. The measurements were made with a simple two-fluid manometer with pressure taps located 6 inches upstream and downstream of the flame arresters. An entrance length of 6 feet preceded the sample. A schedule 40 2-inch-diameter steel pipe was used and flow rates of water up to 66 gal/min at 60°F were available.

Figure 43 is a plot of pressure drop through the 1/2-inch × 0.050-inch flame arrester for various bulk flow velocities. Theory predicts that for laminar flow through the arrester cell the pressure drop should have the form

$$\Delta P = \frac{32 L \mu \bar{V}}{D^2 g_c} + K \rho \bar{V}^2$$

where,

L = length of arrester

μ = absolute viscosity of the fluid

D = equivalent diameter of a passage in the arrester

$\bar{V}$ = bulk flow velocity through the arrester

ρ = density of the fluid

K and g_c = constants

Table 13. Results of Pressure Drop Measurements with Flame Arresters.

Flow Rate (gal/min)	Bulk Water Velocity (ft/sec)	Net Pressure Drop Through Arrester[a] 1/2 × 0.050 inch (psi)	1 × 0.050 inch (psi)
7.6	0.73	0.045	0.075
19.7	1.9	0.093	0.200
28.5	2.7	0.144	0.333
32.7	3.1	0.169	0.400
42.4	4.0	0.233	
53.3	5.1	0.316	
66.0	6.3	0.429	

[a]Corrected for pressure drop through straight pipe section.

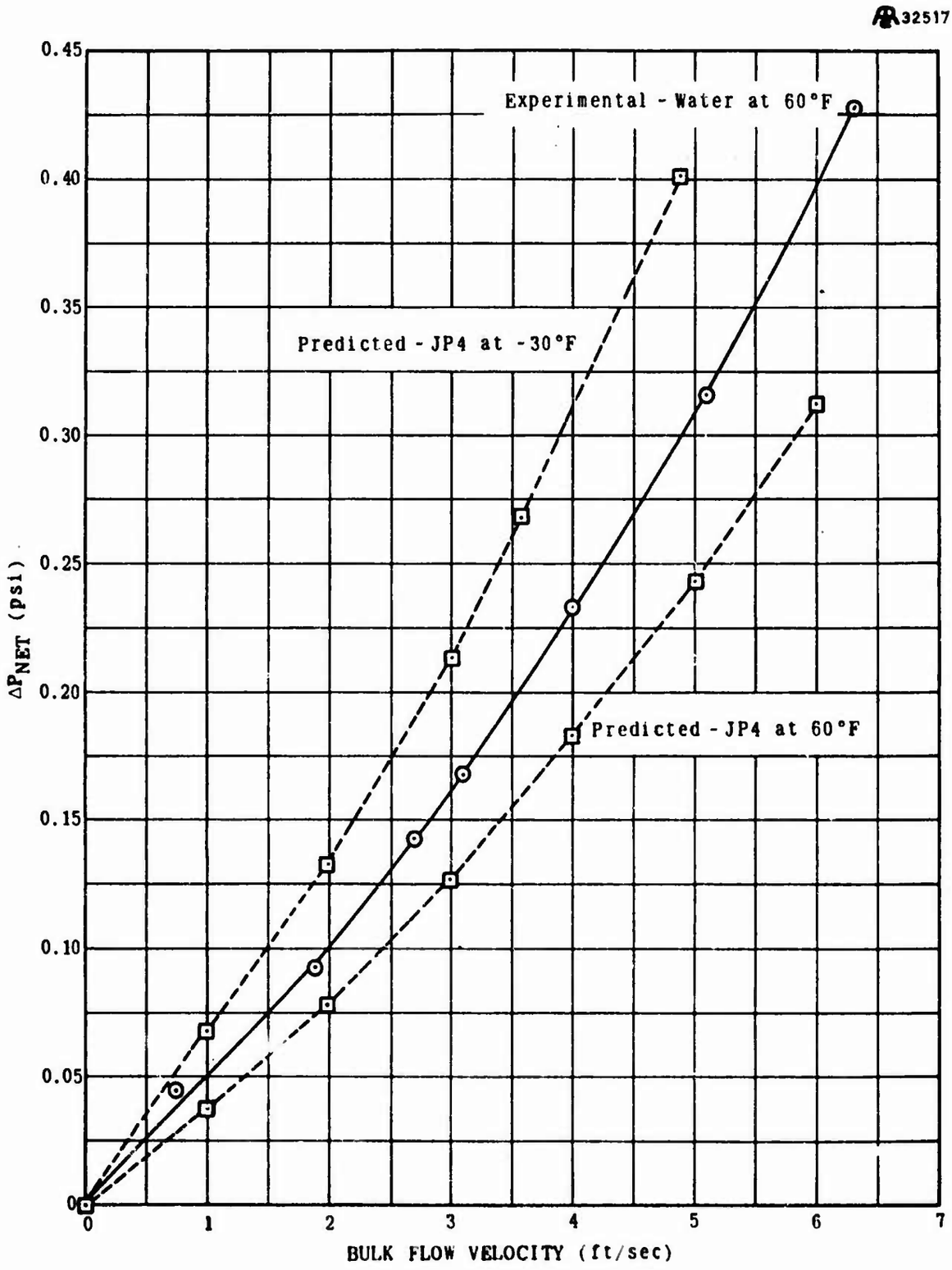

Figure 43. Flame Arrester Pressure Drop Versus Bulk Flow Velocity (1/2 In × 0.050 In Arrester).

The first term arises from skin friction losses; the second arises from entrance and exit losses due to flow constriction. Reference to Figure 43 shows that in the range of interest the pressure drop is nearly a linear function of the bulk flow velocity, indicating that the flow through the arrester is indeed laminar and that entrance and exit losses are negligible (i.e., K = 0). A calculation of the Reynolds number through one of the arrester passages (D = 0.050 inch) for a bulk velocity of 4 ft/sec gives:

$$Re = \frac{\bar{V}D}{\nu} = \frac{4 \times 0.00416}{1.1 \times 10^{-5}} = 1510$$

This value emphasizes that the flow is in the laminar regime.

Because of the above facts it is possible to estimate the pressure drop for the same arrester and flow velocity with JP-4 as the working fluid. Using the pressure drop equation with K = 0 gives

$$\Delta P_{JP-4} = \frac{\mu JP\text{-}4}{\mu \text{ water}} \quad \Delta P \text{ water}$$

Figure 43 shows a plot of ΔP_{JP-4} as calculated from the above equation for temperatures of -30°F and 60°F.

From the Boeing analysis of the fuel tank vent system[11] one can find the existing pressure drops at various flow rates for JP-4 at 60°F. Table 14 summarizes these data together with the additional pressure drops from the 1/2-inch and 1-inch arresters.

Table 15 gives values of the maximum allowable fueling rates with and without the 1/2-inch and 1-inch arresters placed in the vent tube.

It is concluded that the additional pressure drop introduced by either arrester does not significantly alter the maximum allowable fueling rates as long as they remain clean and free of dirt. Additionally it will be shown, in the Icing Analysis (Section 5.3) that the inclusion of these types of arresters in the vent tube when operating as designed will not introduce an undue pressure drop hazard during severe flight venting operations, provided no icing has occurred.

Table 14. Pressure Drop Through 707 Aircraft Vent System During Fueling.

Fueling Position	Fueling Rate JP-4 @ 60°F (gal/min)	Bulk Velocity (ft/sec)	Existing ΔP (Vent System) (psi)	ΔP 1/2-inch Arrester (psi)	ΔP 1-inch Arrester (psi)	ΔP Total 1/2-inch Arrester (psi)	ΔP Total 1-inch Arrester (psi)
Wing Center Section Tank	50	0.84	0.38	0.03	0.07	0.41	0.45
	100	1.48	1.50	0.06	0.14	1.56	1.69
	250	4.1	9.60	0.19	0.44	9.79	10.04
No. 1 Tank	50	0.82	0.24	0.03	0.07	0.27	0.31
	100	1.68	0.95	0.06	0.14	1.01	1.09
	250	4.10	5.70	0.19	0.44	5.89	6.14
No. 2 Tank	50	0.82	0.38	0.03	0.07	0.41	0.45
	100	1.68	1.50	0.06	0.14	1.56	1.64
	250	4.10	9.00	0.19	0.44	9.19	9.44
Outboard Reserve Tank	50	0.82	3.3	0.03	0.07	3.33	3.37
	100	1.68	12.0	0.06	0.14	12.06	10.14
	250	4.10	68.0	0.19	0.44	68.19	68.44

Table 15. Allowable Fueling Rates with Arresters in Place.

Fueling Position	Maximum Allowable ΔP (psi)	Allowable Fueling Rate Without Arrester (gal/min)	With Arrester 1/2-inch (gal/min)	With Arrester 1-inch (gal/min)
Wing Center Section Tank	4.96	178	176	173
No. 1 Tank	5.17	239	235	230
No. 2 Tank	7.94	230	227	223
Outboard Reserve Tank	5.41	65	65	64

5.2 FLAME HOLDING

The possibility exists that a lightning-initiated flame may propagate to the face of a flame arrester and stabilize on the arrester face if a combustible mixture is flowing out through the arrester. The arrester acts as a flame holder even though it has arrested flame propagation. As heat from the stabilized flame flows into the metal of the arrester the temperature of the arrester increases. As the temperature of the arrester increases its quenching effectiveness decreases because the arrester material no longer represents as large a heat sink. It may be possible for flame to propagate through the arrester if its temperature becomes too large. Eventually the arrester material will attain an equilibrium temperature whose value depends on the thermal conductivity of the arrester, and heat transfer rate to the surrounding environment.

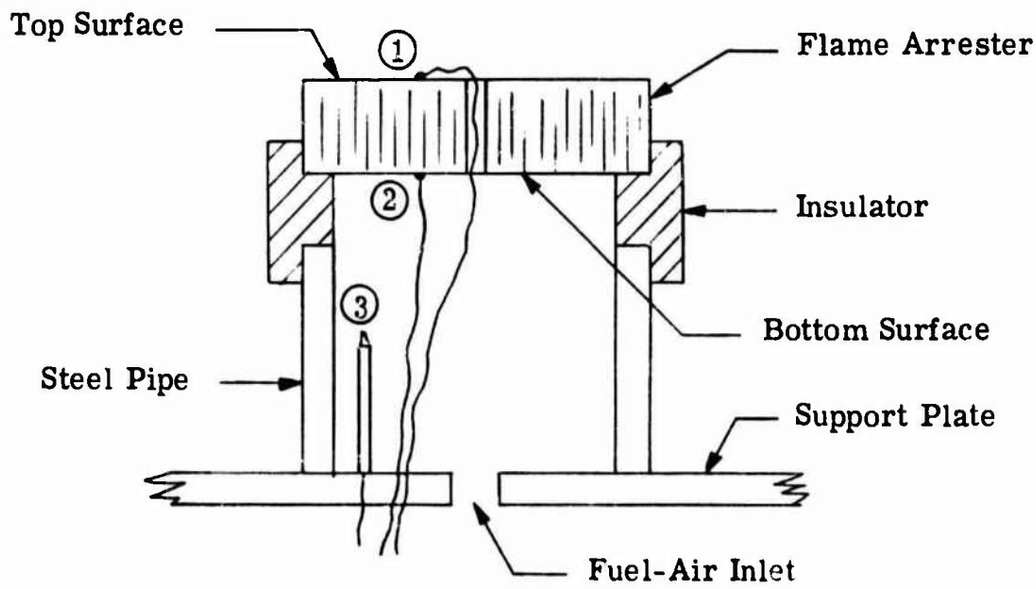

Figure 44. Schematic Diagram of Flame Holding Apparatus.

A test was conducted to determine whether the 1/2-inch × 0.050-inch and 1-inch × 0.050-inch stainless steel arresters could be penetrated in this fashion. The apparatus is shown schematically in Figure 44. The arrester was insulated from the plenum in order to minimize heat losses at the edge. Propane-air mixture was supplied at the inlet. Thermocouples 1 and 2 were used to indicate the temperatures of the top and bottom surfaces of the flame arrester. Thermocouple 3 indicated whether flame flashed through the arrester. The millivolt outputs of the thermocouples were monitored with a potentiometer.

The top and bottom equilibrium temperatures of the flame arresters were measured for various values of the flow velocity and air-fuel ratio. The results (see Figure 45) show that the bottom surfaces of the arresters attain their maximum temperatures when the gas flow is just sufficient to maintain a stable flame cone at the cell opening. This result was expected as previous studies have shown that heat transfer to the cell rim is maximized under this condition. Furthermore heat transfer from the arrester material to the flowing fuel-air mixture is reduced as flow is reduced. The mixture ratio which resulted in maximum arrester temperature was approximately 1.15 fraction stoichiometric based on propane weight.

Having selected the most stringent flow and mixture conditions, time histories of the top and bottom temperatures were obtained. (See Figure 46.) After temperature equilibrium was achieved the gas flow was reduced in an effort to induce flashback. No flashback occurred for either the 1/2-inch × 0.050-inch or 1-inch × 0.050-inch arrester. For the 1/2-inch × 0.050-inch arrester an equilibrium temperature of 708°F at the bottom surface was obtained in approximately 5 minutes. The 1-inch × 0.050-inch arrester reached a maximum temperature of 477°F in approximately 10 minutes.

It is important to realize that flashback through heated channels which are normally quenching should not be confused with the concepts of autoignition or hot surface ignition. Flashback will occur when the rate of heat loss to the channel wall is insufficient to quench the flame. In this case the wall acts as an inadequate heat sink and not as an ignition source. The

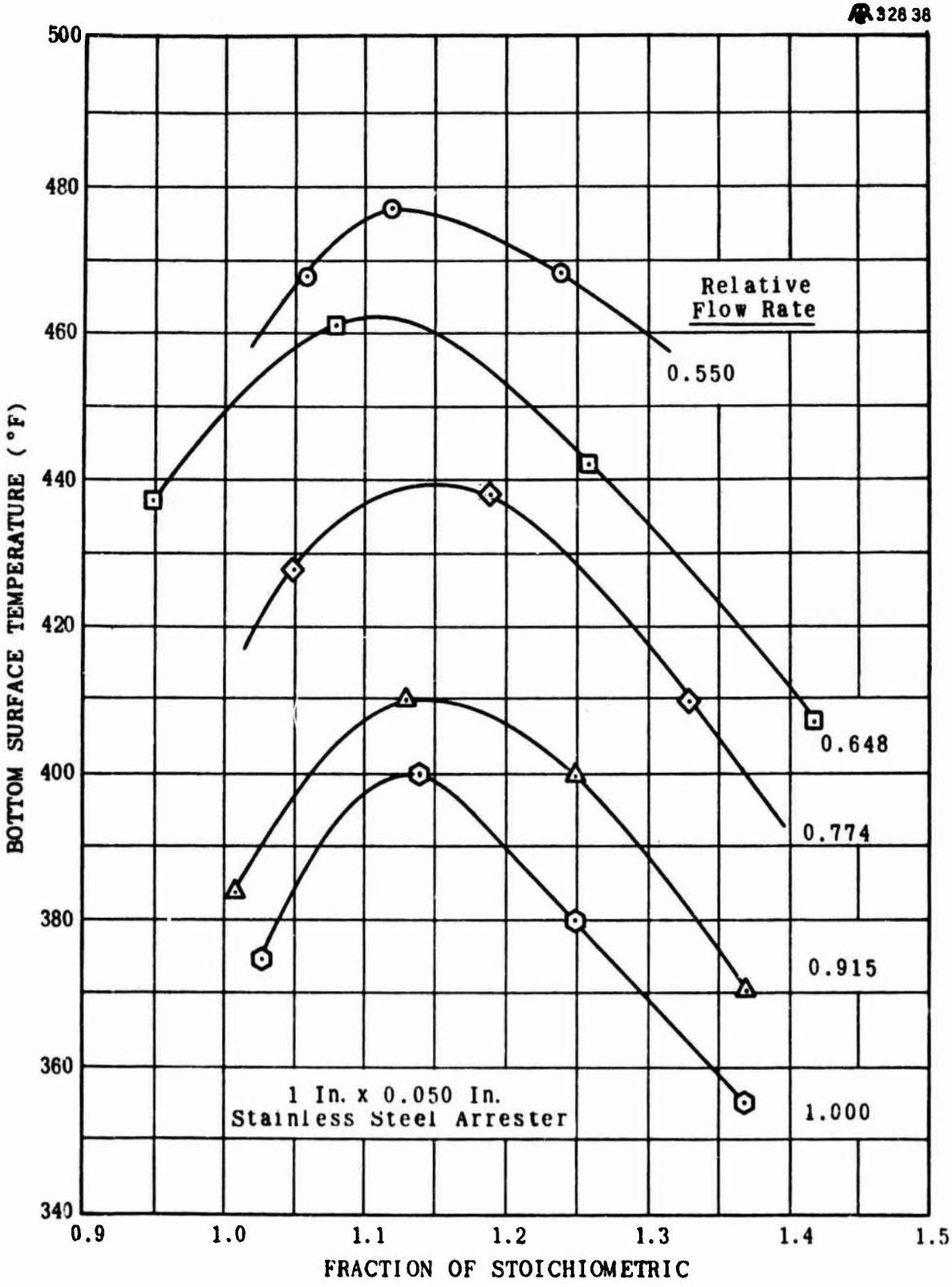

Figure 45. Flame Arrester Surface Temperature for Various Flow Rates and Mixture Ratios.

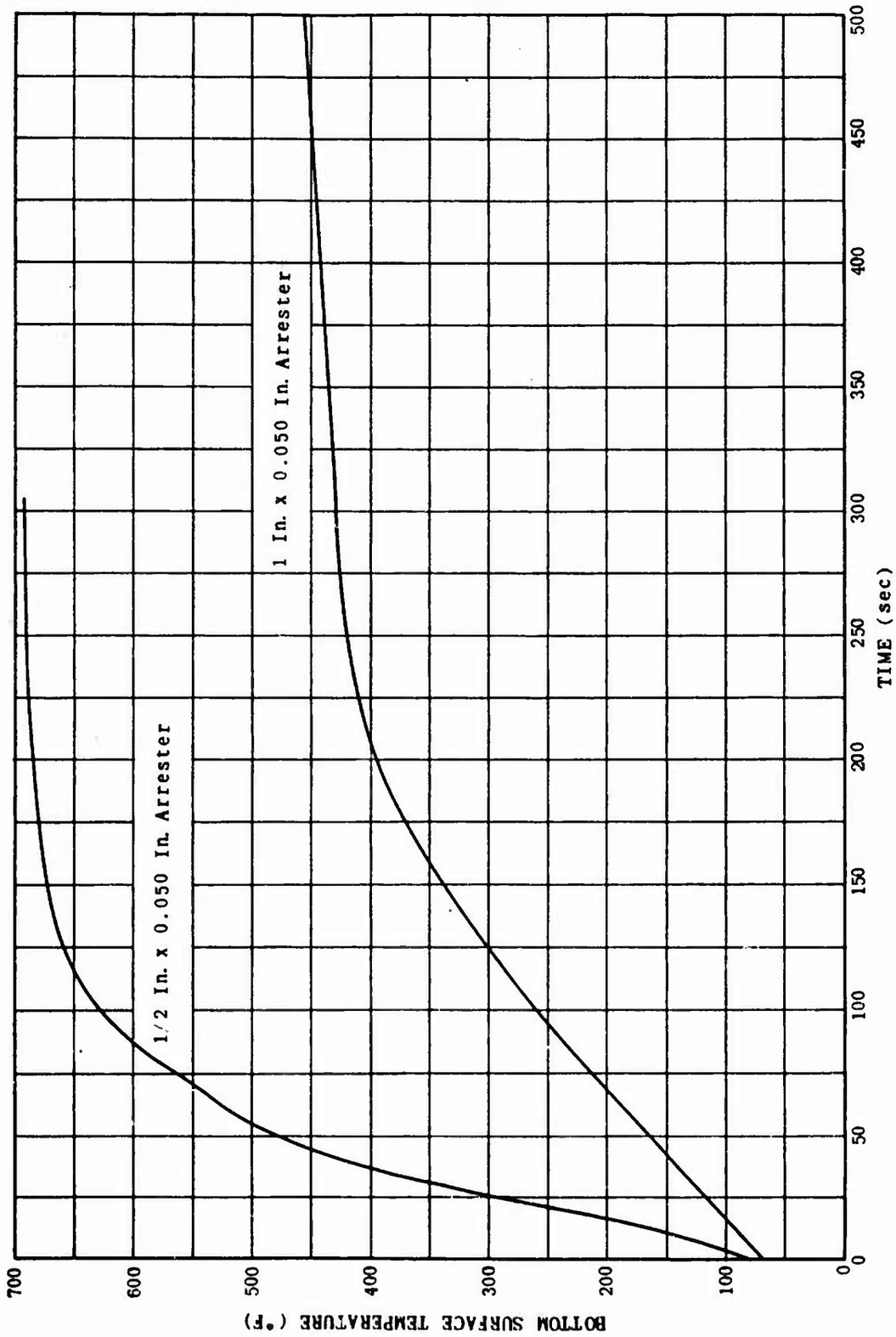

Figure 46. Time History of Flame Arrester Surface Temperature.

ignition of combustible mixtures by hot surfaces involves different phenomena than those described. In this process a portion of the combustible gas must dwell near a hot surface for a time such that chemical heat evolution is produced in a volume in excess of heat dissipation to the surroundings. The dwell time (commonly termed "ignition lag") is a function of the heat transfer characteristics of the gas and heat source, as well as the kinetics of the combustion process. For this reason the geometry of the heat source and the flow field around the heat source are critical factors in determining whether ignition will occur. It is incorrect to assume that a heat source whose temperature exceeds the ignition temperatures quoted in the literature necessarily causes ignition. However the quoted values of hot surface ignition temperatures may be used as order-of-magnitude estimates of the actual case if no experimental data is available. For instance methane and ethane have hot surface ignition temperatures of the order 960°F given by reference 7. Ignition of JP-6 vapors by hot wires depends on the wire diameter. Ignition temperatures range from 1085°F to 1880°F for heat sources with diameters of 0.75 inch and 0.016 inch respectively.[26] Other paraffins would exhibit roughly the same behavior.

It is apparent that the temperatures of 708°F and 477°F attained at the back surfaces of the 1/2-inch × 0.050-inch and 1-inch × 0.050-inch arresters in the present experiments were not sufficient to cause ignition of the propane-air mixture. Experiments should be performed for other fuels. Additionally the problem of flashing of liquid fuel on the hot surface of the flame arrester should be investigated, though the sequence of events leading to ignition in this manner seem remote. If a problem does arise it may be alleviated by reducing the front-to-back thermal conductivity of the flame arrester or by increasing its heat transfer efficiency.

5.3 ICING

5.3.1 Discussion of Icing Problem

Aircraft icing occurs by two distinct mechanisms (a) condensation and freezing of water vapor onto the structure, and (b) impingement of supercooled water droplets and/or freezing rain. These two mechanisms are distinct in that in item a the liquid water content appears as a fluid which behaves like a perfect gas; while in item b the liquid water content is contained in discrete particles which have mass and volume and thus obey the dynamical laws of motion although they are liable to evaporation.

For the usual problem of external icing of aircraft structures, the supercooled water droplets represent, by far, the most severe hazard, and the bulk of the literature on aircraft icing is devoted to this area. Ice accumulation of a structure is a highly individual phenomenon, and tests under icing conditions are always run if a potential hazard is thought to exist.

For icing of a flame arrester located well inside the vent tube we must discuss both icing mechanisms mentioned above. The more difficult of the two problems is the impingement of supercooled droplets. In order to determine if a given droplet will survive the rather tortuous entrance into the vent outlet and then impinge onto the flame arrester, it is necessary to solve for the trajectory which is described by the equations of motion of a particle in a fluid. The major difficulty is that the flow field is not known for any except the simplest of shapes, and the entrance configuration is not one of these. Should the vapor pressure of the air surrounding the droplets be diminished for any reason, the droplets will very quickly evaporate.

In the only reported icing tests of this vent scoop panel and outlet,[19] it was reported that the ice accumulation around the external scoop was within permissible limits and that liquid water moving on the surface of the wing did not enter the vent outlet. However, no data were reported as to the quantity or size of droplets that were ingested into the ducted flow (if any).

For the Stokes flow regime (Re <1),the drag force on a particle is proportional to its diameter. Thus we can see that only a very small particle would have a drag force comparable in magnitude to its inertia force. The more massive water droplets in the air stream over the wing will not track well and will impinge on the entrance section to the vent duct. The smaller particles will be entrained in the fluid and will follow the fluid around the flame arrester elements and will not impact there unless they happen to approach an element with a certain region A_1 as shown below. In all probability, a significant amount of the water of the non-impacting droplets will be evaporated from the droplets as they pass through the flame arrester and will enrich the moisture content of the through-flowing air.

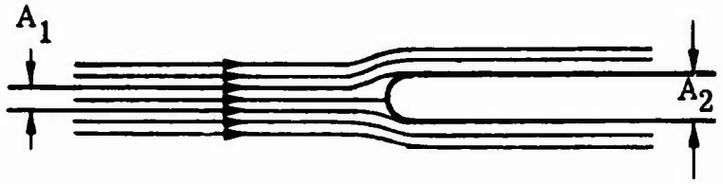

FLAME ARRESTER ELEMENT

This catching phenomenon is described by a collection efficiency, E, given by

$$E = \frac{A_1}{A_2}$$

Icing due to condensation of water vapor onto a colder structure is assumed to occur by diffusion of the water vapor through the boundary layer to the surface where freezing occurs. The diffusion is promoted by a concentration gradient which exists because the liquid water content of saturated air decreases with the decreasing temperature as the structure wall is approached. The diffusion to a cylindrical surface is assumed to be a reasonable approximation of the diffusion to the leading edge of a flame arrester element.

5.3.2 Air Flow in Vent Duct

For a constant rate of descent, $\frac{dh}{dt}$, from some altitude, air will flow into the evacuated portion of the fuel tanks in order to maintain pressure equilibrium between the atmosphere and the tanks. Let us assume that the pressure drop in the duct is negligible so that tank pressure is always equal to atmospheric pressure. Then the weight rate-of-flow, $\dot{m}$ into the tank is

$$\dot{m} = V_{tank} \frac{d\rho}{dt} \text{ (lb/sec)}$$

where

V_{tank} ~ volume of the tank which is empty of fuel (ft^3),

$\frac{d\rho}{dt}$ ~ rate of change of atmospheric weight-density with time (lb/ft^3-sec).

The density of the standard atmosphere may be approximated closely by an expression of the form

$$\rho = A\, e^{-Bh}$$

where h is altitude in feet, and where for $0 < h < 35{,}000$ feet the constants A and B have the values

$$A = 0.07651$$
$$B = 3.1958 \times 10^{-5}$$

Since

$$\frac{d\rho}{dt} = \frac{d\rho}{dh}\,\frac{dh}{dt}$$

the weight rate-of-flow becomes

$$\dot{m} = V_{tank} \frac{d\rho}{dh}\,\frac{dh}{dt} = -B\rho\, V_{tank} \frac{dh}{dt} \qquad (1)$$

The velocity of the flow through the vent tube, v, is given by

$$v = \frac{\dot{m}}{\rho\left(\frac{\pi D^2}{4}\right)} \quad \text{(ft/sec)} \tag{2}$$

where $\pi D^2/4$ is the area of the vent tube cross section (ft^2). Substituting equation (1) into (2) gives

$$v = \frac{-4\ B\ V_{tank}}{\pi D^2}\ \frac{dh}{dt} \tag{3}$$

We see that the mass flow rate increases exponentially with time but the flow velocity is constant. We may evaluate equations (1) and (3) for the worst situation; i.e., when the fuel tank is empty of fuel and the aircraft is executing an emergency descent of 15,000 ft/min. Then,

$$V_{tank} = (11{,}000\ \text{gal})\ (0.1337\ ft^3/\text{gal}) = 1470.7\ ft^3$$

$$D = (5.0\ \text{in}) = 0.4167\ \text{ft}$$

$$\frac{dh}{dt} = -15{,}000\ \text{ft/min} = -250.0\ \text{ft/sec}$$

$$h\,(\text{ft}) = 35{,}000 - 15{,}000\ t\ \ (t\ \text{minutes})$$

Hence

$$\dot{m} = (1470.7)\ (-3.1958 \times 10^{-5})\ (-250.0)\ (0.7651)e^{-3.1958 \times 10^{-5}h}$$

$$\dot{m} = 0.9\ e^{-1.1185 + 0.003707t} \quad \text{(lb/sec)}$$

The mass flow rate is seen to vary from 0.294 lb/sec at 35,000 ft to 0.9 lb/sec at sea level. The flow velocity in the 5-inch vent tube is constant.

$$v = \frac{-4\,(1470.7)\ (3.1958 \times 10^{-5})}{\pi\ (0.4167)^2}\ (-250.0) = 86.2\ \text{ft/sec}$$

Assuming incompressible flow, the velocity at various locations in the vent outlet can be calculated. The rectangular entrance has an area of 26.5 in^2, hence the velocity there is

$$v = \frac{19.62\ in^2}{26.5\ in^2}\ (86\ ft/sec) = 64\ ft/sec$$

The exit from the box section is a circular section with a 1-inch segment removed and has an area of 16.91 in^2. The velocity there is

$$v = \frac{19.62\ in^2}{16.91\ in^2}\ (86\ ft/sec) = 100\ ft/sec$$

5.3.3 Icing Due to Supercooled Water Droplets

The following quantitative discussion is presented as indicative of the icing problem which is associated with supercooled water droplets. The physical model is highly simplified in order to lend itself to analysis.

The vent scoop panel is located L = 6 ft from the leading edge of the wing in the streamwise direction. For an emergency rate of descent, an often used design point[11] is 10,000 ft/min, at 27,000 ft altitude and Mach number 0.85. Under these conditions, the free-stream velocity is v_∞ = 850 ft/sec, the kinematic viscosity is $\nu = 3.178 \times 10^{-4}\ ft^2/sec$ and the Reynolds number is

$$Re = \frac{v_\infty L}{\nu} = 1.6 \times 10^7$$

This predicts a turbulent boundary layer on the wing at the vent outlet whose thickness, δ, is

$$\delta = 0.37\ L\ (Re)^{-1/5} = 0.965\ in$$

The velocity distribution in a turbulent boundary layer is accurately given by the 1/7-power law

$$\frac{u}{v_\infty} = \left(\frac{x}{\delta}\right)^{1/7} \tag{4}$$

where u is the velocity at location x normal to the wing surface. This velocity distribution is shown in Figure 47a.

By continuity, the flow into the vent outlet must equal the flow taken from the boundary layer. That is

$$\text{entrance velocity} \times \text{area} = \int_0^H u(x)\, x\, dx$$

$$(64 \text{ ft/sec})\ (265 \text{ in}^2) = \int_0^H v_\infty \left(\frac{x}{\delta}\right)^{1/7} x\, dx = \frac{7}{15} v_\infty \left(\frac{H^{15}}{\delta}\right)^{1/7}$$

Solving for H, the thickness of the layer which is ingested into the duct, we get

$$H = \left\{\frac{(64)\,(26.5)\,(15)\,(0.965)^{1/7}}{(7)\,(850)}\right\}^{7/15} = 0.60 \text{ in}$$

Thus we see that the lower 60 per cent of the boundary layer contributes the flow (and thus the water droplets) which enters the vent outlet. Since the free-stream velocity is an order of magnitude larger than the duct velocities, we will assume that any particle which negotiates this first corner will successfully pass the rest and will ultimately arrive at the location of the flame arrester in the vent tube.

In order to estimate particle trajectories around the entrance corner, the simplified flow fields shown in Figure 47b and Figure 47c are suggested as embodying the primary features of the real flow field and perhaps bracketing the size particles which are admitted.

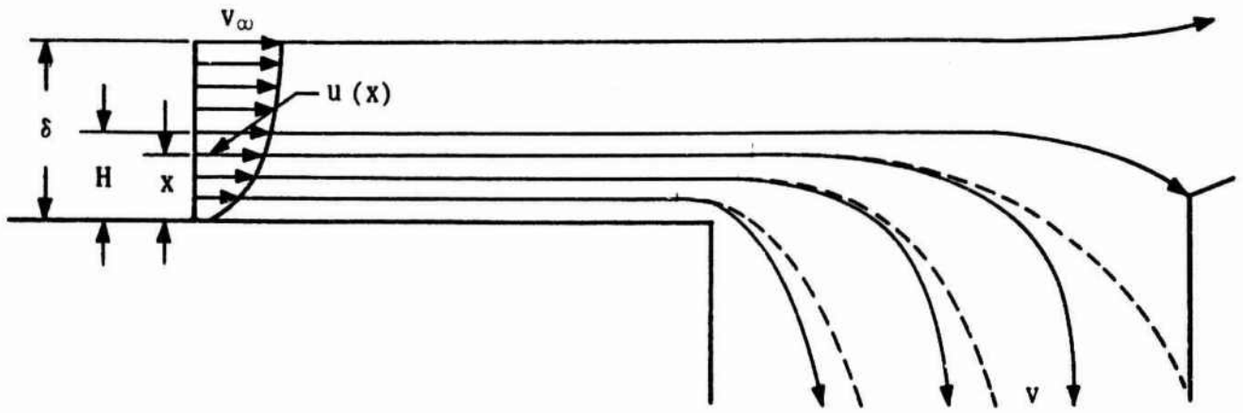

a. Typical Inlet Flow Field

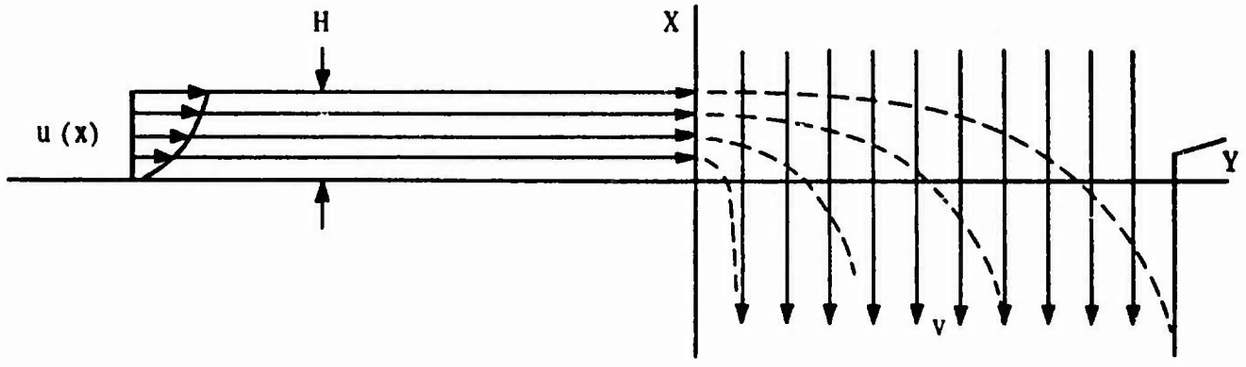

b. Model Flow Field

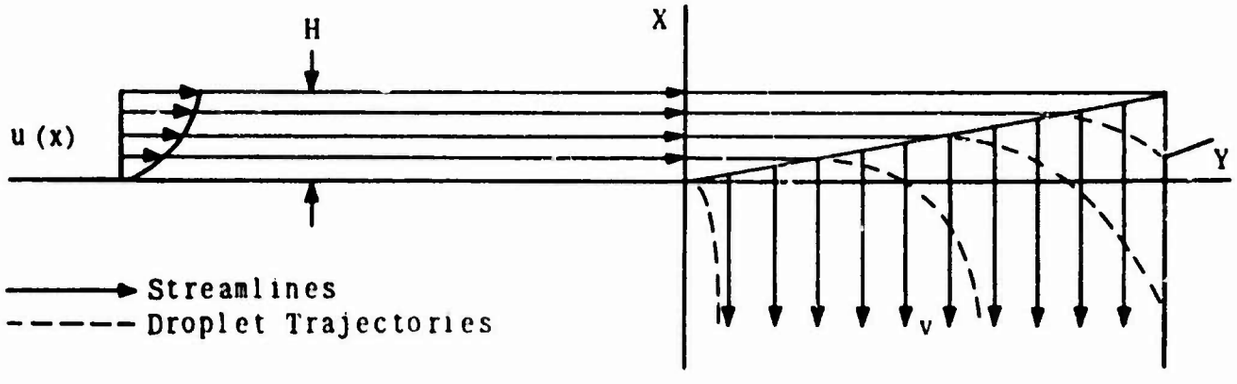

c. Model Flow Field

Figure 47. Flow Fields for Icing Analysis.

In the first model shown in Figure 47b, the particle is assumed to be inserted with initial velocity u(x) at right angles to the duct velocity v. When the equations of motion for a particle of mass m with drag force $F_D = Kv$ are integrated and initial conditions applied, the resulting displacements are

$$x = -\lambda (u - v)\left(1 - e^{-t/\lambda}\right) - vt$$

$$y = \lambda u \left(1 - e^{-t/\lambda}\right)$$

where $\lambda = \frac{m}{K}$ can be considered as a time constant for the system. We see that the horizontal displacement, y, exponentially approaches its maximum value of λu as $t \to \infty$, irrespective of the duct velocity, v.

We are interested in determining the diameter of the particle, d_p, that just reaches the opposite wall; i.e., $y = \lambda u = 1/6$ ft. Particles larger than this will impact on the wall and freeze there, while smaller particles will enter into the duct.

Above, it was stated that the drag force is assumed proportional to the first power of the particle velocity with respect to the fluid. This is true only for Stokes flow where $F_D = (3\pi\mu\, d_p)\, v$. It will be seen that the water droplets which are of the proper size to enter the inlet scoop have a Reynolds number range $10 \leq Re \leq 100$. This is above the regime where Stokes theory is applicable ($Re < 1$) and, in fact, Stokes formula is too small by a factor of from 2 to 5. A rough correction then is to introduce a factor of 4 if we are to use Stokes formula. This is done in the following analysis. Thus

$$F_D = 4\,(3\pi\mu\, d_p)\, v = Kv$$

where

$$K = 12\pi\mu\, d_p$$

μ = fluid absolute viscosity, 3.15×10^{-7} lb-sec/ft^2

Then

$$\lambda = \frac{m}{K} = \frac{\rho_w \left(\frac{\pi d_p^3}{6} \right)}{12\pi\mu d_p} = \frac{\rho_w d_p^2}{72\mu}$$

where

ρ_w = mass density of water, 1.778 lb-sec^2/ft^4

We set $\lambda u = 1/6$ ft and solve for the particle diameter, d_p.

$$d_p = \sqrt{\frac{12\mu}{\rho_w u}}$$

The initial velocity, u, is dependent on the location in the boundary layer as was seen in equation (4).

We are interested in values of x only as great as H, the thickness of the injected layer, so we may introduce the dimensionless distance $\frac{x}{H}$ and equation (4) can be written

$$u = \left(\frac{x}{H} \frac{H}{\delta} \right)^{1/7} v_\infty$$

Inserting this expression into the previous equation gives

$$d_p = \left\{ \frac{12\mu}{\rho_w \left(\frac{x}{H} \frac{H}{\delta} \right)^{1/7} v_\infty} \right\}^{1/2} = \left\{ \frac{12\mu}{\rho_w v_\infty} \left(\frac{\delta}{H} \right)^{1/7} \right\}^{1/2} \left(\frac{H}{x} \right)^{1/14}$$

Evaluating the constant term in this expression we find

$$\left\{ \frac{12\mu}{\rho_w v_\infty} \left(\frac{\delta}{H} \right)^{1/7} \right\}^{1/2} = 5.02 \times 10^{-5} \text{ ft} = 15.3 \text{ microns}$$

Then the equation for d_p simplified to

$$d_p = 15.3 \left(\frac{H}{x}\right)^{1/14} \text{ microns} \qquad (5)$$

where, x, is the distance above the plate.

This equation probably represents an upper bound on the maximum size of particles that may enter, because our model subjects the particle to large drag forces beginning at y = 0. In the real flow field, the particle only gradually encounters drag forces as it proceeds from y = 0 toward the far wall, as the trajectories in Figure 47a show.

A second model which may represent a lower bound to the maximum particle size that enters is sketched in Figure 47c.

This model is exactly like the previous one except that the particle is assumed to be drag-free until it reaches the diagonal line given by

$$y = \frac{1}{6} \frac{x}{H}$$

That is

$$\lambda u = \frac{1}{6} \left(1 - \frac{x}{H}\right)$$

Solving for d_p as before, we find that now

$$d_p = 15.3 \left(\frac{H}{x}\right)^{1/14} \left(1 - \frac{x}{H}\right)^{1/2} \qquad (6)$$

Equations (5) and (6) are plotted in Figure 48 as well as the estimated mean. Both theories allow very large size droplets to enter the duct if they originate very near the wing surface. This is as it should be, because at the very bottom of the boundary layer, the velocity is so low that the droplet has almost no inertia and drag forces will always predominate irrespective of droplet size.

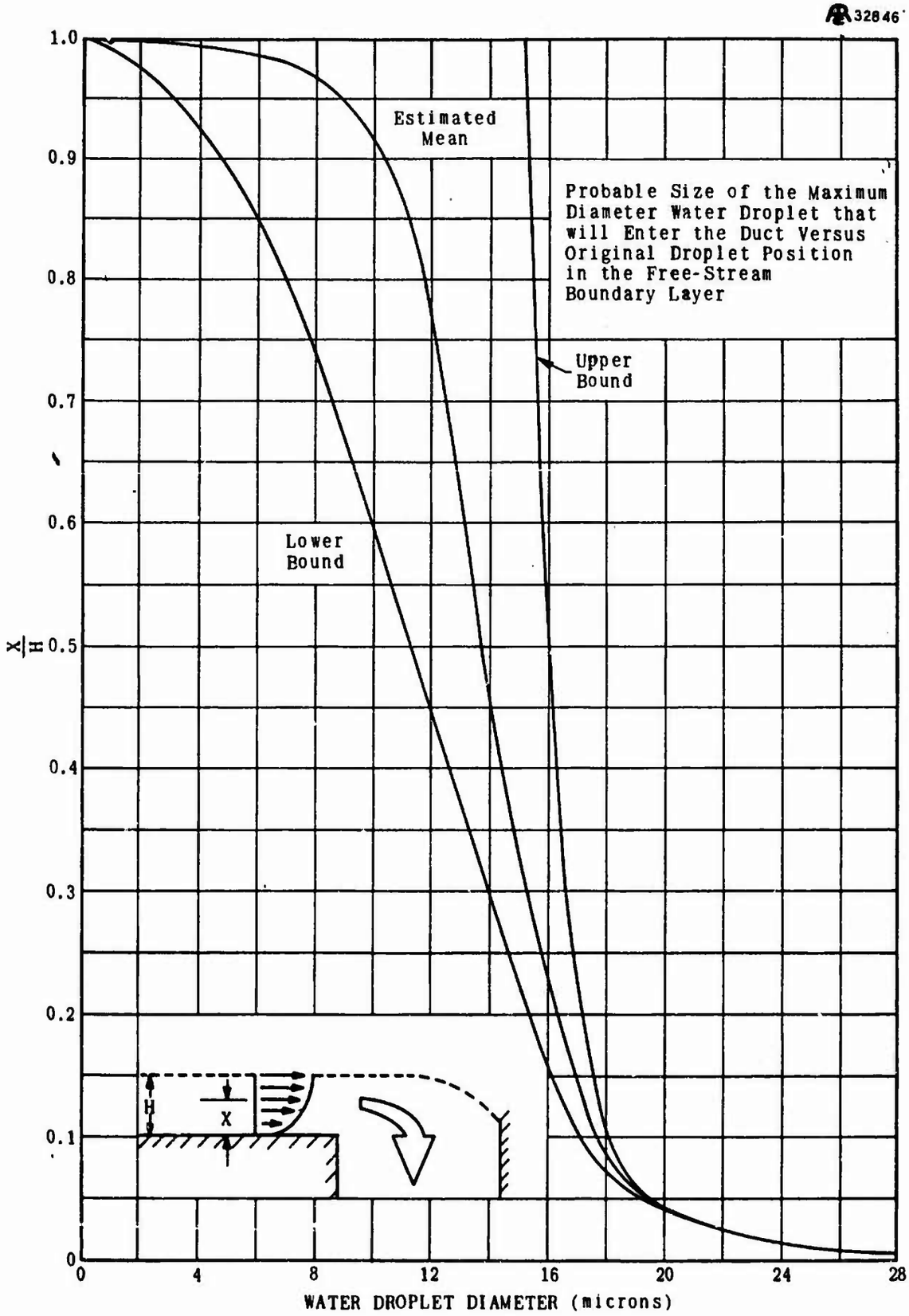

Figure 48. Water Droplet Diameter Versus Position in Free Stream Boundary Layer.

If we assume that the boundary layer contains a homogeneous distribution of all size droplets, then the probability that a droplet of any given size will approach in the boundary layer between $\frac{x}{H} = 0$ and $\frac{x}{H}$ is just $\frac{x}{H}$. For example the probability of a particle exceeding 20 microns and still getting into the duct is seen in Figure 48 to be about 0.04.

The complete probability curve for any size particle entering the duct is plotted in Figure 49 for the mean curve of Figure 48. Also shown on this plot is the collection efficiency, E, for a flame arrester element over which the flow with various size droplets is flowing. This concept is based on a discussion by E.G. Richardson[20] of the paths of particles impinging on a cylinder normal to the flow. The collection efficiency, E, is a function of the particle parameter P, which is defined by

$$P = \frac{d_p^2 \, v \, \sigma}{q \, t_w \, \mu}$$

where

$\sigma \sim$ specific gravity of the drop relative to the fluid, $62.4/0.0765 = 815$

$d_p \sim$ diameter of the particle, ft

$v \sim$ velocity of the flow, ft/sec

$t_w \sim$ thickness of the walls in the flame arrester, ft

$\mu \sim$ fluid kinematic viscosity, 1.545×10^{-4} ft^2/sec

The probability that a particle having entered the vent tube will encounter an element of the flame arrester depends upon the area of the duct cross section that is blocked by the flame arrester. A typical flame arrester will block only about 10 per cent of the total duct area so that the probability that a particle will impact the arrester is 0.1E. The probability that a particle will enter the inlet scoop and impact the flame arrester is then $0.1E\left(\frac{x}{H}\right)$. These probability curves are summarized in Figure 49. We see that water droplets having a diameter of about 8 microns have the best chance of contributing to

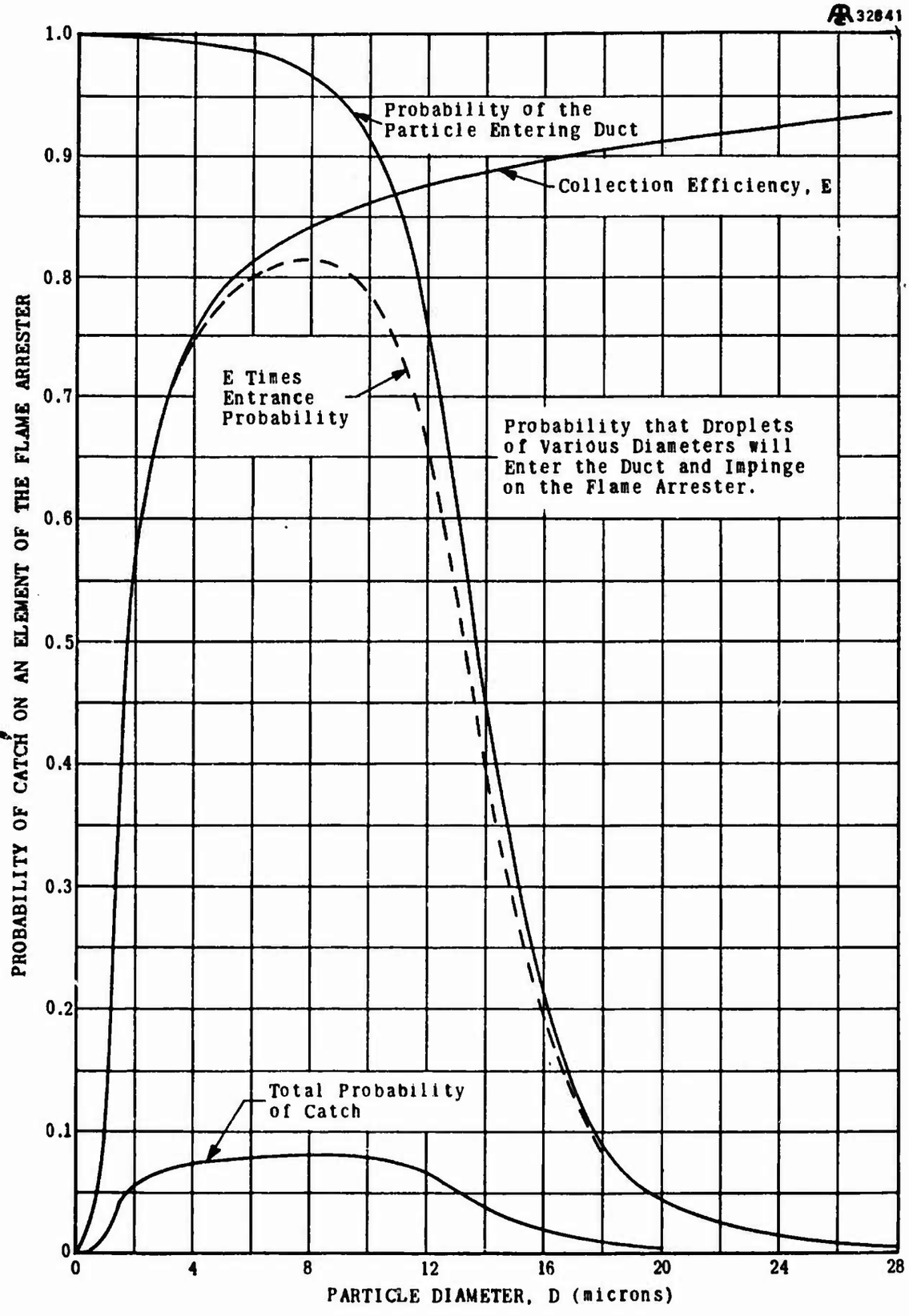

Figure 49. Probability of Water Particle Entering Duct.

the icing of a flame arrester. The probability of their completing their journey, however, is low — only about 0.08. This implies that a long icing period would be required to accumulate a significant deposit of supercooled water droplets on the flame arrester.

Figure 50 is taken from reference[21] and shows the exceedance probability for various drop diameters. Eight-micron drops are seldom encountered as can be seen by the large exceedance probability for a mean-effective diameter of eight microns. In any encounter, however, some of the drops would be of the most favorable size for injection into the vent outlet.

Further analysis of the icing due to supercooled water droplets seems unjustified in view of the rather crude flow models which must be assumed. It seems clear, however, that vent outlet configurations can be designed to be quite selective to the size particles which can be admitted.

5.3.4 Water Content in Saturated Air

For temperatures below 60°C, the specific weight of vapor is given by the ideal gas law to within 0.5 per cent

$$\frac{P_{sv}}{W_v} = 0.08206 \frac{T}{M}$$

where

P_{sv} ~ saturated water vapor pressure (atmospheres)

W_v ~ saturated water vapor density (Kg/m^3)

T ~ temperature (°K)

M ~ molecular weight; $H_2O = 18$

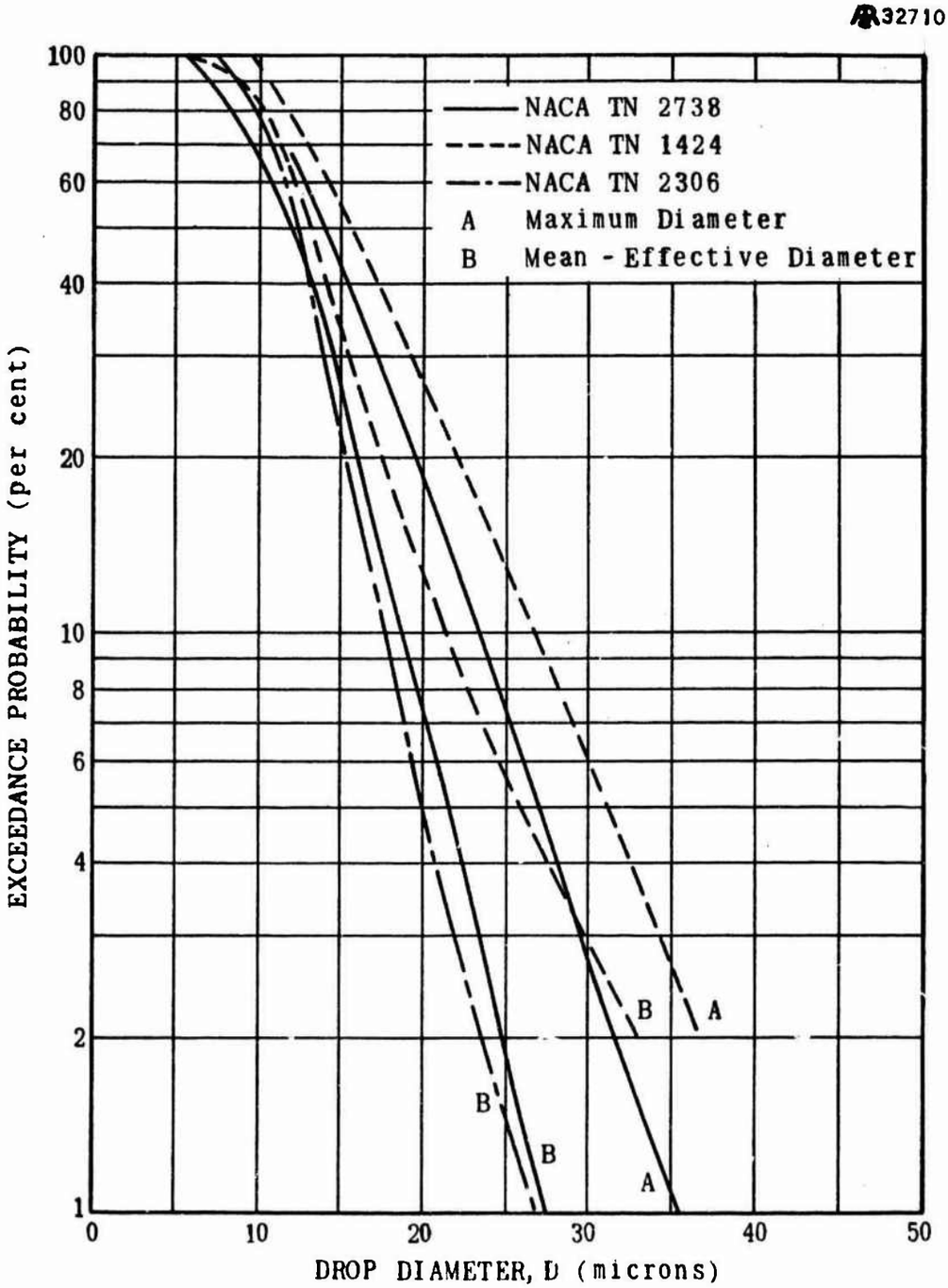

Figure 50. Exceedance Probability for Drop Diameter (from FAA ADS-4)

The mass of water vapor present per unit volume of saturated air is then

$$W_v = \frac{\frac{18}{T}\frac{P_{sv}}{760}}{82.06} = 288.62\ \frac{P_{sv}}{T}$$

where

P_{sv} ~ saturated vapor pressure (mm Hg)

W_v ~ saturated vapor specific weight (gm/m^3)

Using data for pressure of saturated water vapor[22] we find that W_v may be approximated by an expression of the form

$$W_v = Ae^{BT} \tag{7}$$

where the empirical constants are found to be

$$A = 0.65 \times 10^{-4}$$

$$B = 0.05071$$

and T is to be in °F.

5.3.5 Steady-State Temperature Lag

The temperature of the standard atmosphere is linear with altitude from sea level to 35,000 ft. If the airplane descends at a constant rate, the air which will flow into the vent tube will have linearly increasing temperature with time. The flame arrester and adjacent vent tube and airplane structure will tend to remain at the colder temperatures associated with the higher altitudes.

After some time has elapsed the flame arrester temperature will be increasing at the same rate that the air temperature is increasing but will be lagging by a constant amount ΔT. This steady-state temperature lag depends, in part, on the rate that heat is being transferred from the arrester to the aircraft structure.

The smaller the temperature lag, ΔT, the less likely it is that condensation will occur. The most favorable situation then is for the flame arrester to be thermally insulated from the airplane. The degree of insulation may affect the induced electric arcing characteristics. The assumption of an adiabatically insulated flame arrester is a good approximation of the real situation because a flame arrester may be designed to have a very low rate of heat conduction in the radial direction. The following analysis calculates the steady-state lag in an insulated flat plate over which an ever-warming air is moving.

For a flame arrester 0.5-inch deep, it is unlikely that fully-developed flow will occur within the passages of the arrester, so the Reynolds number will be based on an equivalent flat plate.

$$Re_x = \frac{vx}{\nu}$$

For $v = 86$ ft/sec, $x = 0.5$ in $= 0.04166$ ft, and $1.766 \times 10^{-4} \leq \nu \leq 4.037 \times 10^{-4}$ ft^2/sec, we calculate

$$8.87 \times 10^3 \leq Re \leq 2.03 \times 10^4$$

Since the critical Reynolds number is 3.2×10^5 for a plate,[23] the boundary layer may be assumed to be laminar and the maximum thickness of the boundary layer is

$$\delta \; 5 \sqrt{\frac{\nu x}{v}} = 2.21 \times 10^{-3} \text{ ft} = 2.65 \times 10^{-2} \text{ in}$$

Thus the boundary layer thickness is less than half the distance between successive elements if they are no closer than 0.06 inch.

The temperature lag, ΔT, in a flat plate of thickness t_w being heated from both sides is given by

$$\Delta T = \left\{ \frac{\rho_w C \left(\frac{t_w}{2} \right)}{\bar{h}} + \frac{\left(\frac{t_w}{2} \right)}{2\alpha} \frac{dT}{dt} \right\} \tag{8}$$

where

$\rho_w \sim$ density of the wall

$t_w \sim$ thickness of the wall

$C \sim$ specific heat of the wall

$\bar{h} \sim$ average heat-transfer coefficient

$\alpha = \frac{k_w}{\rho_w C} \sim$ thermal diffusivity of the wall

$\frac{dT}{dt} \sim$ rate of change of air temperature with time

$k_w \sim$ thermal conductivity of the wall

The average heat-transfer coefficient, $\bar{h}$, for flow over a flat plate is given by[24]

$$\bar{h} = \frac{2k\,Nu}{x} = \frac{2K}{x} \; 0.332 \; \sqrt[3]{Pr} \; \sqrt{Re_x}$$

where

$Nu \sim$ Nusselt number

$Pr \sim$ Prandtl number

$Re_x \sim$ Reynolds number based on length x

$x \sim$ length of the flat plate

$k \sim$ thermal conductivity of the flowing gas

We will compute the extreme values of $\bar{h}$ for the temperature range of the air flow. At $T = -66.4°F$; $Re = 8.87 \times 10^3$; $Pr = 0.730$; $k = 0.011$ Btu/hr ft °F, $\bar{h} = 14.867$ Btu/hr ft °F. At $T = 40.6°F$; $Re = 2.03 \times 10^4$; $Pr = 0.715$; $k = 0.0135$ Btu/hr ft °F, $\bar{h} = 27.414$ Btu/hr ft °F.

We will use the averaged value of heat-transfer coefficient

$$\bar{h} = 21.1 \frac{\text{Btu}}{\text{hr ft}^2\ °\text{F}} = 0.3517 \frac{\text{Btu}}{\text{min ft}^2\ °\text{F}}$$

For a stainless steel wall we have the following properties

$$\rho_w = 7.70\ \text{gm/cm}^3$$

$$C = 0.142\ \text{cal/gm°C}$$

$$k_w = 0.082\ \text{cal/cm°C sec}$$

Then

$$\alpha = \frac{k_w}{\rho_w C} = \dot{m}\ 0.075 \frac{\text{cm}^2}{\text{sec}} = 4.84 \times 10^{-3} \frac{\text{ft}^2}{\text{min}}$$

Also

$$\rho_w C = 1.093 \frac{\text{cal}}{\text{cm}^3\ °\text{C}} = 68.22 \frac{\text{Btu}}{\text{ft}^3\ °\text{F}}$$

We may replace the rate of change of temperature by the product

$$\frac{dT}{dt} = \frac{dT}{dh} \cdot \frac{dh}{dt}$$

$\frac{dT}{dh}$ is a constant of the standard atmosphere and is found to equal -3.565×10^{-3}° F/ft

Then we have

$$\Delta T = \left[\frac{68.22 \text{ Btu/ft}^3 \text{°F}}{0.3517 \text{ Btu/min ft}^2 \text{°F}} \left(\frac{t_w}{2} \right) + \frac{\left(\frac{t_w^2}{2} \right)}{2(4.84 \times 10^{-3}) \text{ ft}^2/\text{min}} \right] \times (-3.565 \times 10^{-3} \text{°F/ft}) \frac{dh}{dt}$$

For thin walls $t_w << 1$ and the second term is negligible compared to the first. Hence

$$\Delta T \text{ (°F)} = 0.346 \, t_w \frac{dh}{dt} \tag{9}$$

As an example of the size of ΔT, for $t_w = 0.001$ inch, and $\frac{dh}{dt} = 15{,}000$ ft/min, $\Delta T = 0.48$°F. The actual temperature lag will vary with radial distance from the center of the duct, thus ice will form least in the center of the arrester and most on the outer surfaces.

5.3.6 Ice Deposition Due to Condensation

The rate at which water vapor arrives at the surface of the plate is given by a local mass transfer coefficient, h_D, which is determined by considering the diffusion rate of water vapor through air. For the thin flat plate, the mass transferred to the leading edge may be approximated by considering the analogous problem of mass transfer to the front half of a cylinder normal to the flow, as shown below.

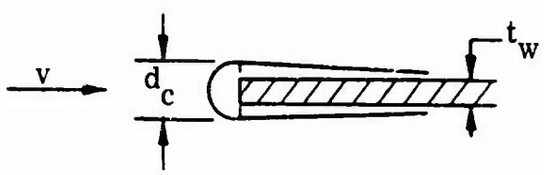

Water condensing on a flat plate is discussed by Eckert[24] and the analogy between heat-transfer and mass-transfer is made. In the present analysis, the mass-transfer coefficient to a cylindrical body will be calculated by analogy with the heat-transfer coefficient developed on pages 184-187 of the above reference.

The rate of condensation of water on a cylinder is given by

$$\dot{m}_w = \bar{h}_D \ (W_\infty - W_w) \ \ (lb/ft^2 min)$$

where $\bar{h}_D$ ~ average mass transfer coefficient over the front half of a cylindrical body.

W_∞ ~ specific weight of free stream saturated air (lb/ft^3)

W_w ~ specific weight of saturated air at the wall (lb/ft^3)

We will find it convenient to assume that the flame arrester temperature is lagging the free-stream air temperature by an amount ΔT (° F). It is this steady-state temperature difference that causes the condensation and freezing of the saturated water vapor. Then we may write

$$W_\infty - W_w = \frac{dW_v}{dT} \ \Delta T \ \ (lb/ft^3)$$

Hence

$$\dot{m}_w = \bar{h}_D \ \frac{dW_v}{dT} \ \Delta T \ \ (lb/ft^2\text{-}min) \qquad (10)$$

We now proceed to develop a differential equation for d_c, the diameter of the ice cylinder which is assumed to form on the leading edge of the flame arrester element. Leading edge icing may be assumed to be more severe than at any other location of the flat plate as illustrated in the preceding sketch. The differential equation is derived by expressing each term in equation (10) in terms of d_c. This is done in the following paragraphs.

For a known rate of condensation of water from the vapor state, $\dot{m}_w$ (lb/ft^2-min), the rate of ice deposition is

$$\dot{m}_i = 0.917\ \dot{m}_w S \quad \text{(lb/min)}$$

where S is the area to which vapor is condensing and 0.917 is the specific gravity of ice. The volume rate of deposition is

$$\dot{V}_i = \frac{\dot{m}_i}{57.2} = 0.01603\ \dot{m}_w S \quad (\text{ft}^3\text{-min})$$

where 57.2 is the density of ice in lb/ft^3. The volume rate of ice accumulation may be replaced by a semi-circular area of unit width whose diameter is increasing with time.

That is

$$V_i = \frac{\pi d_c^{\,2}}{8} \quad \text{or} \quad \dot{V}_i = \frac{\pi d_c}{4}\ \frac{d}{dt}\ (d_c)$$

But

$$\dot{V}_i = 0.01603\ \dot{m}_w S = 0.01603\ \dot{m}_w \frac{\pi d_c}{2}$$

hence

$$\dot{m}_w = A\ \frac{d}{dt}\ (d_c)$$

where

$$A = 31.1915 \tag{11}$$

In equation (7) we found an empirical expression for the specific weight of saturated water vapor as a function of temperature

$$W_v = 6.5 \times 10^{-5}\ e^{0.05071T}$$

Hence

$$\frac{dW_v}{dT} = 3.296 \times 10^{-6}\ e^{0.05071T}$$

But T is a function of time which depends on the rate of descent

$$T = T_o + \frac{dT}{dh}\frac{dh}{dt}\,t$$

For an initial altitude of 35,000 ft $T_o = -66.4°\,F$, and for a standard atmosphere $\frac{dT}{dh} = -3.565 \times 10^{-3}\ \frac{°F}{ft}$. Hence

$$T = -66.4\ F - 3.565 \times 10^{-3}\ \frac{dh}{dt}\,t$$

Using this expression for T the original formula for $\frac{dW_v}{dT}$ becomes

$$\frac{dW_v}{dT} = Be^{C\frac{dh}{dt}t} \tag{12}$$

where

$$B = 1.137 \times 10^{-7}$$

$$C = -1.808 \times 10^{-4}$$

We determine the average mass-transfer coefficient, h_D, as follows:

The heat-transfer coefficient averaged over the front face of a cylinder of diameter d is approximately (it varies with Pr and Re)

$$Nu_d = 0.7\sqrt{Re_d} = 0.7\sqrt{\frac{vd}{\nu}}$$

Assuming an analogous mass-transfer relationship we may write

$$\frac{\bar{h}_D\, d_c}{D} = 0.7\sqrt{\frac{vd_c}{\nu}}$$

or

$$\bar{h}_D = 0.7\ D\ \sqrt{\frac{v}{d_c\ \nu}}\ \text{(ft/min)} \tag{13}$$

where

$D \sim$ diffusion coefficient for water vapor in air (ft^2/min)

$d_c \sim$ diameter of the leading edge ice deposit (ft)

$\nu \sim$ kinematic viscosity of air (ft^2/sec)

$v \sim$ duct velocity (ft/sec)

It is necessary to know $\bar{h}_D$ as a function of time and rate of descent so we must investigate the values of $\bar{h}_D$ for descent through a standard atmosphere. Eckert[25] gives an expression for D for varying temperature and pressure (p. 512). After changing the units slightly, it is

$$D = \frac{30.442}{P_a}\left(1 + \frac{T}{460}\right)^{1.81}\ (ft^2/min)$$

where

$P_a \sim$ atmospheric pressure in lb/ft^2

$T \sim$ atmospheric temperature in °F

The velocity is a function of $\frac{dh}{dt}$ as was shown by equation (3)

$$v = -5.743 \times 10^{-3}\ \frac{dh}{dt}$$

The term $\frac{D}{\sqrt{\nu}}$ is a function of pressure and temperature and is thus determined by the altitude, assuming a standard atmosphere. Between 35,000 ft altitude and sea level $\frac{D}{\sqrt{\nu}}$ is closely approximated by the exponential function

$$\frac{D}{\sqrt{\nu}} = 1.412\ e^{1.382 \times 10^{-5} h}$$

Then if we make the substitution for altitude

$$h = h_o + \frac{dh}{dt} t = 35{,}000 + \frac{dh}{dt} t$$

we obtain

$$\frac{D}{\sqrt{\nu}} = 2.27\, e^{1.382 \times 10^{-5} \frac{dh}{dt} t}$$

Finally if the expressions for $\frac{D}{\sqrt{\nu}}$ and ν are substituted into equation (13) we arrive at the relationship

$$h_D \sqrt{d_c} = E \sqrt{-\frac{dh}{dt} t}\; e^{F \frac{dh}{dt} t} \tag{14}$$

where

$$E = 0.12174$$

$$F = +1.382 \times 10^{-5}$$

The expression for ΔT for an insulated flat plate was given by equation (9)

$$\Delta T = 0.346\, t_w \frac{dh}{dt}$$

Now equations (11, (12), (14), and (9) may be substituted into (10) to obtain the desired differential equation in the variable d_c. We obtain

$$A \frac{d}{dt} (d_c) = \left[\frac{E}{\sqrt{d_c}} \sqrt{-\frac{dh}{dt}}\; e^{F \frac{dh}{dt} t} \right] \left[B e^{C \frac{dh}{dt} t} \right] \left(0.346\, t_w \frac{dh}{dt} \right)$$

After evaluating the constants and rearranging

$$\sqrt{d_c} \frac{d}{dt} (d_c) = 2.67 \times 10^{-6}\, t_w \left(-\frac{dh}{dt} \right)^{3/2} e^{-1.67 \times 10^{-4} \frac{dh}{dt} t}$$

At time zero there is no ice build-up and $d_c = t_w$. Integrating the above expression from 0 to t gives

$$\frac{2}{3}\left(d_c^{3/2} - t_w^{3/2}\right) = 2.67 \times 10^{-6}\, t_w \sqrt{-\frac{dh}{dt}}\left(e^{-1.67 \times 10^{-4}\frac{dh}{dt}t} - 1\right)$$

Since $e^{-1.67 \times 10^{-4}\frac{dh}{dt}t} >> 1$ for the flight conditions of interest, we may neglect the unity above. Dividing through by $t_w^{3/2}$ we get

$$\frac{2}{3}\left[\left(\frac{d_c}{t_w}\right)^{3/2} - 1\right] = \frac{2.67 \times 10^{-6}}{\sqrt{t_w}} \sqrt{-\frac{dh}{dt}}\, e^{-1.67 \times 10^{-4}\frac{dh}{dt}t}$$

Finally

$$\frac{d_c}{t_w} = \left\{4 \times 10^{-6}\sqrt{\frac{-\frac{dh}{dt}}{t_w}}\, e^{-1.67 \times 10^{-4}\frac{dh}{dt}t} + 1\right\}^{2/3}$$

The time, t, in the above expression is the duration in minutes during which icing may occur. For a single descent from 35,000 ft this is

$$t = \frac{7000 - 35{,}000}{\frac{dh}{dt}} = \frac{-28{,}000}{\frac{dh}{dt}}$$

where 7000 ft is the altitude at which 32° F occurs in the standard atmosphere. If no melting occurs between n consecutive descents, then the total time for icing is

$$t = \frac{-28{,}000\, n}{\frac{dh}{dt}}$$

Substituting t into the expression for $\frac{dc}{t_w}$

$$\frac{d_c}{t_w} = \left\{ 4 \times 10^{-6} \sqrt{- \frac{\frac{dh}{dt}}{t_w}} \; 107.2^n + 1 \right\}^{2/3} \qquad (15)$$

Thus we see that the ratio of the ice diameter to the original wall thickness, $\frac{dc}{t_w}$, is a relatively weak function of the ratio $\frac{dh/dt}{t_w}$ but a very strong function of the number of descents, n.

This equation is plotted in Figure 51 for the extreme values of $\frac{dh/dt}{t_w}$ and as a function of the number of descents. It can be seen that regardless of the rate of descent, $\frac{dh}{dt}$, or wall thickness of the arrester elements, t_w, only two descents would cause an excessive amount of ice to form on the flame arrester under the assumed meteorological conditions.

The allowable icing shown in this figure is based on pressure drop considerations which are discussed in the next section.

5.3.7 Pressure Drop in Air Across Flame Arrester

If overflow occurs during fueling of the aircraft, the excess fuel must be permitted to exit through the vent tube without incurring a large pressure loss. Otherwise, excessive positive pressures may rupture the fuel cell. On the other hand, during rapid descent the atmospheric pressure is increasing and air must be free to pass into the fuel cell to prevent an undesirable negative pressure and possible collapse of the bladder tanks. In practice, the allowable negative pressure is the smaller of the two design limits due to the use of bladder-type tanks. The pressure drop in air through the vent tube is considered further in this section.

A Boeing report[11] gives the allowable tank pressure differentials for bladder tanks to be +3.50 psi and -0.36 psi. A ram recovery factor of +0.55q is stated to exist at the vent outlet. For an emergency descent rate

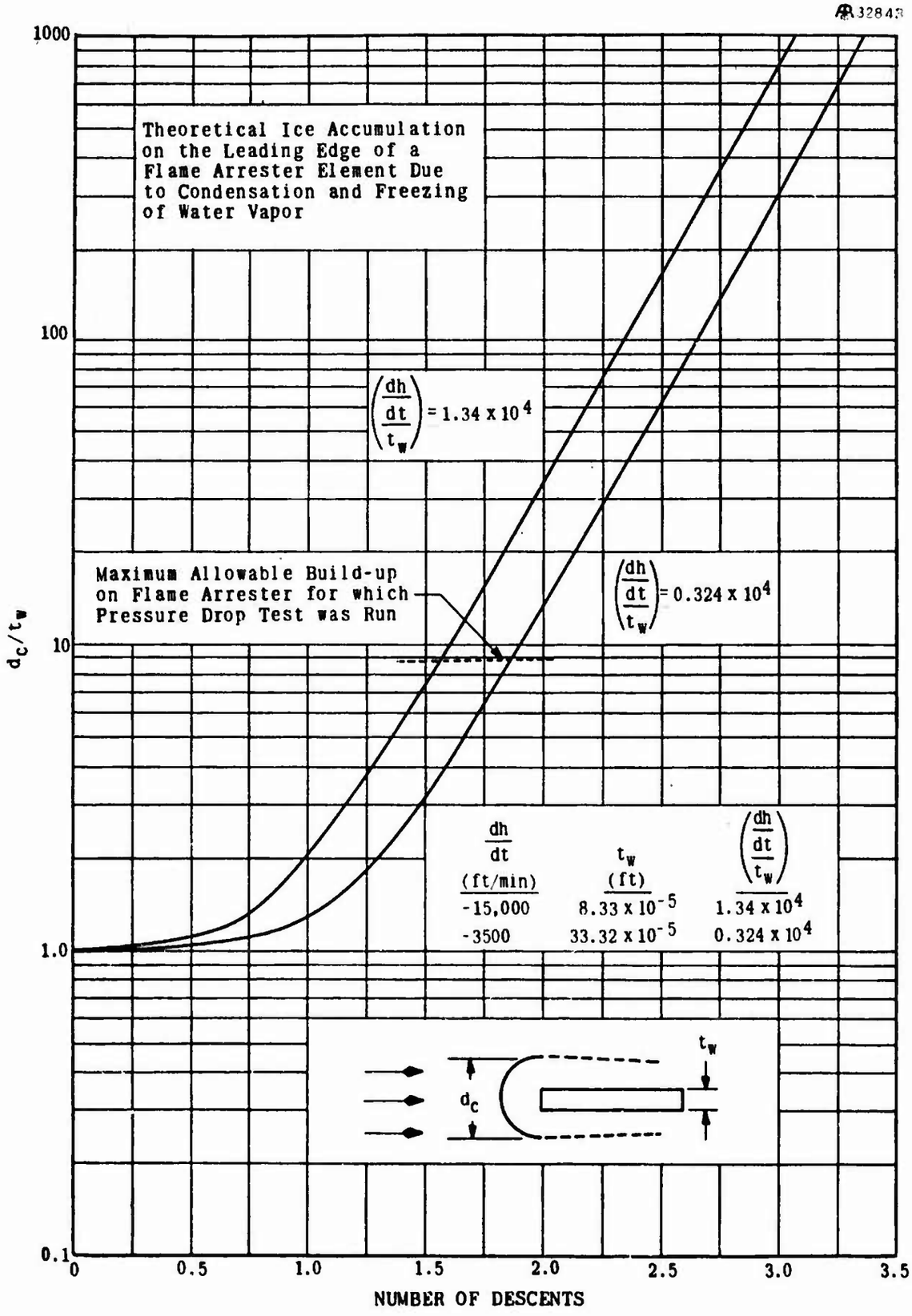

Figure 51. Theoretical Ice Accumulation on Flame Arrester.

this is a positive pressure of 1.0 psi to 1.5 psi. Further it is stated that the pressure in the cavity which surrounds the bladder tanks actually lags the increasing ambient pressure by about 0.5 to 1.5 psi depending on the altitude and on the particular one of three center wing section tankage configurations which are possible in the 707-120 series airplanes. From this information we see that under normal conditions the bladder tanks are under a positive pressure even during emergency descent rate conditions.

The pressure drop in the present vent system between the inlet scoop and the wing center section bladder tanks is given as nominally 0.39 psi. Thus, using the allowable maximum pressure differential of -0.36 psi, we calculate that the pressure drop across any proposed flame arrester must be less than about $1.5 + 0.39 - 0.36 \approx 1.5$ psi or $3.0 + 0.39 - 0.36 \approx 3.0$ psi dpending on the particular configuration.

Hoerner[25] summarizes the results of several investigations of pressure drop across radiator cores in ducts and presents curves which bound the loss coefficients of "typical radiator cores" for varying velocity. For velocities between 60 ft/sec and 100 ft/sec $\xi = 3$ to 6 where

$$\xi = \frac{\Delta p}{\frac{1}{2}\rho\, w^2}$$

or

$$\Delta p = \frac{1}{2}\xi\,\rho\, w^2$$

and where

$\Delta p \sim$ pressure drop across the core (lb/ft^2)
$\xi \sim$ loss coefficient for the radiator core
$\rho \sim$ density of the air flow ($lb\text{-}sec^2/ft^4$)
$w \sim$ velocity in the radiator core (ft/sec)

The pressure drop across an actual flame arrester was measured for water flow as reported in Section 5.1. The particular arrester was 1/2-inch deep with 2-mil wall thickness and 50-mil maximum distance between

walls. By Reynolds number analogy the test data were converted to loss coefficient for air. The data are plotted in Figure 52. For a vent velocity of 86 ft/sec which corresponds to an emergency rate of descent, ξ is seen to be 2.9.

The velocity in the flame arrester core, w, increases above the velocity in the duct, v, in direct proportion to the area decrease caused by blockage of the flame arrester and any ice which may be present on it.

$$A_d\, v = (A_d - A_b)\, w$$

where

$A_d \sim$ cross section area of the duct, $\pi D^2/4$

$A_b \sim$ cross section area blocked by the flame arrester core

If we define a blocking efficiency, $\eta = \dfrac{A_b}{A_d}$, the above equation can be rearranged to give

$$W = \left(\frac{A_d}{A_d - A_b}\right) v = \frac{v}{1 - \eta}$$

With this equation, Δp can be expressed in terms of the blocking efficiency.

$$\Delta p = \frac{\xi \rho}{2\,(144)} \left(\frac{v}{1 - \eta}\right)^2$$

We have seen that the maximum allowable value for the pressure drop is $\Delta p = 1.5$ psi and that the vent tube velocity is proportional to the rate of descent, $v = -5.743 \times 10^{-3} \dfrac{dh}{dt}$, where $\dfrac{dh}{dt}$ is in ft/min. Substituting these two equations into the preceding expression for Δp

$$1.5 = \frac{\xi \rho\, (-5.743 \times 10^{-3})^2}{288\,(1 - \eta)^2} \left(\frac{dh}{dt}\right)^2$$

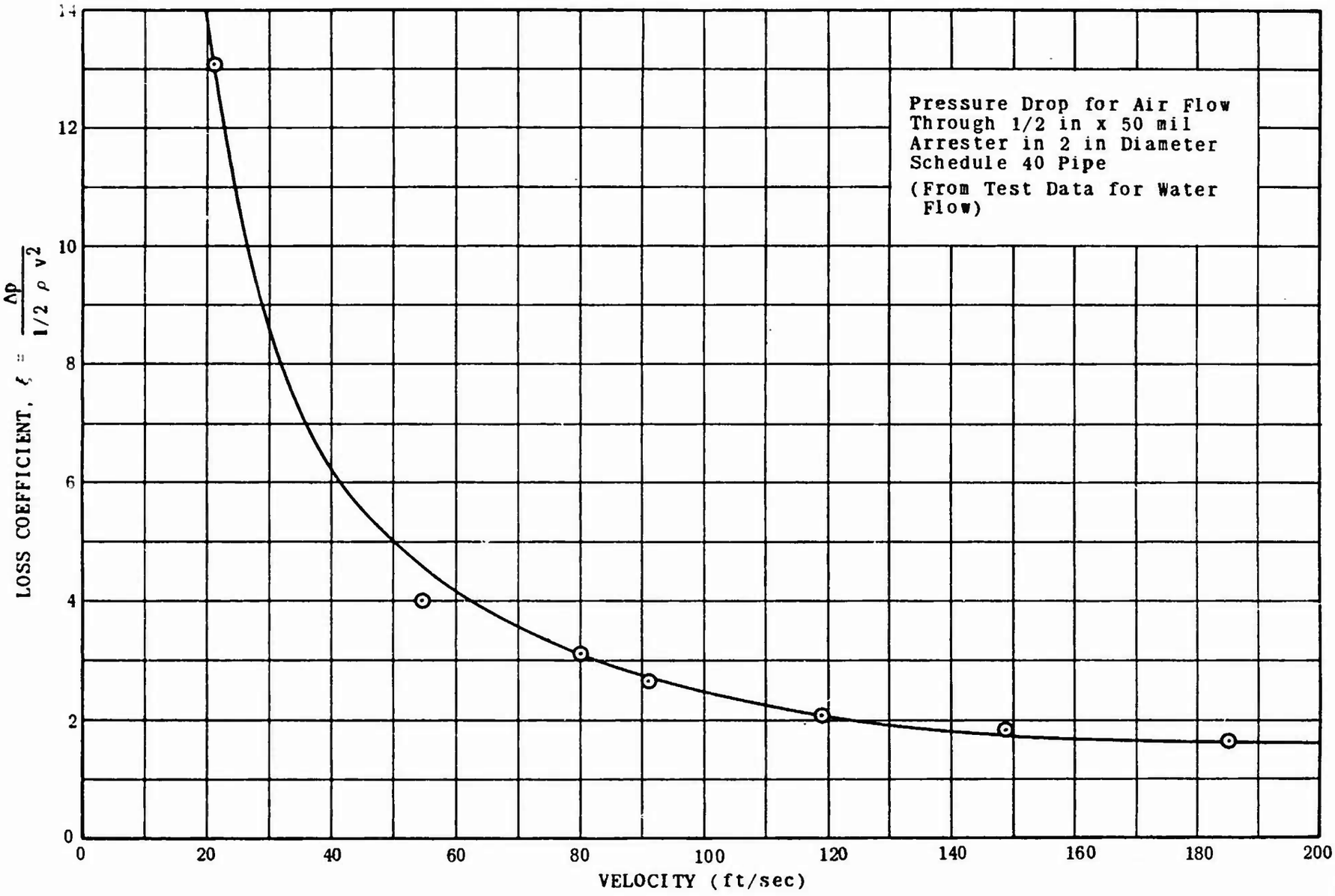

Figure 52. Pressure Drop Through Flame Arrester.

Thus we can write an expression for the allowable blocking efficiency, η, in terms of the descent rate $\frac{dh}{dt}$. After some rearranging we have

$$\eta = 1 - 2.33 \times 10^{-5} \left|\frac{dh}{dt}\right| \qquad \eta < 1$$

This shows that high blocking efficiencies (large amounts of icing) are permitted if the descent rate is low. If, however, we insist that the maximum blockage be such that the emergency rate of descent is safe at all times, then for $\frac{dh}{dt}$ = 15,000 ft/min.

$$\eta_{(\text{allowable})} = 1 - 2.33 \times 10^{-5} (15000) = 0.651$$

The blocking efficiency of a flame arrester depends on the wall thickness of the elements (which includes ice if present), the distance between elements, and the particular grid configuration. Table 16 gives formulas for typical flame arrester configurations.

The arrester for which pressure drop test data was obtained was of type (c) as listed in the table. For this particular arrester we may calculate the permissible icing.

$$1.813 \frac{t_w}{e} \frac{d_c}{t_w} = \eta_{(\text{allowable})}$$

$$\frac{d_c}{t_w} = \frac{(0.651)(0.050)}{(1.813)(0.002)} = 9.0$$

This limit was plotted in Figure 51 as previously mentioned.

5.3.8 Icing Summary and Discussion

Contributions to icing of a flame arrester in the vent tube have been shown to arise to two distinct mechanisms: entrainment of supercooled water drops from the free-stream air flow, and by condensation and freezing of saturated water vapor onto the colder flame arrester. Both of these icing

Table 16. Blocking Efficiency, η, for Typical Flame Arrester Configurations.

Flame Arrester Configuration	Total Length of Grid, L_T	Total Blockage $A_b = L_T \cdot t_w$	$\eta = \frac{A_b}{A_d}$
(A) Parallel Plates 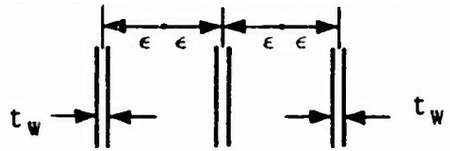	$\frac{A_d}{2\epsilon}$ [a]	$\frac{A_d}{2} \frac{t_w}{\epsilon}$	$\frac{1}{2} \frac{t_w}{\epsilon}$
(B) Square Grid 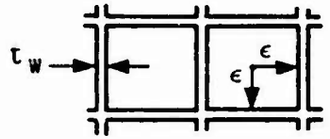	$\frac{A_d}{\epsilon}$	$A_d \frac{t_w}{\epsilon}$	$\frac{t_w}{\epsilon}$
Triangular Grid 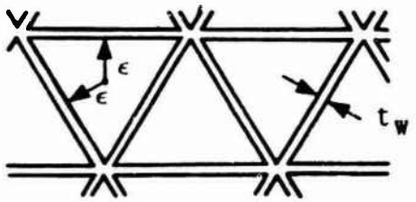 or Hexagonal Grid 			
(C) Corrugated Grid 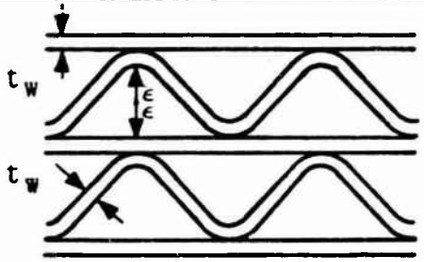	$\frac{A_d}{2\epsilon}$ (1 + 2.625)	1.813 $A_d \frac{t_w}{\epsilon}$	1.813 $\frac{t_w}{\epsilon}$

[a] A_d is the Area of the Duct in Which the Grid is Installed.

AR328239

mechanisms can only occur during descent of the airplane when the fuel tanks are "breathing" in, and both icing rates increase with rapid rates of descent.

Simplified models of the flow field into the vent tube outlet show that the rapid turning allows only small water droplets to enter. The 8-micron diameter drops appeared to be most easily admitted, but drops of this small size are not often encountered. More accurate estimates of water drop impingement must depend on actual icing tests.

Ice accumulation by condensation can only occur if the flame arrester is cold enough to supersaturate the air which is flowing over it. The amount of temperature lag between the air and the flame arrester depends on the thermal and heat-transfer properties of the arrester, both of which may be controlled by the arrester design.

Ice from condensation during an emergency rate of descent is not excessive, but only two repeated normal descents through a saturated atmosphere with no melting occurring between descents can accumulate an excessive amount of ice as shown in Figure 51.

No attempt was made in the computations to take into account the release of latent heat of the condensing water vapor to the walls of the flame arrester. This heat is applied at the ideal place to reduce the temperature lag of the arrester relative to the inflowing air temperature and its neglect only increases the conservative position of the computational results of the icing analysis.

6.0 DISCUSSION AND CONCLUSIONS

6.1 SUMMARY

The conclusions obtained directly from the experimental and analytical studies are presented below. Following the conclusions, a summary discussion is presented of the lightning protection measures for 707 aircraft fuel systems.

6.1.1 Experimental Conclusions

(a) If lightning can initiate combustion by striking near the vent outlet then it is possible, under certain conditions, that the flame can propagate through the vent system into the fuel tanks.

(b) Flames initiated by simulated lightning will propagate through the vent duct at speeds up to 150 ft/sec and generate pressures up to 15 psig. The flame speed and pressure generated appear to be dependent upon the total energy deposited in the vicinity of the vent outlet by the discharge and are not strongly dependent upon the voltage and current rates of rise.

(c) The 707 vent duct and surge tank act as an organ pipe and provide flame speeds greater than the usual turbulent burning velocities due to large pulsing mass flows in the duct. Suitably timed repeated lightning strokes might reinforce the resonance amplitude of the vent tube and provide still greater flame speeds.

(d) A simple laboratory apparatus has been developed and duplicates the range of flame speeds and pressures in a duct generated by large energy discharges.

(e) Flame arresters located at certain positions in the vent duct will prevent simulated lightning initiated flames from propagating through the duct into the surge tank and fuel tanks.

(f) The flame arrester openings should have characteristic cell dimensions of the order of 0.050 inch. Stainless steel honeycomb or rolled corrugated strip with cell depths of 1 inch are satisfactory.

(g) Flame arresters located in the 707 vent duct near the vent outlet are ineffective due to the inward mass flow developed in the duct by the simulated lightning discharge. Flame arresters located near the surge tank are effective.

(h) Screens and wire gauzes are ineffective in stopping the high-velocity flame fronts generated by certain types of simulated lightning.

(i) A theory has been developed, based on experimental data, which qualitatively explains the mechanism of flame propagation into the vent system. This theory suggests that a careful acoustic analysis of the system should be an important consideration in locating any flame arresters.

(j) Two stainless steel flame arresters, one 0.5-inch deep and one 1-inch deep, with 0.050-inch openings when acting as a flame holder under the most severe heat transfer conditions reach equilibrium temperature within a few minutes and this temperature is not sufficient to cause flashback through the arresters.

(k) The pressure drop introduced by the 1/2-inch and 1-inch deep flame arresters with 0.050-inch openings is a small fraction of the total pressure drop through the vent system and would require a small decrease in allowable fueling flow rate to maintain the design pressure drop through the vent system.

(l) Flames which traverse the vent tube in times of 18 msec or more (i.e., equivalent to average flame speeds of 140 ft/sec or less) were prevented by industrial-type explosion suppression systems from propagating through the surge tank.

(m) Flames which traverse the vent tube in times of 11 msec or less (i.e., equivalent to average flame speeds of 230 ft/sec or greater) were not prevented from propagating through the surge tank by industrial-type explosion suppression systems.

(n) The industrial-type explosion suppression system will prevent flames, whose speeds are comparable to the maximum flame speeds measured during simulated lightning experiments, from propagating through the surge tank into the reserve tank. The margin of safety of this particular system is limited since the system may not be effective for somewhat higher flame speeds.

(o) There was no evidence of plasma (i.e., high ion concentration) penetration into the vent outlet and vent tube from simulated lightning strikes directly to the vent outlet with energy releases exceeding ten times that of previous investigations. However, the plasma test was not completely satisfactory because of limitations of time and because of external electromagnetic interference with the plasma probes.

(p) There was no evidence of pressure ratios exceeding 2 generated in the vent tube by simulated lightning strikes directly to the vent outlet.

6.1.2 Analytical Conclusions

(q) A continuous net outflow rate of 5 ft/sec is required to prevent flashback in the 5-inch diameter vent tube either through the core of the gas flow or along the walls. Since flames may propagate into the duct at speeds approaching 150 ft/sec, a minimum total outflow rate of the same order may be required to provide the desired outflow conditions at all times.

(r) The use of mechanical valves in the vent tube to isolate flow paths is not an effective or practical technique to prevent flame propagation through the vent system.

(s) The use of bladders which separate bulk-fuel from air is an accepted containment method. However, since the fuel may permeate the bladder material, a flammable mixture may still exist in the region between the bladder and the wing skin.

(t) Inerting systems can be effective in preventing flammable mixtures from occurring, but very large quantities of inerting gas may be required to assure nonflammability of the mixture under all conditions.

(u) Icing calculations show that under the most severe aircraft descent rate in the most severe atmospheric environment for icing, the 1-inch deep 0.050-inch opening, 5-inch diameter flame arrester will not be sealed with ice.

(v) Icing calculations show that under the most severe atmospheric icing conditions, the 1-inch deep, 0.050-inch opening, 5-inch diameter flame arrester may be sufficiently blocked after a few normal descents to create buckling pressures in the fuel tanks during an emergency descent. This may not be a sufficient margin of safety and icing tests are recommended.

6.1.3 Summary Discussion

A stainless steel flame arrester 1-inch deep, 5 inches in diameter with 0.050-inch openings located near the surge tank will prevent flame propagation into the surge tank under all the conditions tested. The arrester is simple and can be retro-fitted. Pressure drop and flame holding characteristics of this arrester do not add significant additional hazards. Icing calculations show that under severe conditions ice will form on the arrester but it will not seal closed. Added protection may be achieved by enlarging the arrester and duct diameter prior to entering the surge tank. There appears to be sufficient room in the 707 wing tip to increase the arrester area several-fold. This will reduce the flow approach velocity and also increase the area over which ice may be deposited. If further protection is desired to assure continuous openings in the vent, a flame arrester protected by-pass tube with a blowout panel could be installed to rupture if pressure drop through the system becomes excessive. The use of electrical, hydraulic or pneumatic de-icing systems would also protect against severe icing

Since arresters with larger openings of different areas and geometries may be effective, further work is needed to optimize the arrester design with respect to cell size, position, area, thickness, geometry, pressure drop, pressure relief, icing and plugging characteristics. This would permit full evaluation of this protection technique to obtain the proper basis for integration of the arresters into the aircraft, after which a flight test program could commence.

Similarly, explosion suppression systems appear to offer satisfactory protection from flames propagating through the vent system. However, more work is needed to optimize the design effectiveness, safety, maintenance and

weight. The effectiveness of these systems in preventing explosions caused by direct strikes to tanks should be evaluated. It may be possible to retro-fit explosion suppression systems into existing aircraft.

Another possible approach would be the use of increased vent velocities. New aircraft designs might consider the use of a scoop to bring in air, mix it with the fuel tank effluent and provide the required high exit velocities to the mixture.

At this time, the most promising device for protection against flame propagation through the aircraft vent system appears to be a flame arrester. Explosion suppression systems, increased vent velocities, and possibly inerting, show some promise and should continue to be considered.

6.2 ADVANTAGES AND DISADVANTAGES OF PROTECTION SCHEMES

Method	Advantages	Disadvantages
Flame Arresters	Very effective, reliable Simple, no moving parts Easily retro-fit Inert, non-corrosive Low weight Low unit cost	Potential plugging and icing hazard Compromised by one large opening
Explosion Suppression	Effective against typical flame speeds Can be retro-fit Circuit can be checked Can repeat cycle Relatively long term suppression	Not effective against high flame speed Toxic, corrosive agent Explosive components Complex - questionable reliability Potential malfunction due to dirt, defective parts Weight, cost Inadvertent actuation
Increased Vent Velocity	Can be effective No moving parts Simple	Major modification Needs high velocity Leading edge icing Minimize or negate tank positive pressure
Mechanical Valves	--	Not practical Not effective
Bladders	--	May not be effective
Inerting	Can be effective Inert agent Can be intermittent	High pressure storage Large storage capacity Special regulators and valves needed Somewhat complex

BIBLIOGRAPHY

1. Robb, J., Newman, M., et al., Lightning Hazards to Aircraft Fuel Tanks, NASA TN4326, September 1958.

2. Viemeister, P.E., The Lightning Book, Doubleday and Co., Inc., 1961.

3. Tilson, S., Environmental Electricity, Science and Technology, No. 25, January 1964.

4. Lockheed Service Digest No. 48, March 1964.

5. Blanc, M.V., Guest, P.G., von Elbe, G., Lewis, B., J. Chem. Phys. Vol. 15, p. 798, 1947.

6. Lewis, B., von Elbe, G., Combustion, Flames and Explosions of Gases, 2nd Ed., Academic Press, N.Y., 1961.

7. Van Dolah, R.W., Zabetakis, M.G., Burgess, D.S., Scott, G.S., Review of Fire and Explosion Hazards of Flight Vehicle Combustibles, ASD Technical Report 61-278, Bureau of Mines, U.S. Dept. of the Interior, April 1961 and Supplement 1, April 1962.

8. Palmer, K.N., Review of Information on Selected Aspects of Gas and Vapor Explosion, Journal of the Institute of Fuel, 1956.

9. Gerstein, M., Investigation of Mechanism of Potential Aircraft Fuel Tank Vent Fires and Explosions Caused by Atmospheric Electricity, NASA TN D-2240, January 1964.

10. Kirschner, O.E., NFPA Aviation Bulletin No. 161, July 1956.

11. Nordstrom, D.C., Analyses of the 707-120 and -220 Fuel Tank Vent System, Boeing Doc. No. DC 1493, The Boeing Company.

12. Fuel Vent System Flight Test - Boeing 707, Pan American Airline Report No. ME-138, January 31, 1964.

13. Harris, Grumer, von Elbe, Lewis, Third Symposium on Combustion, Flame and Explosion Phenomena, Williams and Wilkens, Baltimore, 1949, p. 80.

14. Friedman, R., Third Symposium on Combustion, Flame and Explosion Phenomena, Williams and Wilkens, Baltimore, 1949.

15. Friedman, R. Johnston, W., Journal of Applied Physics, Vol. 21, No. 8, pp. 791-795, August 1950.

16. McAdams, Heat Transmission, 3rd Edition, McGraw Hill Co., Inc., New York, 1954.

17. Williams, D., Bollinger, L., Third Symposium on Combustion, Flame and Explosion Phenomena, Williams and Wilkens, Baltimore, 1949, p. 176.

18. Electrostatic Discharges in Aircraft Fuel Systems, Coordinating Research Council, Proj. No. CA-22-59, July 1961.

19. Ruggeri and von Glahn, Investigations of Aerodynamic and Icing Characteristics of Recessed Fuel-Vent Configurations, NACA TN-1789, 1949.

20. Aerodynamic Capture of Particles, Edited by E.G. Richardson, Pergamon Press, 1960.

21. Engineering Summary of Airframe Icing Technical Data, FAA ADA-4, 1964.

22. Handbook of Chemistry and Physics, 24th Edition, p. 1979, Chemical Rubber Publishing Co.

23. Schlichting, H., Boundary Layer Theory, Pergamon Press, 1955.

24. Eckert and Drake, Heat and Mass Transfer, McGraw-Hill, 1959.

25. Hoerner, S.F., Fluid-Dyanic Drag, Published by author, Midland Park, New Jersey, 1958.

26. Ignition Characteristics of Fuels and Lubricants, Tech. Doc. Rep. No. APL-TDR-64-25 - AF Aero Propulsion Laboratory, Wright-Patterson Air Force Base, December, 1963.

APPENDIX A

LIGHTNING AND TRANSIENTS RESEARCH INSTITUTE ARTIFICIAL LIGHTNING DISCHARGE FACILITIES USED IN ATLANTIC RESEARCH CORPORATION FUEL VENT STUDIES

Prepared by

Lightning and Transients Research Institute

Lightning and Transients Research Institute Artificial Lightning Discharge Facilities Used in Atlantic Research Corporation Fuel Vent Studies

The artificial lightning discharge facilities used in the Atlantic Research Corporation fuel vent studies have been set up to reproduce the particular characteristics of natural lightning discharges to aircraft which would be of most significance in studying ignition and flame propagation in vent tubes and flame arresters.

The specific waveforms used were based on Lightning and Transients Research Institute's 15-year analysis of lightning damage to aircraft parts, over one-thousand aircraft flight damage questionnaires, in flight research programs and in a study of natural cloud to ground discharges triggered by rocket-borne wires off the Lightning and Transients Research Institute's research ship "Azara".

As most of the accumulated data has come from aircraft flight damage records, the rates of rise of current and charge transfers must be obtained by duplicating these effects in the laboratory. As no data are accumulated unless there is damage serious enough to require shop repair of the aircraft, the data represents in effect the high side of the normal distribution curve of magnitudes. A summary of the magnitudes of the various stroke parameters is presented in Table A-1 recognizing that the average values represent the average from damage reports rather than the true average, as many strikes are unreported and these average estimated values are extrapolated to a maximum and a possible upper limit value. In these fuel vent studies, the maximum rather than the average recorded values were considered to be of most importance in studying possible hazards mechanisms.

A lightning discharge may be characterized by the effects it produces, the magnetic force on conductors and sparking at poor connections produced by the high currents, the blast effects produced by the high energies in the expanding spark channel, the metal pitting and holes produced by the heavy charge transfers and the streamering and puncture of dielectrics induced by the tremendous potentials. Earlier Lightning and Transients Research Institute

Table A-1. Characteristics of Natural Lightning Discharges to Aircraft.

	Average	Maximum	Possible Upper Limit
Current/amps/μsec	50,000	500,000	1,000,000
Rate of rise	10,000	200,000	500,000
Charge - coulombs	50-200 (weighted)	600	1,000
Voltage	10^8	0.5×10^9	10^9

high-voltage facilities for reproducing these effects are illustrated in Figure A-1, along with the associated current waveforms.

The U. S. Air Force and U. S. Navy have established in Mil-A-9094C a specification describing similar discharges for the testing of aircraft lightning arrester susceptability to damage. However, this composite discharge is not entirely suitable for testing ignition and propagation mechanisms in fuel vents. It specifies long duration components lasting up to a second which are less applicable for these studies, for as the aircraft moves past the ionized stroke channel at approximately 0.8 feet/millisecond, the mid span vent location is passed in a few milliseconds. Also, structural damage, holes, etc. in adjacent areas should have little effect on propagation mechanisms other than through internal joint sparking as covered in Lightning and Transients Research Institute internal sparking studies. What are required, however, are high-current and high current rate of rise discharges with maximum amplitude.

Two types of discharges were used in the tests, a high energy discharge with a current of 250,000 amperes, (more than double the 100,000 amperes specified in Mil-A-9094C) a slowly rising front of 50 microseconds and a long tail of 300 microseconds utilizing a source voltage of only about 25 kilovolts, maximum, and a second steep front of wave discharge (high current rate of rise) reaching about 50,000 amperes in one microsecond utilizing one million volts as a driving source to obtain the steep wavefront. These test discharges fall between the average and maximum values of current and current rate of rise shown in Table A-1. The charge transfer of the high-energy discharge was only about 9 coulombs, but as pointed out previously this is of less importance in these vent propagation studies of a mid span vent past which the stroke should be swept in a few milliseconds by the windstreams.

The potentials used in the tests were limited to about one million volts using close electrode spacings to assure that the discharge would strike directly into or near the vent outlet. With higher potential and longer arc lengths, it would have been very difficult to direct the strike into the relatively shielded vent area. The high potential was required principally to obtain a high rate of rise of current.

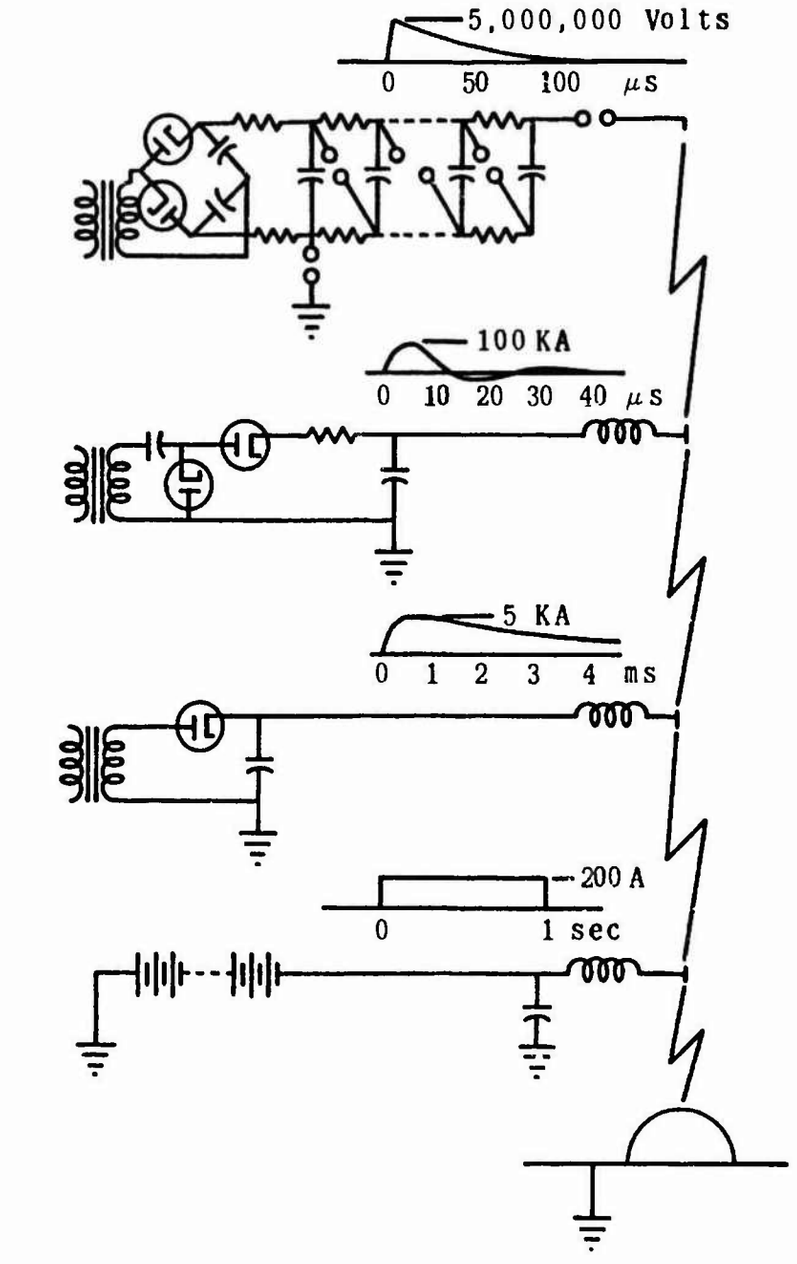

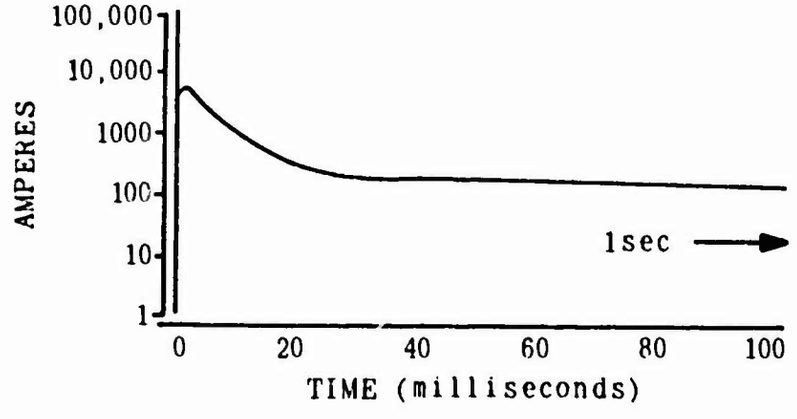

Figure A-1. Artificial Lightning Generator With Multiple Current Component Sections, and Resultant Composite Output Current Waveform.

Both discharges were made oscillatory in order to obtain maximum currents. Waveforms are illustrated in the oscillograms of Figure A-2, and schematic circuit diagrams are shown in Figure A-3 for the two generators. The high current generator was essentially a large capacitor bank and is shown in Figures A-4 and A-5. The steep front generator was a Marx type of high-voltage impulse generator in which a bank of capacitors were charged in parallel and discharged in series, and it was specially designed with minimum inductance to produce maximum rates of rise of current. To further reduce inductance the generator was positioned at an angle to minimize lead lengths as illustrated in Figure A-6. A photograph of the generator in operation, showing the two parallel capacitor-spark gap columns, is shown in Figure A-7.

Of particular interest, in addition to the electrical characteristics of the discharges, were the associated pressure waves. The variations in pressure wave peaks with current, current rate of rise, and with the mass of vaporized material are illustrated in Figure A-8. The study of the mass of vaporized material is of interest as aluminum foil conductors were used to trigger the low voltage arcs. With the Marx generator output of one million volts, no trigger conductors were required. The pressure oscillograms indicated that the pressure peaks are more affected by total energy than by current rate of rise. The pressures measured in these studies correlate well with the pressures measured near a triggered natural lightning discharge from the Lightning and Transients Research Institute's Research Schooner "Azara" as reported in an earlier NASA-FAA sponsored report.*

The artificial lightning discharge currents and current rates of rise used in these studies correspond to the more severe discharges recorded to date on aircraft but it must be emphasized that they do not represent the most severe discharges to be expected.

* Investigation of Mechanisms of Potential Aircraft Fuel Tank Vent Fires and Explosions Caused by Atmospheric Electricity. Final Report Contract No. NASr-59 May 31, 1963.

NOT REPRODUCIBLE

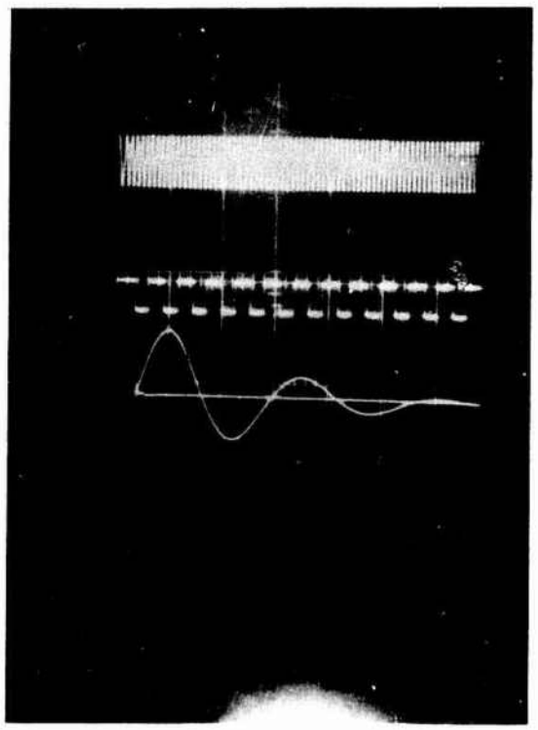

Figure A-2a. Typical High-Current Waveform, 150 Ka. and 100 Microsec./Unit.

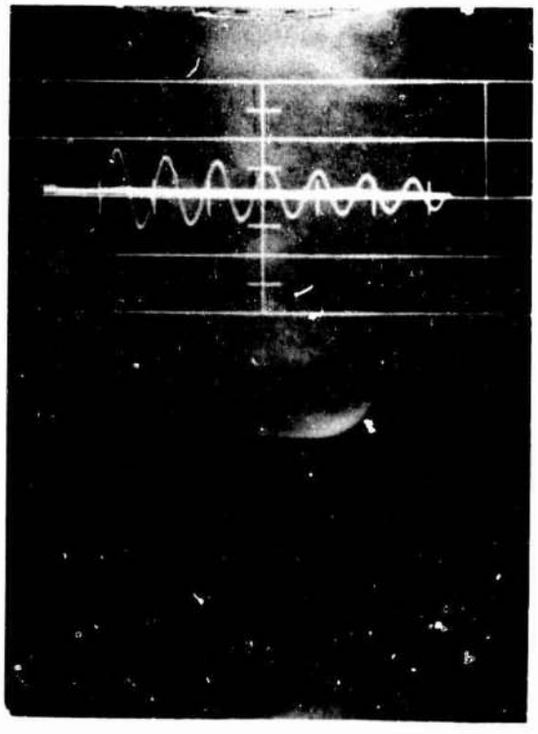

32938

Figure A-2b. Typical Current Waveform From High-Voltage Generator, 50 Ka. and Five Microsec./Unit.

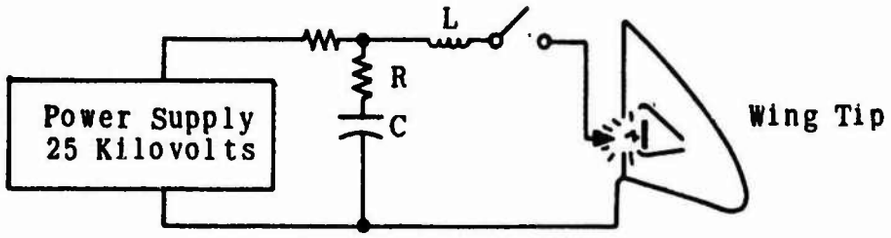

Figure A-3a. Circuit Diagram of High-Energy Generator Which Produces 250,000 Amperes Current Reaching Crest in 50 Microseconds.

NOT REPRODUCIBLE

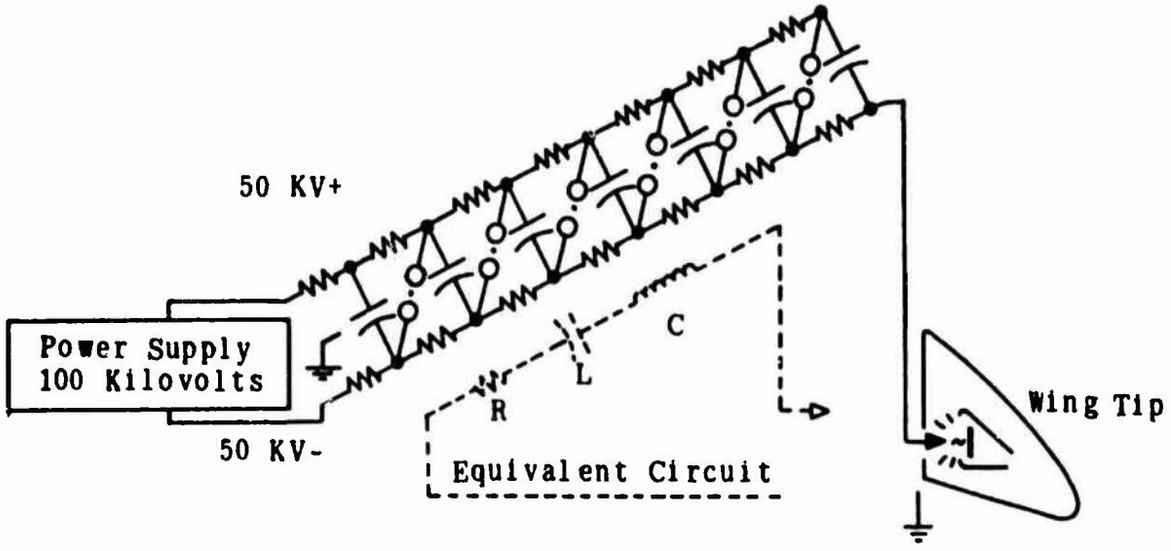

Figure A-3b. Marx Generator Circuit Used to Produce High-Current Rate of Rise Discharges Reaching 50,000 Amperes Crest in About One Microsecond.

NOT REPRODUCIBLE

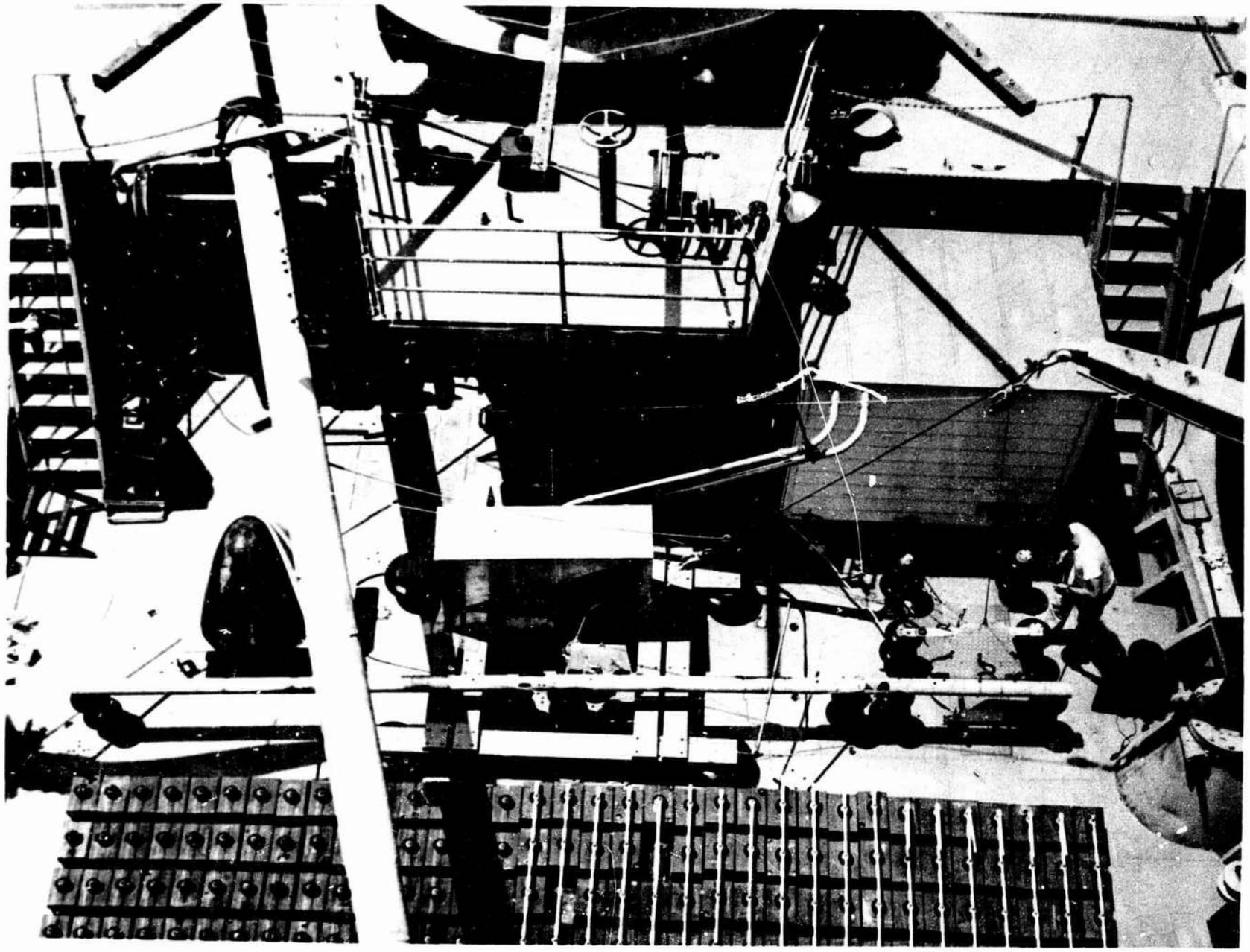

Figure A-4. High-Current Generator and Test Apparatus.

329 29

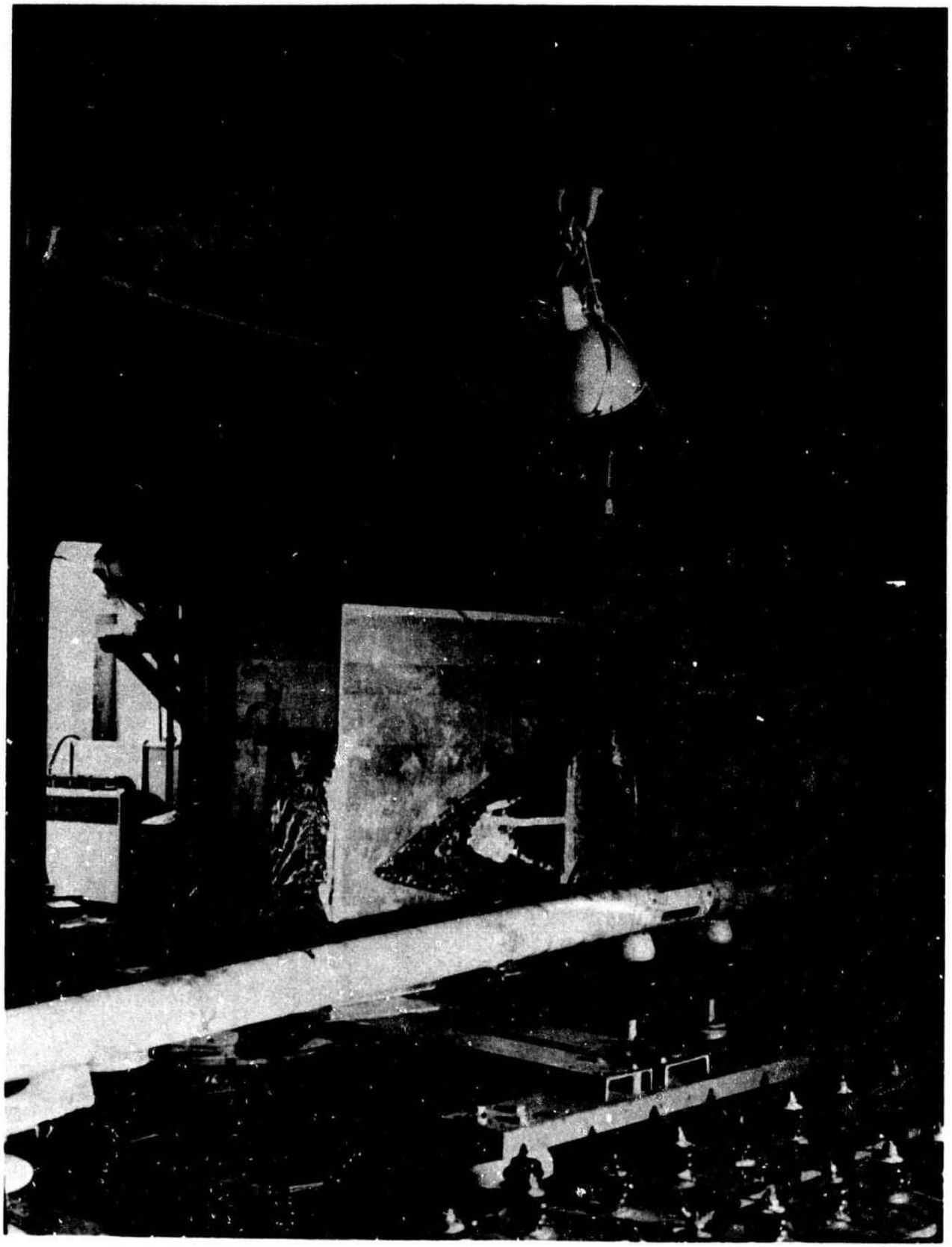

329 30

Figure A-5. Atlantic Research Test Apparatus at High-Current Generator.

NOT REPRODUCIBLE

603233

NOT REPRODUCIBLE

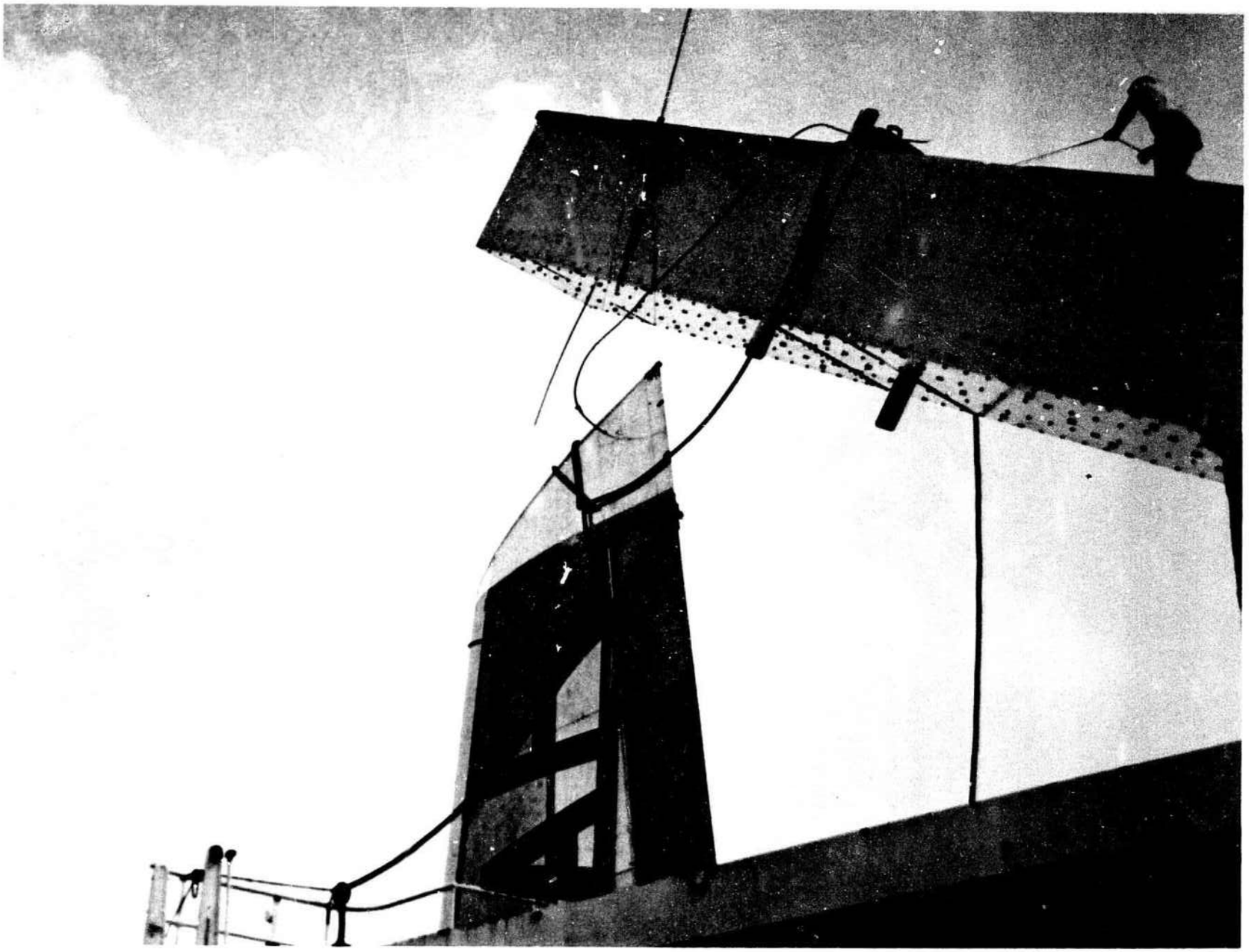

32932

Figure A-6. High-Voltage Generator and Test Wing.

6C 3233

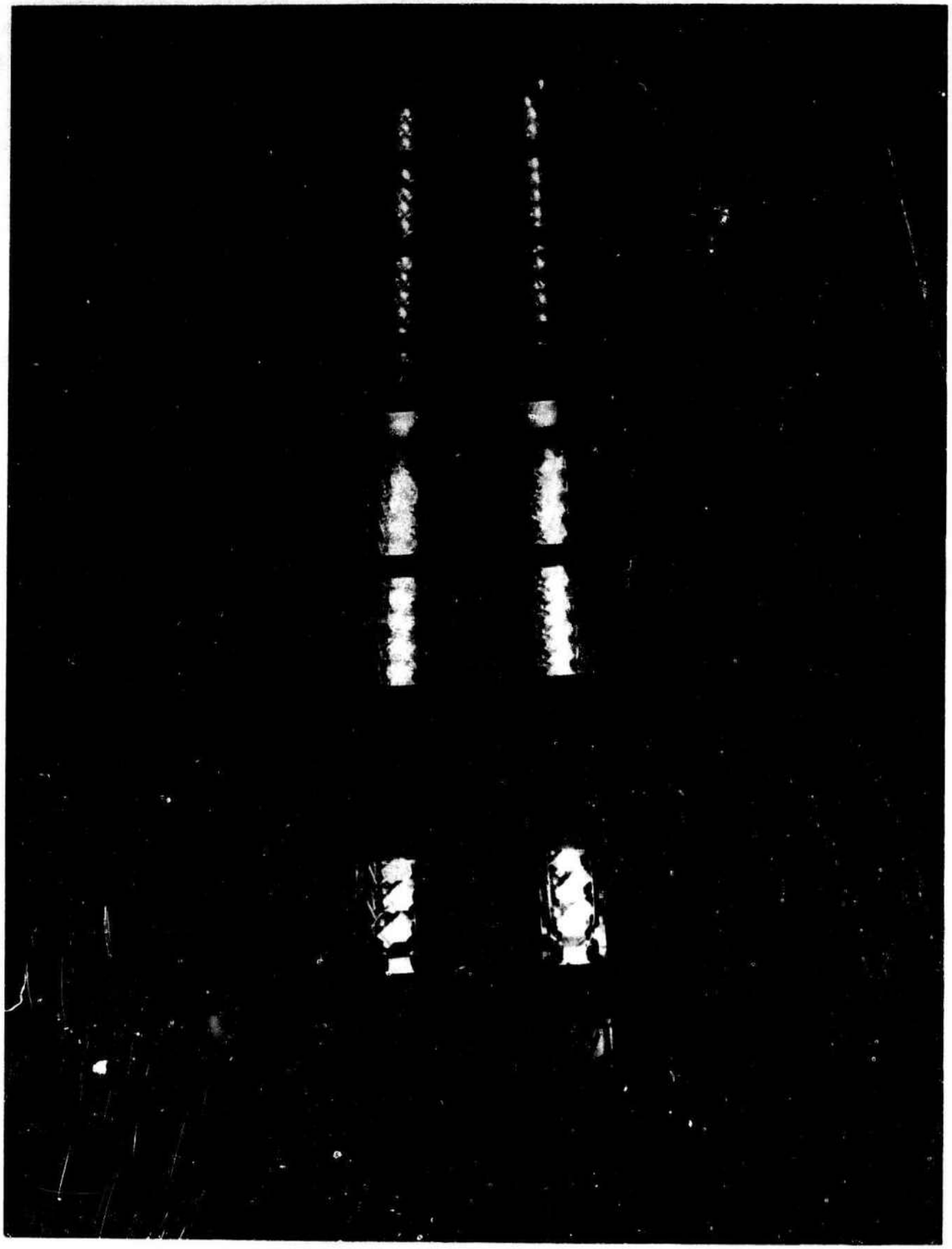

AR 32931

Figure A-7. High-Voltage Generator in Operation.

NOT REPRODUCIBLE

603133

All pressures - 9 psi/div. , currents - 30,000 amps/div, sweeps-200 usec/div.

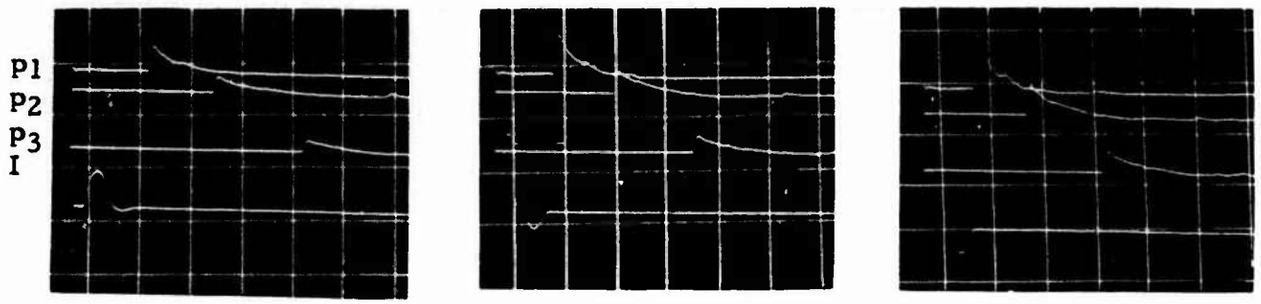

Figure A-8a. Pressure Wave Variation With Discharge Current 0.003 inch × 0.375 inch Aluminum Foil Strip Used to Initiate Discharge.

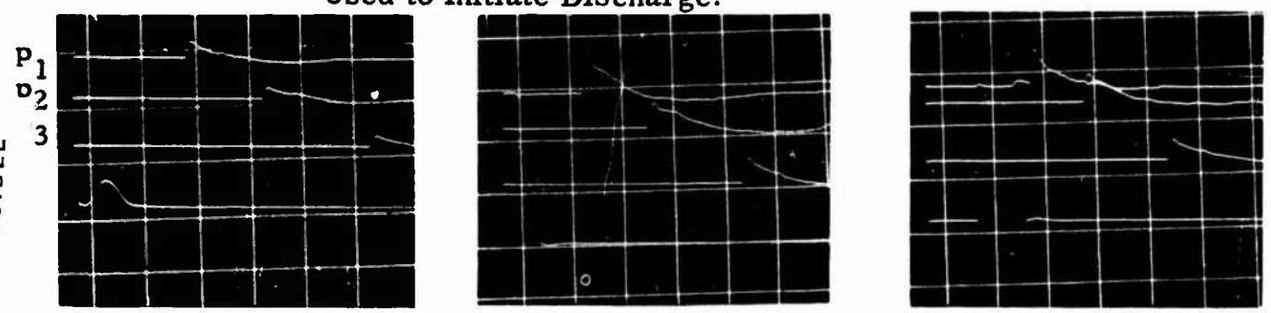

Figure A-8b. Pressure Wave Variation With Discharge Current 0.015 inch Diameter Copper Wire Used to Initiate Discharge.

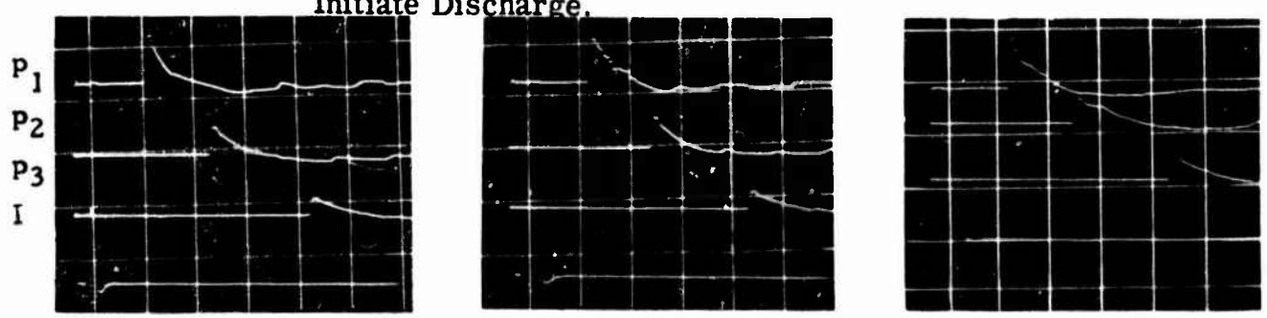

Figure A-8c. Pressure Wave Variation With Current Rate of Rise.

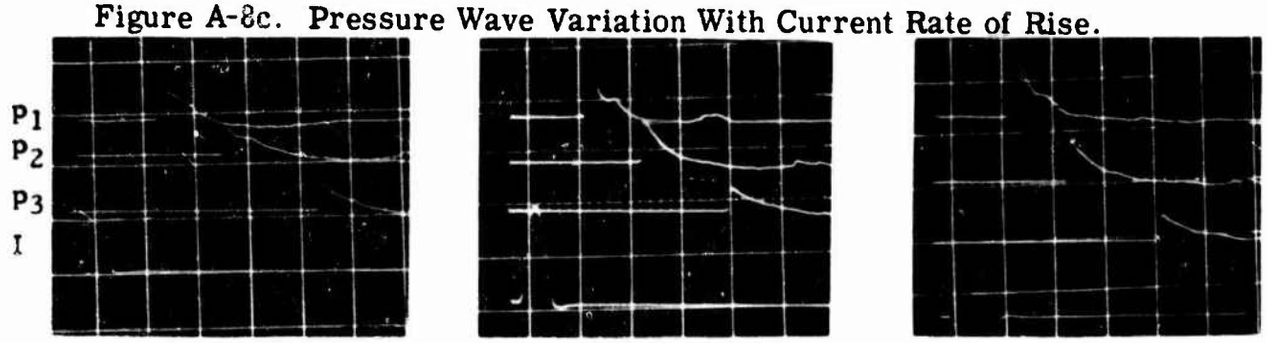

a)0. 015 " wire b) plus 2 grams water c) alum foil 3x375 mil

Figure A-8d. Pressure Wave Variation With Mass of Vaporized Material.

NOT REPRODUCIBLE

607233

APPENDIX B

FLAME ARRESTER CONFIGURATIONS

Title: 0.055 Inch Accordion

Material: Aluminum

Manufacturer: Twin Industries Inc.

Typical Cell:

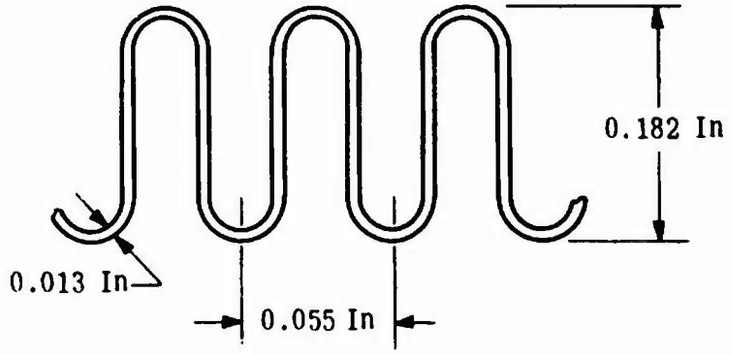

Depth: 1/2 Inch

Title: 0.055 Inch Screen

Material: Copper

Typical Cell:

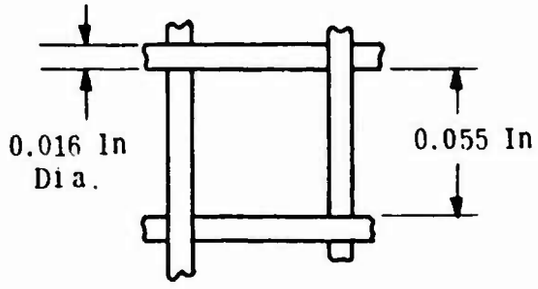

Title: 0.100 Inch Screen

Material: Copper

Typical Cell:

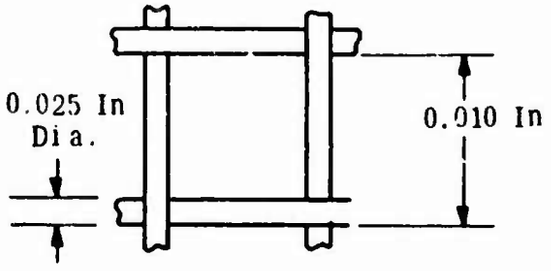

Appendix B
Description of Flame Arresters

Title: 1/2 Inch Ceramic

Material: Cercor

Manufacturer: Corning Glass Work, Inc.

Typical Cell:

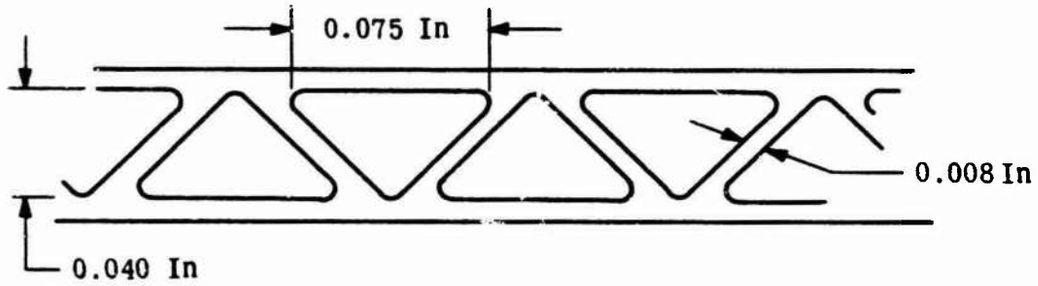

Depth: 1/2 Inch

Appendix B
Description of Flame Arresters

Title: 1/2 Inch x 0.050 Inch

Material: Stainless Steel

Manufacturer: Twin Industries Inc.

Typical Cell:

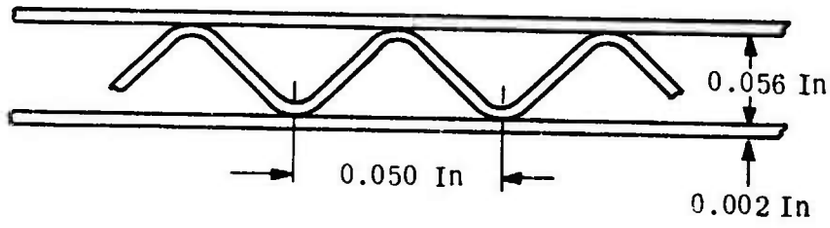

Depth: 1/2 Inch

Title: 1 Inch x 0.050 Inch

Material: Stainless Steel

Manufacturer: Twin Industries Inc.

Typical Cell:

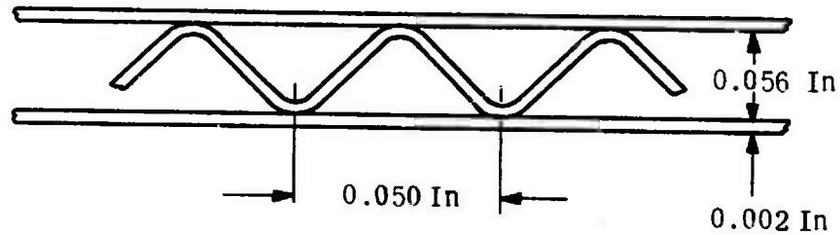

Depth: 1 Inch

APPENDIX C

EXPLOSION SUPPRESSION SYSTEMS
GENERAL INFORMATION

EXCERPTS FROM FENWAL, INCORPORATED PROPOSAL NO. PS-139 ISSUED JANUARY 23, 1964*

INTRODUCTION

The history of losses of combat aircraft during World War II definitely indicated the inherent hazard that is carried in fuel tanks. The majority of losses in the combat aircraft occurred as the result of fuel tank explosions. These experiences prompted an investigation by the Royal Aeronautical Establishment of Farnborough, England, to determine methods by which these explosions could be eliminated. The outcome was the development of an Explosion Suppression System based upon the high speed actuation of an extinguishing system during the incipient stages of the explosion.

This method was proven satisfactory through extensive testing and service on combat aircraft. Recognition of the effectiveness and practicability of this system is evidenced by the establishment of a U. S. Military Specification MIL-F-25648 for the use of this system to achieve fire and explosion suppression in aircraft fuel tanks and fuel tank cavities.

Over the past several years, an extensive industrial program has been under way in the United States to apply explosion suppression systems to various hazardous processes. Over one hundred (100) systems are in service at present, and actual suppressions of incipient explosions total twenty (20). In all of these, the structural damage was completely eliminated, permitting continued operation of the plant.

TECHNICAL DISCUSSION

Vent System

The vent system on the 707 consists of a series of ducts connecting the various fuel tanks to a surge tank located at each wing tip. The exit to atmosphere is accomplished by a single duct from the surge tank to the lower surface. The capacity of the surge tank is approximately fifteen (15) gallons and the duct to the lower surface approximately 24 inches in length. The duct length between the outboard reserve tank and the surge tank is negligible, and a direct opening must be assumed.

*Release of this information approved by G. J. Grabowski, Manager, Protection Systems.

Suppression System

To protect the vent system from an explosion initiated by an ignition source outside the vent opening, the Suppression System must be capable of detecting the incipient condition. Since the flame must pass through the duct to the surge tank, the installation of a radiation sensitive detector in the duct would provide an early signal for actuation of the suppressing devices. These devices would be installed in the surge tank and outer bay of the reserve tank to extinguish the flame as it enters. The installation of the suppressor in the reserve tank is necessary due to the opening between the tanks.

Explosion Detector

The detector consists of a sensing element and a control unit. The detector is sensitive to the visible and near-IR radiation levels of the type encountered with fuel explosions and provides an output as the radiation level increases. The control units connect to a wire bridge explosive switch which actuates the suppression device. The entire system is designed to meet MIL-E-7894A.

Suppressors

The suppressor distributes the extinguishing agent at extremely high speeds to inhibit the combustion process. The liquid agent is contained in a tubular suppressor with a material of construction of stainless steel. The 250 cc's of agent is discharged at high speeds when the explosive charge at the center is actuated by the electrical pulse from the control unit. The explosive force ruptures the suppressor wall along scored lines thus providing a definite failure pattern and preventing fragments from being thrown into the tank.

System Wiring

Standard aircraft wire may be used to connect DC supply leads to the system, except where the presence of RF fields exist in the vicinity of the detector. The leads from the output of the detector to the input of the control unit must be single conductor shielded wire.

COPY

DATA SHEET

500 cc Suppressor

92000-X

OPERATION:	Hydrostatic pressure is created by the explosive actuator rupturing the hemisphere along pre-scored lines. Agent is expelled at a dispersal velocity greater than 200 ft/sec.
ENVIRONMENTAL CONDITIONS:	
TEMPERATURE:	180° F Maximum
PRESSURE:	20 Psia Maximum
ELECTRICAL DATA:	
MIN. FIRING CURRENT:	1.0 Amp
REC. FIRING CURRENT:	5.0 Amp
DETONATOR RESISTANCE:	1.0 Ohm Nominal
HAZARDOUS LOCATION:	Designed for class I Groups C and D
HEMISPHERE MATERIAL:	Nickel-plated copper
AGENT:	Determined by customer application
WEIGHT:	7 Pounds Maximum
RECONDITIONING:	The entire assembly is expendable
STORAGE TEMPERATURE:	160° F Maximum

HEALTH HAZARDS AND PRECAUTIONS FOR THE SAFE HANDLING AND USE OF BROMOCHLOROMETHANE*

The Dow Chemical Company, Midland, Michigan
Biochemical Research Department
March 23, 1956

INTRODUCTION

The following statements on health hazards are as complete as available toxicological information permits. The precautions for safe handling and use are necessarily general in nature since detailed recommendations can be made only for the specific exposures and circumstances of each individual use. Inquiries about operations and uses may be addressed to The Dow Chemical Company. Assistance in evaluating the health hazards of particular plant conditions may be obtained from certain consulting laboratories and from State Departments of Health or of Labor, many of which have an Industrial Hygiene Service.

OUTLINE OF HAZARDS AND PRECAUTIONS

Bromochloromethane has an anesthetic action at high concentrations - Avoid exposures to high concentrations of vapor which cause such effects as staggering, dizziness, incoordination, stupor, confusion, headache, nausea or unconsciousness.

Mildly irritating to the skin - Avoid prolonged and repeated contacts on the skin. Do not wear contaminated clothing or shoes.

---

*Also known as Methylene Chlorobromide, Chlorobromomethane, and CB

SUMMARY OF HAZARDS

The acute toxic action of Bromochloromethane is manifest by typical anesthetic effects such as are produced by ethyl ether. This anesthetic action is sufficient to produce drunkenness, unconsciousness, and mortality if the exposure is prolonged after the occurrence of unconsciousness. Bromochloromethane has no other important toxic action; significant injury is not possible in the absence of definite anesthetic effects, and residual injury is not likely following complete recovery from the anesthetic effects.

Studies on the effects of repeated exposures have shown that a number of animal species can tolerate repeated 7 hour exposures to a vapor concentration of several hundred ppm with but very little evidence of injury. It appears therefore that the chronic toxicity is very low and that adverse effects may not be expected from repeated exposure at concentrations without minimal anesthetic effects such as lightheadedness, dizziness, stupor, mental confusion, or incoordination.

Like many organic solvents Bromochloromethane has a mild irritating action on the skin. A rash may result from prolonged and repeated contact.

It should be recognized that the accidental swallowing of appreciable quantities may lead to more or less serious injury.

PRECAUTIONS FOR SAFE HANDLING

Due to the high volatility of Bromochloromethane some precautions are advisable. Under particularly unfavorable circumstances of extensive volatilization and of poor ventilation, in which high vapor concentrations may result, exposed persons should be protected by ar approved gas mask with a canister affording protection against organic vapors, or by an oxygen or air supplied mask. For regular operations, provision should be made to keep vapor concentrations sufficiently low to avoid symptoms. Although specific

recommendations for safe concentrations cannot be made at present, it is doubtful if concentrations can exceed 500 ppm for extended periods without some adverse effect.

Precautions should be taken to avoid prolonged and repeated contacts on the skin, particularly through contamination of shoes and clothing.

Measures should be taken to avoid accidental ingestion. The material should be kept in appropriately labelled containers and should be stored where it is not available to children.

WHAT TO DO FOR EXPOSURES

Exposures should be terminated at once in the event of definite symptoms, and a physician should be called if effects seem to be at all marked. If breathing stops, artificial respiration should be started at once.

If the material gets into the eyes, these should be washed thoroughly with flowing water and a physician should be seen for medical care.

If the liquid is accidentally swallowed, vomiting should be induced as quickly as possible and a physician should be called.

If clothing or shoes become contaminated with this material, they should be promptly removed and not worn again until entirely free of the material.

HAZARDS IN THE USE OF BROMOCHLOROMETHANE AS A FIRE EXTINGUISHING AGENT

In the use of a vaporizing liquid fire extinguishing agent such as Bromochloromethane, there are questions regarding the acute hazard from exposure to the vapors of the agent and also to the thermal-decomposition products.

When relatively large quantities of Bromochloromethane are used in confined spaces, so that high concentrations of vapor may accumulate,

there is a possibility of anesthetic effects. This possibility does not seem to constitute a particularly serious hazard because of the improbability of there being a sudden incapacity or unconsciousness without warning.

The thermal-decomposition products of Bromochloromethane consists of halogen acids, halogens and other compounds that are highly irritating and toxic. It is doubtful that these substances greatly increase the normal hazards of smoke and gas from fires, particularly since the halogen acids are quite painful to the eyes and nose, and give excellent warning of their presence in excessive amounts. It is always necessary to avoid breathing the gas and smoke, irrespective of the extinguishing agent used.

The incidental hazards due to the presence of Bromochloromethane in fire extinguishing equipment are not unusual due to the poor capacity for producing serious organic injury.

We may conclude, therefore, that Bromochloromethane is a fire extinguishing agent that offers distinct advantages as far as health hazards are concerned and that it can be used quite safely when the particular hazards of fire fighting are recognized. Those incidental hazards that may arise through leaks in containers and through deliberate mis-use are not unusual and are no greater than those hazards presented by other commonly available substances.

BIBLIOGRAPHY

1. Unpublished data
   The Dow Chemical Company

2. Toxicity and Narcotic Action of Monochloromonobromomethane with Special Reference to Inorganic and Volatile Bromide in Blood, Urine and Brain
   J.L. Svirbely, B. Heyman, W.C. Alford and W.F. von Oettingen
   Journ, of Ind. Hygiene and Toxicology, Vol. 29, 382 (1947)

3. Pathologic Changes Produced by Monochloromonobromomethane B. Highman, J.L. Svirbely, W.F. von Oettingen, W.C. Alford and L.J. Pecora Archives of Pathology 45, 299-305 (1948)

4. Life Hazards and Nature of the Product Formed when Chlorobromomethane Extinguisher Liquid is Applied to Fires.
The Underwriter's Laboratories, Inc.
Bulletin of Research No. 42 - August 1948.

A Letter from Mr. P.C.C. Brown

Vice President - Engineering

Graviner Incorporated
Rockville, Maryland

dated April 15, 1964

COPY

Graviner Incorporated
628 Lofstrand Lane · Rockville · Maryland · 20850
Telephone · Area Code 301-762-4422

April 15, 1964

Atlantic Research Co.
Shirley Hwy. & Edsall Rd.
Alexandria, Virginia

Attention: Mr. Christian Bolta

Subject: Aircraft Fuel Tank Explosion Protection

Gentlemen:

Further to our discussions of Tuesday, April 7th, we are pleased to provide more information on our explosion protection systems and their service record.

As you are probably aware, the need for some form of explosion protection in the fuel tanks of military aircraft became evident during World War II, and Graviner began development of a suitable system, under a Government study contract in 1952; an essential parameter of the program being that the finally developed system must utilize components capable of being installed in all types of aircraft. The program resulted in a standard range of equipment available for installation in military bomber and transport aircraft during 1956, and it was immediately put into the current turbojet bomber production. The system has been installed in the various tactical freighters and strike aircraft designed and produced since then for both the Royal Air Force and the Royal Navy.

Early work in the field of explosion detection was concentrated on pressure rise detectors but it soon became obvious that if these were to be sufficiently sensitive to achieve rapid detection, they would also be triggered by aircraft maneuvers. Continuing work was therefore directed toward surveillance detection of the burning mixture. Infra-red detection was discarded because of the temperature limitations on the cell which caused increasing attenuation above 20°C, such that detection of weak mixture explosions within suitable time factors was not possible. Photomultiplier cells which were predominantly blue sensitive in the visible light range were finally chosen because they will satisfactorily detect all explosion flames from full rich to full weak mixture strengths.

COPY

Photomultiplier tubes are extremely sensitive devices since the initiating photo-cathode emission is increased by as many as a million times as the electrons of the original emission bombard successive targets through nine or more stages. An antimony surface at the cathode will give a blue sensitive cell which is easily able to see the poor radiation of weak mixture flames. At the same time, the cell has sufficient sensitivity in the red area to see the greater radiation level present in rich mixture burning.

The Graviner explosion protection system was therefore designed around a photomultiplier capable of detecting 0.03 lux since it was shown that weak mixture, rich mixture, mist and breathing explosions would provide from 0.1 to 12 lux at 3 ft. from the ignition source. Pressure rises not exceeding 1.5 p.s.i. during suppression in fuel cells larger than 10 gallons was taken as the criterion.

The detector form and design, as put into service, is shown on our Data Sheets E1, E5 and E6. The signal from the P.M. tube is used to trigger an electronic relay and energy from a capacitor storage is released to suitably disposed suppressors, shown on Data Sheets E2 and E7. Suppressant is dispersed throughout the vapor space inhibiting the further spread of the explosion flame front and inerting the remaining volume. Tests at Colnbrook have shown that the volume will remain inert for periods up to 20-30 minutes depending upon the ambient conditions, changes to them, and the agent used. In general, the low vapor pressure agents, such as CB, will not give good persistence. A powerpack is used to provide the special voltages required by the P.M. tube and illustrated on Data Sheet E3. The weight quoted would be much reduced by the introduction of various new and proved design techniques.

Service experience with the system has been satisfactory but because of its military significance it is not possible to quote service in terms of flying hours, etc. We feel it is significant that the system has been specified for and installed in additional aircraft designs since its first introduction into service in 1957. Only the electronic relay - a cold cathode tube - has given poor service, and the current design standard is expected to show much improved performance. No electric/electronic components are lifed, and only the explosive actuator in the suppressors has an installed life - 3 years.

COPY

Graviner Incorporated
628 Lofstrand Lane
Rockville, Maryland

Continuation Sheet

-3-

Systems are currently flying in two different types of turbojet and turboprop, strike and transport aircraft of the Royal Air Force.

Very truly yours,

GRAVINER INCORPORATED

/s/ P.C.C. Brown

P.C.C. Brown
Vice President - Engineering

PCCB/jp